**Professur für Hydrologie**
Albert-Ludwigs-Universität Freiburg im Breisgau

Barbara Sailer

# Climate change scenarios in international river basins: Is the uneven distribution of water resources increasing?

Masterarbeit unter Leitung von
Dr. Kerstin Stahl
Freiburg im Breisgau, Dezember 2013

**Professur für Hydrologie**
Albert-Ludwigs-Universität Freiburg im Breisgau

Barbara Sailer

# Climate change scenarios in international river basins: Is the uneven distribution of water resources increasing?

Referent: Dr. Kerstin Stahl
Koreferent: PD Dr. Jens Lange

Masterarbeit unter Leitung von
Dr. Kerstin Stahl
Freiburg im Breisgau, Dezember 2013

# Table of Contents

# List of Figures

# List of Tables

# Abstract

Water availability will be a major challenge for human society in the $21^{st}$ century, globally but also in the 279 existing international river basins. Projections about climate change show changes in the hydrological cycle leading to large impacts on water resources. Studies about climate change were mostly applied globally or as case studies for a specific river basin and the results based on the simulations of one hydrological model.

In this study, a model ensemble of six global hydrological models, all forced by three different general circulation models, is used to calculate the expected changes in hydroclimatic conditions due to climate change in international river basins. The main focus is on the changes in riparian countries within one basin and the differences among them because these differences could lead to tensions and conflicts.

Different indices stating the conditions about water availability and reliability are calculated for three future time periods following the two IPCC emission scenarios A2 and B1. These are used to quantify the future changes in water availability in the riparian countries of transboundary river basins.

The projected changes are not continuous over the three 30-yearly time periods between 2010 and 2100. However, generally the results show that the international river basins in the northern latitudes, in sub-Saharan Africa excluding the southern part, most basins in South America and in Central and South East Asia will experience increasing water availability while a decrease is projected for the international basins in Southern and South Eastern Europe, basins in the northern and southern parts of Africa and most basin in the Middle East. Mostly the changes among the countries of an international basin are comparable but there are also basins in which the projections for the riparian countries differ. Examples are the Nile basin, the basins in Southern Africa, the Tigris-Euphrates basin and the Orinoco basin.

The comparison of differences in water availability and reliability shows that the transboundary basins with the highest disparities among its riparian countries are predominantly situated in the transition zone from the Sahara to sub-Saharan Africa. Due to

climate change differences between the countries within a basin will increase in most basins. Exceptions are the basins in Europe, some basins in Central Asia and the Middle East as well as the basins in Southern Africa.
The results are based on naturalized model runs, which means that only the effects of climate change are included but no human impacts such as increasing water withdrawals or demographic trends are represented. These factors will also lead to changes in the water availability in transboundary basins and further investigations should be made in these areas to establish adequate management plans for international river basins.

**Keywords:**
International river basins, basin country polygon, water availability, climate change, emission scenarios, hydro-climatic variability, model ensemble, hydrological models, global circulation models

# Zusammenfassung

Veränderungen in der Wasserverfügbarkeit stellen eine der großen gesellschaftlichen Herausforderungen im 21. Jahrhundert dar, global gesehen aber auch in den 279 internationalen Flussgebieten. In Zukunft wird es durch den Klimawandel zu Veränderungen im hydrologischen Kreislauf kommen, die großen Einfluss auf die Wasserressourcen haben werden. Studien zum Klimawandel wurden oft global oder anhand von Fallstudien für ausgewählte Flussgebiete durchgeführt. Die Resultate basierten meinst auf den Simulationen eines hydrologischen Modelles.

In der vorliegenden Studie werden die durch den Klimawandel verursachten Veränderungen der hydroklimatischen Bedingungen innerhalb eines internationalen Flussgebietes mit Hilfe eines Modellensembles aus sechs hydrologischen Modellen und drei Klimamodellen berechnet. Das Hauptaugenmerk liegt dabei auf den hydroklimatischen Veränderungen der einzelnen Anrainerstaaten in einem Flussgebiet und den Unterschieden zwischen ihnen. Diese Unterschiede können zu Spannungen und Konflikten zwischen den Nachbarländern führen.

Verschiedene Indizes, durch die Aussagen über die Wasserverfügbarkeit und deren Variabilität getroffen werden können, werden für drei Zukunftszeiträume berechnet. Anhand dieser werden die durch den Klimawandel verursachten Veränderungen der Wasserverfügbarkeit in den einzelnen Anrainerstaaten der internationalen Flussgebiete quantifiziert.

Die prognostizierten Veränderungen sind über die drei 30-jährigen Zeitperioden zwischen 2010 und 2100 nicht in allen Anrainerstaaten der internationalen Flussgebiete kontinuierlich. Sie zeigen aber einen generellen Trend, der in den grenzüberschreitenden Flussgebieten der nördlichen Breiten und in Afrika südlich der Sahara mit Ausnahme der Gebiete südlich des Kongos sowie für die meisten internationalen Flüsse in Südamerika, Zentral- und Südostasien eine Zunahme des Wasserdargebots vorhersagt. Zum anderen werden die internationalen Flussgebiete in Süd- und Südosteuropa, in den nördlichen und südlichen Teilen Afrikas und die meisten Flussgebiete im Nahen Osten eine Abnahme in der Wasserverfügbarkeit erfahren. In den meisten internationalen

Flussgebieten ist die Veränderung der Wasserressourcen innerhalb der einzelnen Länder vergleichbar. In einigen Einzugsgebieten unterscheiden sich die vorhergesagten Änderungen für die einzelnen Länder jedoch deutlich. Beispiele sind der Nil, die internationale Flussgebiete im Süden Afrikas, das Tigris-Euphrat Einzugsgebiet und der Orinoco.
Der Vergleich der einzelnen Anrainerstaaten eines internationalen Flussgebietes in Bezug auf Wasserverfügbarkeit und Variabilität zeigt, dass die Gebiete mit den größten Ungleichheiten meist in Übergangebereichen verschiedener Klimazonen liegen. Auffallend viele liegen in der Sahelzone. Die Unterschiede hinsichtlich der Wasserverfügbarkeit zwischen den Ländern eines Einzugsgebietes werden in der Zukunft durch Klimaveränderung in den meisten internationalen Flussgebieten steigen. Ausnahmen bilden die grenzüberschreitenden Gebiete in Europa, Nordafrika, einige in Zentralasien und dem Nahen Osten sowie im Süden Afrikas.
Die Resultate der Studie basieren auf Simulationen, in denen der menschliche Einfluss auf die Wasserressourcen, wie zum Beispiel die vorhergesagte Zunahme der Wasserentnahme oder demographische Entwicklungen, vernachlässigt wurden. Diese Faktoren werden jedoch ebenfalls die Wasserverfügbarkeit in internationalen Flussgebieten beeinflussen. Diese sollten in weiteren Studien analysiert werden um weitreichende Kenntnisse zu erlangen, die für ein an den Klimawandel angepasstes Wassermanagement innerhalb eines internationalen Flussgebietes genutzt werden können.

# 1. Introduction

Water availability will be one of the major challenges for human society in the $21^{st}$ century. It is linked to the wellbeing and economic success of a region. The lack of water limits development in many areas of the world. The complexity of water resources pose challenging management problems. In international river basins the competition over this resource can lead to conflict or cooperation. Projected changes in the hydrological cycle due to climate change can increase the conflict potential especially in transboundary river basins where are large difference in the water availability among the riparian countries and high yearly variability.

## 1.1. International river basins

Water does not adhere to national and political borders. Worldwide there are 279 river basins counted with two or more riparian states (De Stefano et al., 2012). This corresponds with approximately half of the global land surface which is covered by international water resources (Wolf et al., 1999). Most of which are located in Europe (68 transboundary river basins), followed by Africa (64) and Asia (60). In North America lie 46 international river basins, in South America 38 (UN Water, 2013). About two-third of these are shared by two riparian countries. The other third is shared by more than two riparian states. The river with most bordering countries (18) is the Danube river basin in Central and Eastern Europe. A map of the international river basins of the world can be found in the back inside cover of the thesis B.1.
Transboundary river basins play an important role in the water supply for millions of people and in the political stability of countries. Competition over shared water resources has lead to conflict between riparian states, but also to cooperation. Studies about interactions between riparian countries are mostly case studies for selected river basins e.g. the Nile (Smith and AI-Rawahy, 1990; El-Fadel et al., 2003) and the Jordan river basin (Haddadin and Shamir, 2003).
The largest and first empirical study on conflict and cooperation in international river

basins was carried out by researchers of the Oregon State University (Wolf et al., 2003). They developed the Transboundary Freshwater Dispute Database (TFDD) in which all reported water-related events (cooperation and conflict) are collected. Wolf et al. (2003) identified basins at risks using this data about interactions between states bordering the same river. Most of them were cooperative events (1228) while 507 were defined as conflictive events and 96 as non-significant.
The changes in water availability projected by climate change scenarios may present serious management challenges and conflict potential to riparian states. Moreover, water scarcity due to rising water demand is projected to increase in many regions of the world (Alcamo et al., 2007). These factors will intensify security concerns within or among countries or within river basins. De Stefano et al. (2012) identified areas with high potential risk of future hydro-political tension by analyzing the institutional resilience to water variability in transboundary river basins combined with historic and projected variability of runoff.

## 1.2. Climate change scenarios

It is projected that climate change will lead to changes in the distribution of water resources and will intensify the hydrological cycle: increasing water vapor content, changing precipitation patterns as well as intensity and extremes, and changes in run-off and soil moisture (Bates et al., 2008).
Past events indicate significant trends. Precipitation increased in the eastern parts of Northern and Southern America, in Northern Europe and in Northern and Central Asia. In contrast, precipitation decreased in the Sahel, in the Mediterranean area, in Southern Africa and in parts of Southern Asia (Bates et al., 2008).
Projections about future changes due to climate changes are based on future green-house gas emission. They are a product of a very complex system determined by demographic and socio-economic factors and technological changes (Nakicenovic et al., 2000). So it is relatively uncertain how future climate will develop.
The Intergovernmental Panel on Climate Change (IPCC) developed four different storylines for long-term emission scenarios. Each storyline is representing different demographic, technical, social, economic and environmental developments.
In the following, only the two emission scenarios used in this study are described. Descriptions were found in the IPCC special report on emission scenarios (Nakicenovic et al., 2000):

The A2 storyline is describing a very heterogeneous world. The changes are based on regional economic growth. Main themes are self-sufficiency and to keep the local traditions and identities. The world population is steadily increasing. Economics developments are predominantly regionally orientated. Per capita economic growth and changes in technology are more geographically dependent and slower than in other emission scenarios. The predicted increase in temperature for this scenario is about 2.0 to 5.4 degrees Celsius by 2100.
The central elements of the B2 emission scenario are a high level of environmental and social consciousness combined with a global approach to a more sustainable development. It describes a convergent world with a population increase till 2050 and a decline thereafter. There will be rapid changes in the economy towards a service-orientated and information economy. At the same time the material intensity will decrease and clean and resource-efficient technologies will be introduced. The main emphasis is on global solutions towards economic, social and environmental sustainability, including improved social justice but without additionally climate initiatives. The predicted temperature increase ranges from 1.1 to 2.9 degrees Celsius by 2100.

Based on these scenarios a lot of research about climate change was done. Climate model simulations are highly uncertain and depending on the model which was used (Bates et al., 2008; Hagemann et al., 2013). However, projections for changes in precipitation for the 21st century are consistent for some parts of the world. Precipitation will increase in high latitudes and parts of the tropics but decrease in some subtropical and lower mid-latitudes. For annual average river runoff and water availability increase in high latitudes and in some wet tropical areas and decrease over some dry regions, the mid latitudes and in the dry tropics are projected (Bates et al., 2008). Chen et al. (2011) and Hagemann et al. (2013) show a trend suggesting future decrease in runoff in comparison to the present day conditions in different parts of the world: eastern part of Australia, southern part of United States and Africa, north eastern part of South America, Southern Europe, and large parts of the Middle East. Thus a significant reduction in available water resources will occur in many catchments in these regions. For considering the uncertainty in climate change often multiple global climate models were used. But in most of the studies just one or two global hydrological impact models (GHM) were applied (Gosling and Arnell, 2011; Milly et al., 2005; Doell et al., 2003). For example, Doell et al. (2003) used the WaterGap Global Hydrological Model WGHM, calculating water availability indicators. These are taking inter annual and

seasonal variability of runoff and discharge into account. Milly et al. (2005) studied the global pattern trends in streamflow and water availability using an ensemble of 12 global climate models. His findings correlate with the areas of decreasing runoff of the results from Chen et al. and Hagemann. He found increasing trends in runoff in eastern equatorial Africa and the high latitudes of North America and Eurasia. But (Haddeland et al., 2011) shows in the WaterMIP inter-comparison, in which different GHMs and land surface models are compared, that differences between hydrological models are the major source of uncertainty and suggests that not only multiple climate models but also multiple impact models should be used for climate impact studies. There are some first studies using multiple impact models (Chen et al., 2011; Hagemann et al., 2013). Chen et al. (2011) used multiple hydrological models to analyse the changes in the hydrological characteristics of twelve large continental river basins and to assess the uncertainty due to the choice of the global climate model and GHM. This study showed that uncertainties in the hydrological changes are larger due to the choice of the GHM than the choice of the climate model. Also the uncertainties based on the choice of the climate model/GHM model are larger for hydrological changes in the future than for the present condition in the control period.

Climate impact studies were carried out on a global level (Voeroesmarty et al., 2000; Alcamo et al., 2007; Chen et al., 2011; Hagemann et al., 2013) or on the level of river basins for example the Congo river basin (CSC, 2013) or for the Colorado river (Christensen et al., 2004). Voeroesmarty et al. (2000), for example, compared global projections of water availability using the water demand to availability ratio in 2025 relative to 1985. But there is no study which is concentrating on countries lying in the same international river basin.

## 1.3. Objectives

International river basins shared by two or more riparian states offer conflict potential. The conflict potential increases in river basins with large differences in the water availability between riparian countries and where the inter-annual availability of water resources is very variable. Climate change will lead to changes in the global and regional hydrological cycle. These will lead to changes in available water resources in world's international river basins.
In this study, changes in water resources in the riparian countries of international river

basins caused by climate change will be analysed and quantified for the 21st century. Model results of climat impact simulations following the two IPCC emission scenarios A2 and B1 are used as a multi-model ensemble. On the basis of the model ensemble, different indices are developed and calculated to quantify the inequality in available water resources within international river basins. The main focus is on changes over time within one river basin and the increasing or decreasing differences in available water resources among the riparian countries in one international river basins basin.
International river basins with a wide difference in these indices for the riparian states will be identified and analysed for the possible hydro-political conflict potential with help of data of cooperation in this basin.
Furthermore, a uncertainty analysis for the multi modelensemble rssults is carried out.

# 2. Data and Methods

## 2.1. Database and data editing

### 2.1.1. WATCH model data

The model data used in this work was created within the WATCH (WATer and global CHange) project funded by the European Union Sixth Framework Programme (Harding et al., 2011). It brought together the hydrological, water resources and climate communities to improve the knowledge of the terrestrial water cycle. Some important aims were the analysis, quantification and prediction of the components of the current and future global water cycle and related water resources states (Haddeland et al., 2011).
Within the project they developed a consistent set of climate data for use as input: one for the period 1901-2000 (Watch Forcing Data) and one for the future period 2001-2100 (Watch Driving data). These datasets were used to force different global hydrological models (Harding et al., 2011). These output data is the basis for this study.

Future climate projections were estimated by three coupled atmospheric-ocean General Circulation Model (GCM) according to concentrations of greenhouse gases of the IPCC emission scenarios A2 and B1 (Nakicenovic et al., 2000). The used GCMs belong to different model families and were selected by availability of climate model data necessary to force the Global Hydrological Model (GHM) ((Hagemann et al., 2013)):

- ECHAM5/MPIOM (Max Planck Institute of Meteorology)
- IPSL (Institute Pierre Simon Laplace)
- CNRM (Centre National de Recherches Meteorologiques, Meteo-France)

The GCMs have a different number of vertical levels and a different horizontal resolution (Chen et al., 2011). Thus, the GCM data had to be interpolated to a horizontal

resolution of 0.5° ((Hagemann et al., 2013)).
GCM output data also contains a number of significant systematical errors. These data connot be used directly in GHMs and had to be corrected. A daily defined statistical bias correction factor based on the fitted histogram equalization function was applied to the daily land precipitation and mean, minimum and maximum daily land temperature ((Piani et al., 2010),(Hagemann et al., 2013)). The correction factor was derived from observed and simulated data for the period 1960 – 1999 and then applied to the control period 1960 – 1999 and the two scenario (A2, B1) periods 2000 – 2100 of the GCM simulations (Chen et al., 2011).
The bias corrected data was used to force eight different GHMs for the two climate change scenarios A2 (8 GHMs) and B1 (6 GHMs excluding Jules and H08):

- GWAVA (Centre for Ecology and Hydrology (CEH))
- H08r (National Institute for Environmental Studies (NIES))
- JULES (UK Met Office (UKMO))
- LPJmL (Potsdam Institute for Climate Impact Research (PIK))
- MacPDM (University of Reading (NERC))
- MPI-HM (Max-Planck Institute for Meterology (MPI-M))
- VIC (Norwegian Water Resources and Energy Directorate (NVE))
- WaterGAP (University of Kassel (CESR))

These models were used to calculate land surface hydrology and water fluxes at a resolution of 0.5° x 0.5° (about 50 km x 50 km, depending on latitude and longitude). The models differ in their evaporation, snow and runoff schemes, their time steps and in meteorological forcing variables (Tab.2.1). A detailed description about each model is given in Chen et al. (2011).

For the A2 emission scenario simulations for all 8 GHMs were forced by the output of 3 GCMs, while for the B1 emission scenario simulations for only 6 GHMs (excluding h08r and jules) were forced by 3 GHMs. This resulted in 24 and 18 different time series for each hydrological variable, respectively.
The whole global modeling chain developed and used within the WATCH project is

Table 2.1.: Participating models in the WATCH project including their main characteristics, adapted from Haddeland et al. (2011)

| Model | Time step | Meteorological forcing variables [1] | Energy balance | $ET_{pot}$ scheme [2] | Runoff scheme | Snow scheme |
|---|---|---|---|---|---|---|
| GWAVA | Daily | P, T, W, Q, $LW_n$, SW, SP | No | Penman-Monteith | Saturation excess/ beta function [4] | Degree day |
| H08r | Daily | R, S, T, W, Q, LW, SW, SP | Yes | Bulk formula [3] | Saturation excess/ beta function | Energy balance |
| JULES | 1h | R, S, T, W, Q, LW, SW, SP | Yes | Penman-Monteith | Infiltration excess / Darcy | Degree day |
| LPJmL | Daily | P, T, $LW_n$, SW | No | Penman-Monteith | Saturation excess | Degree day |
| Mac-PDM | daily | P, T, W, Q, $LW_n$, SW | No | Penman-Monteith | Saturation excess/ beta function | Degree day |
| MPI-HM | Daily | P, T | No | Thornthwaite | Saturation excess/ beta function | Degree day |
| Vic | Daily/ 3h | P, $T_{max}$, $T_{min}$, W, Q, LW, SW, SP | Snow season | Penman-Monteith | Saturation excess/ beta function | Energy balance |
| WaterGAP | Daily | P, T, $LW_n$, SW | No | Priestley-Taylor | beta function | Degree day |

[1] R: rainfall rate, S: snowfall rate, P: precipitation (rain or snow distinguished in the model), T: air temperature, $T_{max}$: maximum daily air temperature, $T_{min}$: minimum daily air temperature, W: wind speed, Q : specific humidity, LW: longwave radiation flux (downward), $LW_n$: longwave radiation flux (net), SW: shortwave radiation flux (downward), SP: surface pressure.

[2] $ET_{pot}$: potential evapotranspiration.

[3] Bulk formula: bulk transfer coefficients are used when calculating the turbulent heat fluxes.

[4] Beta function: runoff is a nonlinear function of soil moisture.

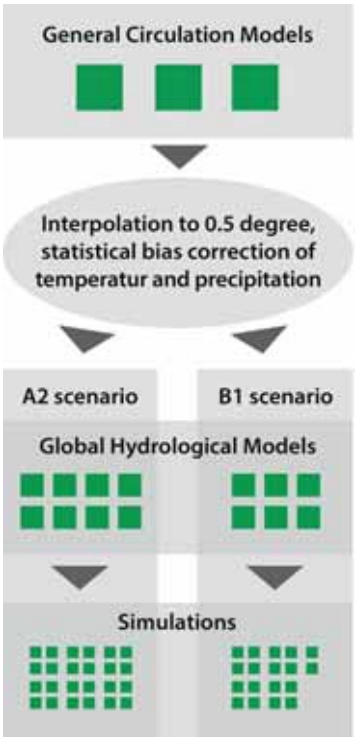


Figure 2.1.: Modelling chain in the WATCH project, adapted of Hagemann et al. (2013).

shown in Figure 2.1. As this work focuses on changes in future available water resources, only the model output data for the main components of the terrestrial water balance are used:

- Precipitation
- Evapotranspiration
- Runoff: Total runoff is the sum of surface and subsurface runoff

Simulation data for the different GCM/GHM model combinations and scenarios (A2 and B1) are available in a monthly resolution for the control period (1960 - 2000) and the future period (2000 - 2100) in NETCDF format. All the GHM runs were natural runs which means that direct anthropogenic influences on the hydrological cycle such as water withdrawals and reservoirs are not considered (Harding et al., 2011).
To work with the output data of all GCM and GHM models the time series of each GHM/GCM model combination had to be brought into the same format. The format corrections were made in the Python programming language using Climate Data Operators (CDO) additionally. The CDO software is a collection of more than 400 operators for standard processing of climate model output data including tools for simple statistical and arithmetic processes, for data selection and sub sampling (Schulzweida et al.,

2012). Besides, due to physically plausibility negative runoff values in different models (GWAVA, LPJmL, and WaterGAP) were set to 0. The amendments made are listed in table 2.2.

Table 2.2.: Data adjustments

| Model output data of | Adjustment | Method |
|---|---|---|
| h08r | reversing latitudes | cdo invertlat |
| macpdm, watergap | renaming cncm3 to cnrm in filename | Python script |
| lpjml, macpdm | set time axis from 1 to 0 | cdo settaxis |
| vic subsurfacerunoff data of IPSL GCM, jules | changing unit from mm/month to mm/s | cdo divc |
| gwava | renaming dimension Time to time and setting time axis to 0 | replace file structure with the structure of lpjml files cdo replace |
| all | setting negative values to 0 | cdo setrtomiss |

### 2.1.2. Geodata of international river basins

The geo data of international river basins made within the Basins at Risk project (Yoffe et al., 2004) are used in this study. ArcGis shape files for the geometry of international river basins and for the Basin Country Polygon (BCP) are available. A BCP is defined as the spatial portion of a basin that is overlapped by a single country(De Stefano et al., 2010). This means every country within one river basin has its own polygon which will be considered in the study. Figure 2.2 shows an example of the BCP of South Africa in the Orange river basin.

The combination of 276 international river basins and 148 riparian states result in 747 BCPs. They cover about 62 million km² of the earth's surface with a total of approximately 2.75 billion people living in this area (De Stefano et al., 2012).

### 2.1.3. Population data

Estimates of human population for the years 1990 and 2000 are available to the public via NASA Socioeconomic data and application center (SEDAC). They provide population data estimates as people per square km in ArcGis raster format. The data set is constructed from using national and sub-national administrative units transforming them to a global grid of a resolution of 2.5 arc (CIESIN/FAO/CIAT, 2005). For this study the data is used in a 0.5° resolution according to the WATCH model output


Figure 2.2.: Example of a basin country polygon.

data. The mean value of these two points of time per grid cell is calculated and used as population data for the time period 1971 to 2000.
For the future period of the years 2010 to 2100 gridded population data of the Greenhouse Gas Initiative (GGI) (Program of the International Institute for Applied Systems Analysis (IIASA)) is used. Documentation about the downscaling methods is found in Gruebler et al. (2007): The population data is based on emission scenarios A2 and B1 of the IPCC Special Report on Emission Scenarios (SRES). These are the high population increase scenario (A2) and low population increase scenario (B1). The B1 population data follows original quantitative scenario characteristics at the level of four world regions (OECD, REF, ASIA and ALM (further information about countries including which world region on http://www.iiasa.ac.at/webapps/ggi/GgiDb/dsd?Action=htmlpagepage=about)). The A2 scenario, however, has been modified. Instead of 15 billion people projected in the SRES scenario, it reaches only 12 billion people by 2100. Scenario indicators were calculated at a spatial resolution of 0.5° x 0.5° following qualitative scenarios of the SRES. The downscaling exercises are scenario dependent and were processed in two steps. First with a combination of decomposition and optimizing the world population scenario results were disaggregated to a level of 185 countries. Afterwards these national results were disaggregated to individual sub-national grid cells taking into account urbanization projections. The data is available for each century in ArcInfo Grid format as population density (people per square km).

For this study the mean value of population for the time periods 2011- 2040, 2041-2070 and 2071 – 2100 is calculated and used. Further, a mean population density value is determined for each BCP using ArcGis zonal statistics.
Although it is not recommended to use the data as individual grid cell informations as projected scenario values (Greenhouse Gas Initiative (GGI) Program of the International Institute for Applied Systems Analysis (IIASA), 2007), it is used in this study. The scenario data has been developed to describe possible spatial patterns. These spatial patterns are also in the grid cell values. By taking the mean value for each BCP, and most BCPs have a size bigger than one grid cell, the data used is already averaged. Also, this study only wants to show possible future trends and not exact values. For this purpose the available population data can be used. le population data can be used.

## 2.2. Methods

Changes in hydrological characteristics and available water resources within international river basins due to climate change are analysed and quantified based on the simulation results of the WATCH project. Different indices are calculated as multi-model ensembles result from the hydrological variables evapotranspiration (potential and actual), precipitation and runoff. For better comparison only the model results of the GHMs which are available for the A2 and B1 emission scenarios are used. This means the ensemble for both emission scenario contains data of 18 different datasets (3 GCMs, 6 GHMs, excluding h08r and jules). The simulation period 1970 - 2100 is subdivided into four time periods each with a length of 30 years. The period of the years 1970 - 2000 functions as a control period for the present status. The three future time periods are 2011 - 2040, 2041 - 2070 and 2071 - 2100. In the following it is referred to them with the center year of the time period: 2025, 2055 and 2085.
The indices are calculated time aggregated on the basis of yearly mean values. The following steps were applied to the results of the hydrological variables evapotranspiration (total and potential), precipitation and runoff for both emission scenarios. For each model combination (GCM-GHM) (all together 18) the yearly mean value for each grid point is calculated using the Python programming language and CDOs. These values were used for further aggregation to thirty yearly mean values [mm/a] for the four different time periods. In addition, the inter-annual standard deviation from the mean was calculated. These new produced NetCDF files are processed with Esri Arc-

Gis. After conversion to raster format, the spatial resolution is refined to a 0.1° x 0.1° raster size. This refinement is made to capture also BCPs with an area smaller than a 0.5 x 0.5° grid cell and can be made because for further analysis only the mean value of the grid points within a BCP are wanted. This mean value of each BCP is calculated using the GIS module Zonal Statistics with the shapefile of the BCP polygons. In this process the mean value of all grid points situated within one polygon/BCP is calculated. In addition, for precipitation and runoff the standard deviation of the grid point values within one BCP is calculated with the same module. This reflects the spatial variation of the value.

### 2.2.1. Indices

Based on these time aggregated values, different indices for each BCP and each timestep are calculated. They were selected to express the water availability as well as the inter-annual variability in the BCPs. Annual mean values of evapotranspiration and precipitation are also considered. These play a significant role in the water balance. Moreover, precipitation is the key climate variable with a major importance for ecosystems and social systems.

Index of Aridity

The Aridity Index (AI) is a measure of the general water balance (Unesco, 1979). The mean values of the different time periods of potential evapotranspiration ($ET_{pot}$) and precipitation (P) are used to calculate the AI (Middleton et al., 1992):

$$AI = \frac{P}{ET_{pot}} \tag{2.1}$$

The index is used to classify hyperarid (AI $< 0.03$), arid (AI = 0.03 - 0.2), semiarid (AI = 0.2 - 0.5), dry subhumid (AI = 0.5 - 0.65) and humid (AI $> 0.65$) regions (Middleton et al., 1992). It is calculated for the model ensemble without gwava because no precipitation data is available for this model and without vic because of missing potential evapotranspiration results.

Spatial and inter-annual variation of precipitation and runoff

The yearly and spatial variability for each grid cell individually is derived from yearly mean values for the hydrological variables runoff and precipitation. The variability of the variables is described by their standard deviation, which is the fluctuation around the mean value (Chen et al., 2011). For better comparison of BCP of different areas and climatic conditions the normalized standard deviation also named coefficient of variation (CV)

$$CV = \frac{\sigma}{\mu} \tag{2.2}$$

where:

| | |
|---|---|
| $\sigma$ | Standard deviation |
| $\mu$ | Mean |

is used to reflect the inter-annual variability of these parameters. The inter-annual variability is the key indicator of the yearly reliability of water availability (Stahl, 2007).

Changes in available water resources

To assess BCPs which are vulnerable to projected climate change in respect of water availability the changes in available water resources are determined. Therefore, available water resources are defined as the total mean annual runoff of the 30 yearly time period minus the mean environmental requirements (EWR) (Chen et al., 2011). The total EWR contain the ecologically relevant low-flow and high-flow components (Smakhtin et al., 2004). Assuming that EWR for a specific catchment, in this study for a BCP, can be roughly approximated by 30% of catchment runoff (Smakhtin et al., 2004) and that these requirements will not significantly change in future, the projected change in available water resource (AWR) can be calculated as

$$\triangle AWR = \frac{(Q_{Scen} - EWR) - (Q_{Con} - EWR)}{(Q_{Con} - EWR)} = \frac{(Q_{Scen} - Q_{Con})}{(Q_{Con} - EWR)} \tag{2.3}$$

where:

| | |
|---|---|
| $\triangle AWR$ | Available water resource [mm/y] |
| $QScen$ | mean annual runoff of scenario period [mm/y] |
| $QCon$ | mean annual runoff of control period [mm/y] |
| $EWR$ | Environmental requirements = 0.3 $/cdot$ $Q_{Con}$ |

Water availabilty per capita

To analyse the significance of low water availability in a BCP, the number of people living within this area has to be taken into account. For this indicator the assumption is made that all the water which will be used by people is coming from the total runoff of the basin. Other fresh water resources like groundwater or man-made sources of freshwater like desalination plants are not taken into account. The water availability per capita is calculated as a mean value per km$^2$ for each BCP.

$$Qcap = \frac{Q}{Cap} \tag{2.4}$$

where:

| | |
|---|---|
| $Qcap$ | Available water resource per capita [m$^3$/y cap] |
| $Q$ | mean annual runoff of time period [m$^3$/y] |
| $Q_{Con}$ | People per km$^2$ |

This indicator is also known as Falkenmark indicator or water stress index and is defined as the fraction of total runoff for human use (**?**)Falkenmark1989). It is widely used because it is easy to apply and understand. **?**Falkenmark1989) set a threshold of 1700m$^3$ water resource per capita per year calculated by estimations of water requirements in domestic, agricultural, industrial and energy sectors, as well as the needs of the environment. Countries with water availability per capita per year under this threshold are set to experience water stress. Countries with values below 1000m$^3$ and 500m$^3$ per capita per year experience water scarcity and absolute water scarcity, respectively. In this study the Falkenmark indicator is applied to the BCPs. However, it has a lot of disadvantages. This indicator does not take into account the availability of the water resource because of the existing infrastructure. Also variations in demand among countries due to culture, lifestyle, climate, etc. are not considered (Rijsberman, 2006). Nevertheless this indicator is used because of the availability of the data.

Hydro-climatic vulnerability index

To bring together the indices stating the water availability situation of a BCP due to its hydro-climatic conditions, a hydro-climatic vulnerability index (hcVI) is applied. Generally, hydro-climatic vulnerability of a region is related to water availability and scarcity as well as to the variability of the water resources. Thus, the choice of indices

using for the composition of the index was made for the Aridity Index (for water availability), the available water per person (for water stress), the spatial variability of precipitation and the inter-annual variability of runoff.
Hence, the hcVI can be expressed as:

$$hcVI = f(P_{WS}, P_{WA}, P_{V_s}, P_{V_t}) \tag{2.5}$$

where:

| | |
|---|---|
| $P_{WS}$ | Parameter for water stress |
| $P_{WA}$ | Parameter for water availability |
| $P_{V_s}$ | Parameter for spatial variability |
| $P_{V_t}$ | Parameter for interannual variability |

All four parameters have the same weight and the value of the hcVI ranges from 0 to 1. '1' indicates the most vulnerable situation according to water availability caused by hydro-climatic factors.

The Aridity Index is a measure of the general water balance and so includes statements about water availability. In areas classified as dry the water availability is lower than in humid areas. Areas with an AI greater than 0.65 are classified as humid (Middleton et al., 1992). Thus, the threshold for the water availability parameter is set to AI = 1. Regions with AI greater 1 should have sufficient water availability.

$$\begin{cases} P_{WA} = 0 & \text{if} \quad AI < 1 \\ P_{WA} = 1 - AI & \text{if} \quad AI < 1 \end{cases} \tag{2.6}$$

The water scarcity parameter is expressed by water which is available per capita and year. It is a measure if a BCP is under water stress or scarcity conditions. The water scarcity parameter can be expressed by comparison of the minimum requirements of water availability per capita (1700 $m^3$/y cap) with the per capita water availability in a BCP:

$$\begin{cases} P_{WS} = 0 & \text{if} \quad Q_{cap} > 1700 \\ P_{WS} = \frac{1700 - Q_{cap}}{1700} & \text{if} \quad Q_{cap} < 1700 \end{cases} \tag{2.7}$$

Another pressure to water availability of a region due to hydro-climatic factors is the variation of water resources. For the spatial variation parameter precipitation,

for the inter-annual variability runoff is taken into account. It is expressed by the coefficient of variation. For the inter-annual variability of runoff the threshold for the most vulnerable situation is set to CV = 0.75 following De Stefano et al. (2012).

$$\begin{cases} P_{V_t} = \frac{Q_{cvt}}{0.75} & \text{if} \quad Q_{cvt} < 0.75 \\ P_{V_t} = 1 & \text{if} \quad Q_{cvt} > 0.75 \end{cases} \tag{2.8}$$

It is assumed that spatial variability has a smaller impact on the interaction between riparian countries in a river basins but it will intensify the impact of inter-annual variability in a BCP. The threshold for a vulnerable situation due to spatial variation of precipitation is set to 0.3.

$$\begin{cases} P_{V_s} = \frac{P_{cvs}}{0.3} & \text{if} \quad P_{cvs} < 0.3 \\ P_{V_s} = 1 & \text{if} \quad P_{cvs} > 0.3 \end{cases} \tag{2.9}$$

### 2.2.2. Future changes

To analyse future changes due to climate change the different indices are compared to the control period 1971-2000. Changes of the three future time periods are calculated relative to the control period.

### 2.2.3. Differences among riparian countries within one international river basin in the indices

In a further step the values of the indices for the riparian countries within one river basin are compared. This comparison is applied to four indices introduced before: precipitation, aridity index, available water resources and inter-annual variability.
River basins with big differences in the values of the different indices are identified. Therefore, the range of the index values of the BCPs within one international river basin is calculated. Making the international river basins comparable to each other, it is normalized with the index mean value of the river basin in the control period:

$$R_{norm} = \frac{I_{Range}}{I_{\mu}} = \frac{I_{max} - I_{min}}{I_{\mu}} \tag{2.10}$$

where:

| | |
|---|---|
| $R_{norm}$ | Normalized Range within basin |
| $I_{Range}$ | Range within a basin |
| $I_{max}$ | Mean |
| $I_{min}$ | Mean |
| $I_{\mu}$ | Mean value of the basin |

Analysing river basins with big differences for disadvantaged (values below the mean value for the basin) and advantaged (value above the mean) BCPs the ratio of the index value relative to the mean value for the basin is calculated. Only BCPs which have an area above 3% of the total basin area are considered.

### 2.2.4. Uncertainties due to the model choice

Another part of this study is the evaluation of the uncertainty in the predicted changes due to the model choice. The uncertainty is approximated by the spread of the model results regarding the choice of GCM or GHM (Hagemann et al., 2013).
This uncertainty analysis is realized for hydrological variables evapotranspiration and AWR and the future time period 2085. Precipitation is not used because it is a forcing variable for the models and the other calculated indices depend on evapotranspiration and AWR.
For the analysis, the changes of evapotranspiration and AWR relative to the control period are not calculated with the model ensemble used before. Instead the changes are calculated as an ensemble mean for each GCM (3) and GHM (6). With these mean values of changes regarding the choice of the GCM or GHM the spread between the models is calculated. To express relative differences between the models, the normalized standard deviation is used (Hagemann et al., 2013).
This means, the mean value of change of the six GHMs is calculated for each GCM. From ensemble mean of each GCM the normalized standard deviation is calculated which reflects the spread with regard to the choice of GCM. To determine the spread due to the choice of GHM the standard deviation is calculated by the GCM ensemble mean values.
The normalized standard deviations due to the model choice are compared for each BCP.

# 3. Results

## 3.1. Conditions in the control period 1971 - 2000

The multi model ensemble results from 6 GHMs and 3 GCMs were used to calculate the mean annual values for the three main components of the terrestrial water balance in the control period (1971- 2000). The annual mean values of precipitation, evapotraspiration and runoff are illustrated in figure 3.1 as BCP based maps. These mean values for each BCP are the reference values for the calculation of future changes.

As expected, the values of the mentioned components in international river basins and its BCPs, individually, are congruent to the world's spatial distribution of these. Nevertheless, it is visible that the annual mean values can differ between countries within one basin.

The spatial distribution of annual mean values of precipitation, evapotranspiration and runoff in the river basins and BCPs, individually, is, as expected, is alike with the worlds distribution of these components. The mean value of precipitation is shown in Figure **??**a. The highest precipitation values are found in the river basins and BCPs of Central America, Northern South America, in the BCPs of Gabon and Equatorial Guinea, the Congo basin and in South East Asia. In these regions annual mean precipitation is between 3000 mm/y and 4600 mm/y. River basins with the lowest annual mean precipitation are located in Northern Africa, the Middle East and Central Asia. Analysing the mean precipitation values within one international river basin, one can see that there basins with high differences in these. Significant disparities can be found especially in basins with bordering countries located in different climate zones. To emphasize are the basins situated at the border of the Sahel zone with Sub Saharan Africa as well as the river basins Niger and Nile, the basins in South East Asia with China as riparian country and also the La Plata basin in South America. For the annual mean evapotranspiration (Fig. 3.1b) and runoff (Fig. 3.1c) the same patterns can be observed.

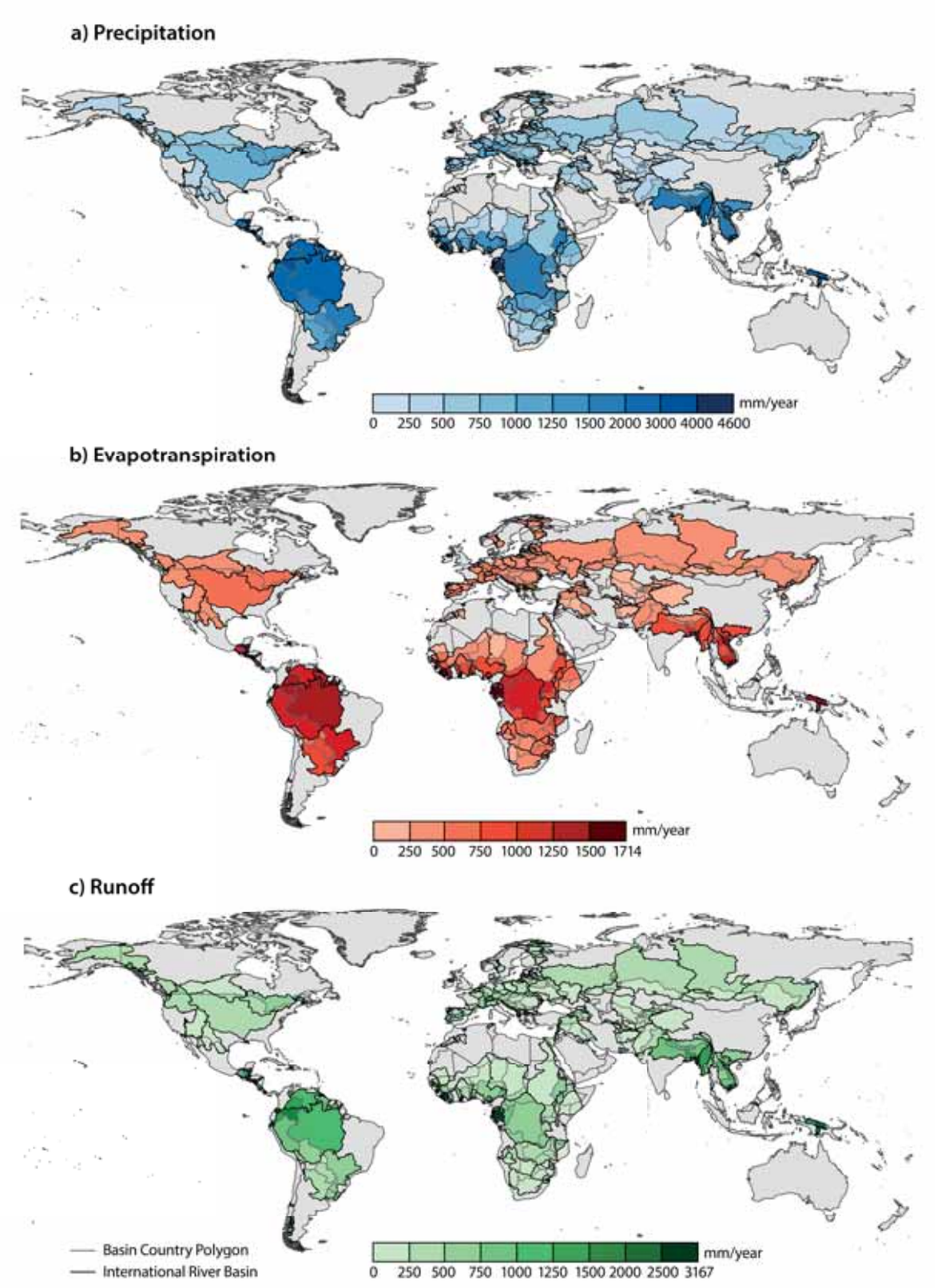


Figure 3.1.: Annual mean values of precipitation (a), evapotranspiration (b) and runoff (c) for the BCPs of international river basins in the control period.

## 3.2. Future changes

### 3.2.1. Changes in annual mean values of evapotranspiration and precipitation

The changes of the annual mean value of the before mentioned variables were calculated for the three future time periods relative to the control period. Generally, the smallest projected changes are observed for evapotranspiration, while the largest changes are projected for runoff.

Changes of evapotranspiration for the three future time periods are presented as BCP based maps in figure 3.2 for the A2 scenario and in figure 3.3 for the B1 emission scenario. In the first time period 2025 and scenario A2, evapotranspiration is projected to increase relative to the control period in most of world's international river basins. Highest rises are projected for river basins in Alaska, Northern Europe, Southern Africa, Western sub-Saharan Africa, East Africa and the river basins in Central Asia (including the countries Pakistan, Western India, Western China Kazakhstan, Kyrgyzstan, Tajikistan, Turkmenistan, Afghanistan and Iran). In these regions, evapotranspiration will increase approximately 10% to 20% is projected. Other regions with increasing evapotranspiration are Central and Eastern Europe, the Middle East, Northern Asia and Southern America. In South East Asia is nearly no change observed. For most of those regions these trends also apply to the projections of the B1 scenario but the predicted increases are smaller. For example, the expected changes in the river basins in Central Asia are about 5% to 10%. In Northern Asia the changes will be smaller than 5% compared to the A2 scenario with 5% to 10%.

Furthermore, in some regions is a negative trend for one scenario predicted while concurrently the other scenario shows a positive trend. For example, in the international basins situated in the belt between the Congo and South Africa (including the countries Namibia, Botswana, Northern South Africa, Zimbabwe, Mozambique, Zambia and Angola), there will be an increase of 5% for the A2 scenario but a decrease of 5% in the B1 scenario. Other regions with an expected increase in scenario A2 and a decrease in scenario B1 are Central America, some BCPs in Western sub-Saharan Africa, the Nile BCP of Egypt and the Jordan BCP of Syria as well as BCPs in South Eastern Europe. Projections of decreasing annual mean evapotranspiration for the river basins in Spain, Portugal, Morocco and Algeria as well as the BCPs in Northern Mexico are congruent for both scenarios but higher for the B1 scenario compared to A2.

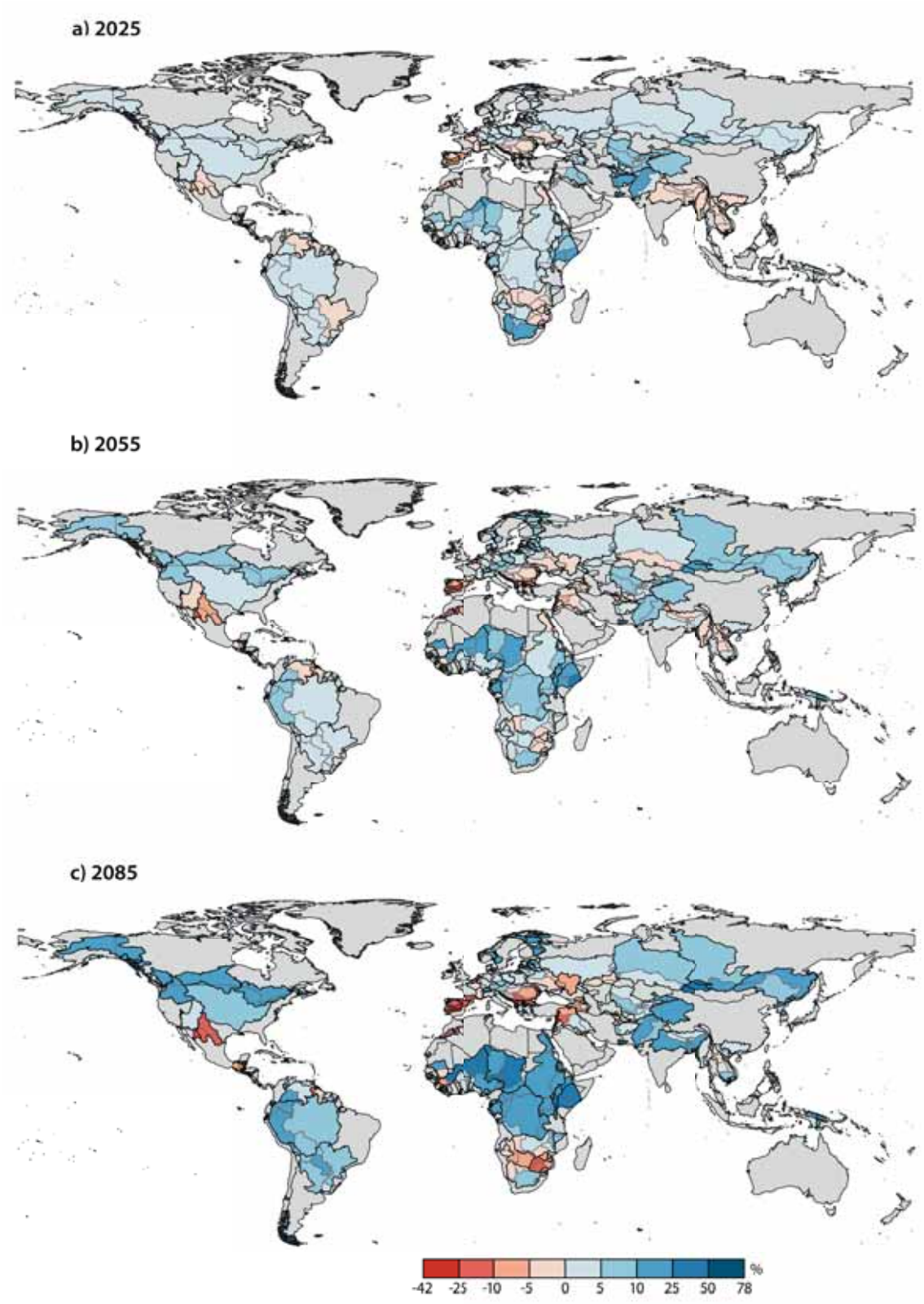


Figure 3.2.: Changes in evapotranspiration in world's international river basin for three future time periods for the A2 emission scenario.

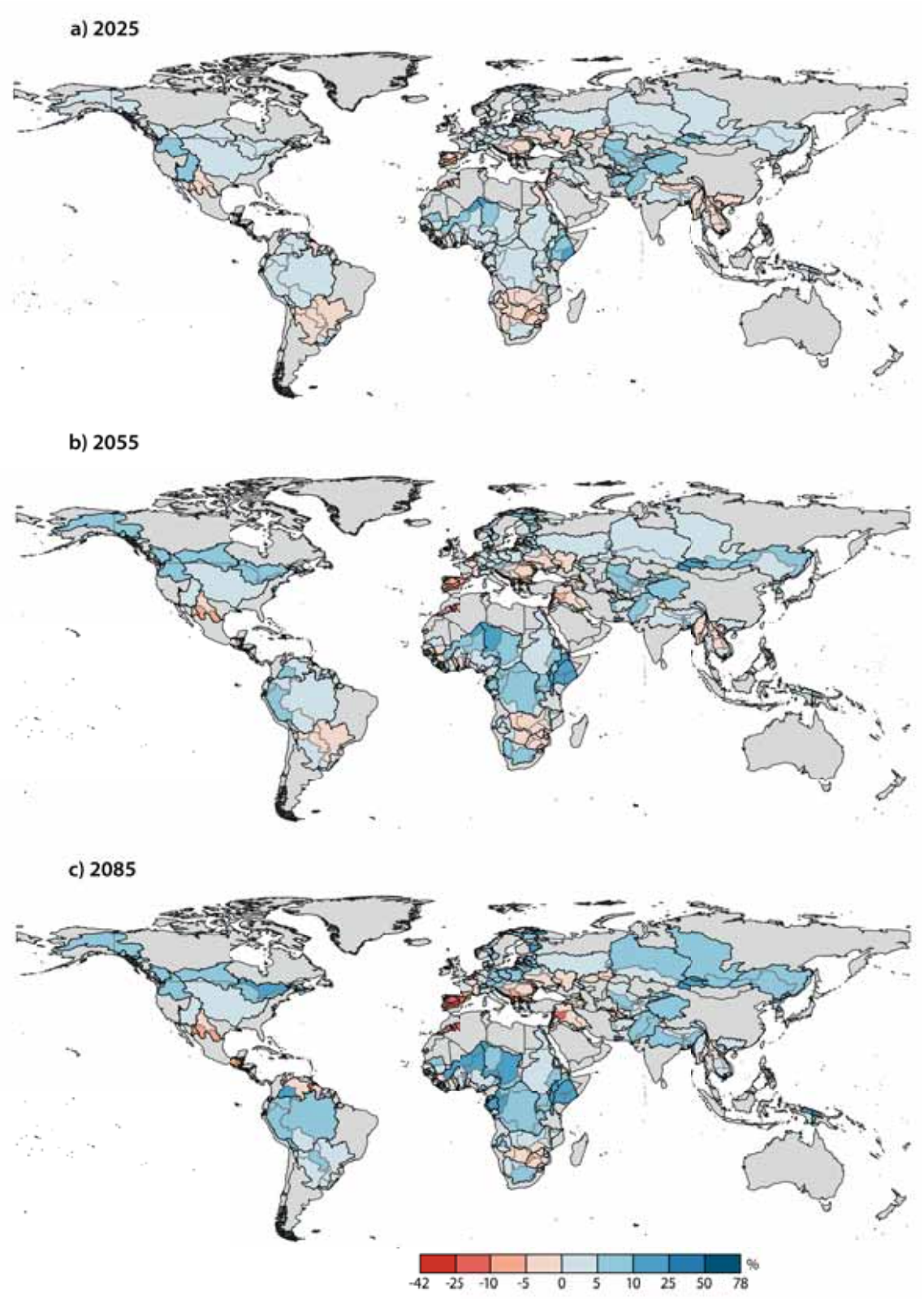


Figure 3.3.: Changes in evapotranspiration in world's international river basin for three future time periods for the B1 emission scenario.

In the next time period 2055, the development will continue and the increasing or decreasing trend will intensify in most BCPs. To mention are the river basins in the Northern latitudes, Central Africa, northern parts of South America (A2 scenario) and South East Asia (A2 scenario) for an intensified increase. In Southern and South Eastern Europe, the projected decrease of evapotranspiration continues and declines about 10% are expected.
In the Middle East plus Egypt different developments are predicted for this time period. In the A2 scenario, the Nile BCP of Egypt, the BCPs in the Jordan Basin and the BCPs in Syria will change from small increase to decrease in evapotranspiration. In other countries of the Middle East, including Georgia, Azerbaijan and Armenia, decreases will be about 5% instead of 5% - 10% in the time period before. For the B1 scenario, there will be a decrease of evapotranspiration. This trend will continue in the far future time period 2085. Also for the A2 scenario a change to decreasing evapotranspiration is expected for the region except for the Tigris-Euphrates BCPs of Iran and Iraq. In these BCPs will be still a small increase relative to the control period. Other areas with projected decrease in evapotranspiration are the international river basins in Southern and South Eastern Europe, in Central America, the BCPs of Northern Mexico and the BCPs situated in the belt between South Africa and the Congo.
Overall, it can be said that predicted changes are higher for the A2 scenario than for the B1 scenario. Also there are regions in which the direction of change is different between the two emission scenarios. To highlight are the La Plata basin and the river basins in the belt between the Congo and South Africa.

The changes in precipitation are visualized in figure 3.4 (A2) and in figure 3.5 (B1). Continuous decrease in precipitation for all three time periods are projected for the international river basins in the following areas: Southern, Central and Eastern Europe, the Jordan basin, Central America with Haiti and the Dominican Republic, in the Amacuro and Essequibo basin (Northern South America), the Orinoco BCP of Venezuela, the La Plata BCP in Brazil and some of the river basins shared by Chile and Argentina. In all other BCPs in Southern America an increase in precipitation is projected. Also in international river basins in sub-Saharan Africa excluding the Western part (Liberia, Cote D'Ivoire, Sierra Leone, Guinea, part of Mali, Senegal, and Mauretania) and the belt between the Congo and South Africa precipitation will increase. The river basins in the Northern latitudes show an increase of precipitation in future. This applies to both scenarios but overall the changes for the A2 projection are higher.

There are also regions for which no continuous trend is simulated. This applies to international river basins located in South East Asia, the Middle East and the belt between the Congo and South Africa. In these basins the prognoses differ most between both emission scenarios. As examples the Ganges-Brahmaputra-Meghna and the Limpopo river basin are mentioned.
In emission scenario B1, the projections in the Ganges-Brahmaputra-Meghna basin show only very slight decreases for the BCPs China (-1.8%) and Myanmar (-0.8%) in precipitation of about 5% and 6%, respectively, in the future time period 2025. Additionally, in the riparian countries Bangladesh and Bhutan precipitation decrease is expected while the projections show increases in the BCPs of India and Nepal. In the far future period 2085, on the contrary, an increase of precipitation in all riparian countries is predicted for the A2 scenario and for the B1 scenario excluding the BCP of China. In Bangladesh and Bhutan increases are projected but they differ among the scenarios. The projections show for Bangladesh 12% (A2) and 9% (B1) increase and for Bhutan 16% and 6%.

In the Limpopo basin, a slight increase is predicted for the riparian countries Botswana, Mozambique and South Africa in scenario A2 while a slight decrease is predicted for Zimbabwe in the near futurue period. In the B1 scenario, decreases of about 0 to 5% are expected for all BCPs in the basin. In the medium future time period 2055, the predictions will change and an increase in precipitation about 0 to 5% is expected for all BCPs. Furthermore, in the A2 scenario, precipitation will increase except for South Africa where it will decrease slightly. In the far future period 2085, opposite developments are predicted for both scenarios. While the projections show nearly no change for South Africa and Zimbabwe an increase in Botswana and Mozambique is predicted in the B1 scenario. In contrast, the multi model results show a decrease greater than 8% for all riparian countries in the A2 scenario.
Generally it can be said, that the river basins and BCPs situated in Central America, Southern, Central and South East Europe and in Northern Africa are expected to experience a decrease of precipitation in the future while the basins located in other parts of the world will experience precipitation increase. The multimodel results also show that the changes are higher in the A2 than in the B1 emission scenario.

Since changes in runoff show similar results to the changes of available water resources (AWR), only those of AWR are described in the following. The changes in runoff show the same patterns, but with smaller changes.

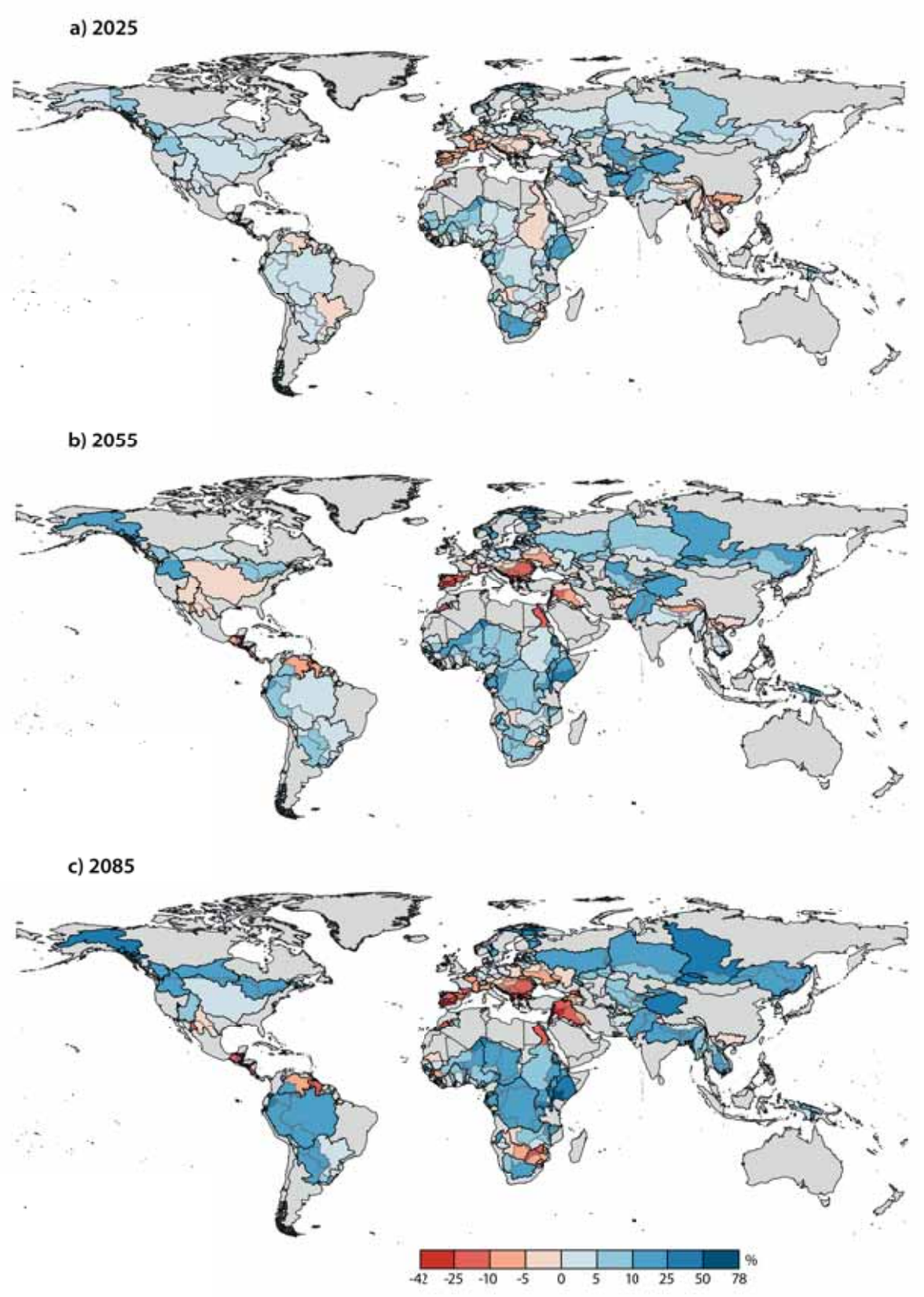


Figure 3.4.: Changes in precipitation in world's international river basin in three future time periods in the A2 emission scenario.

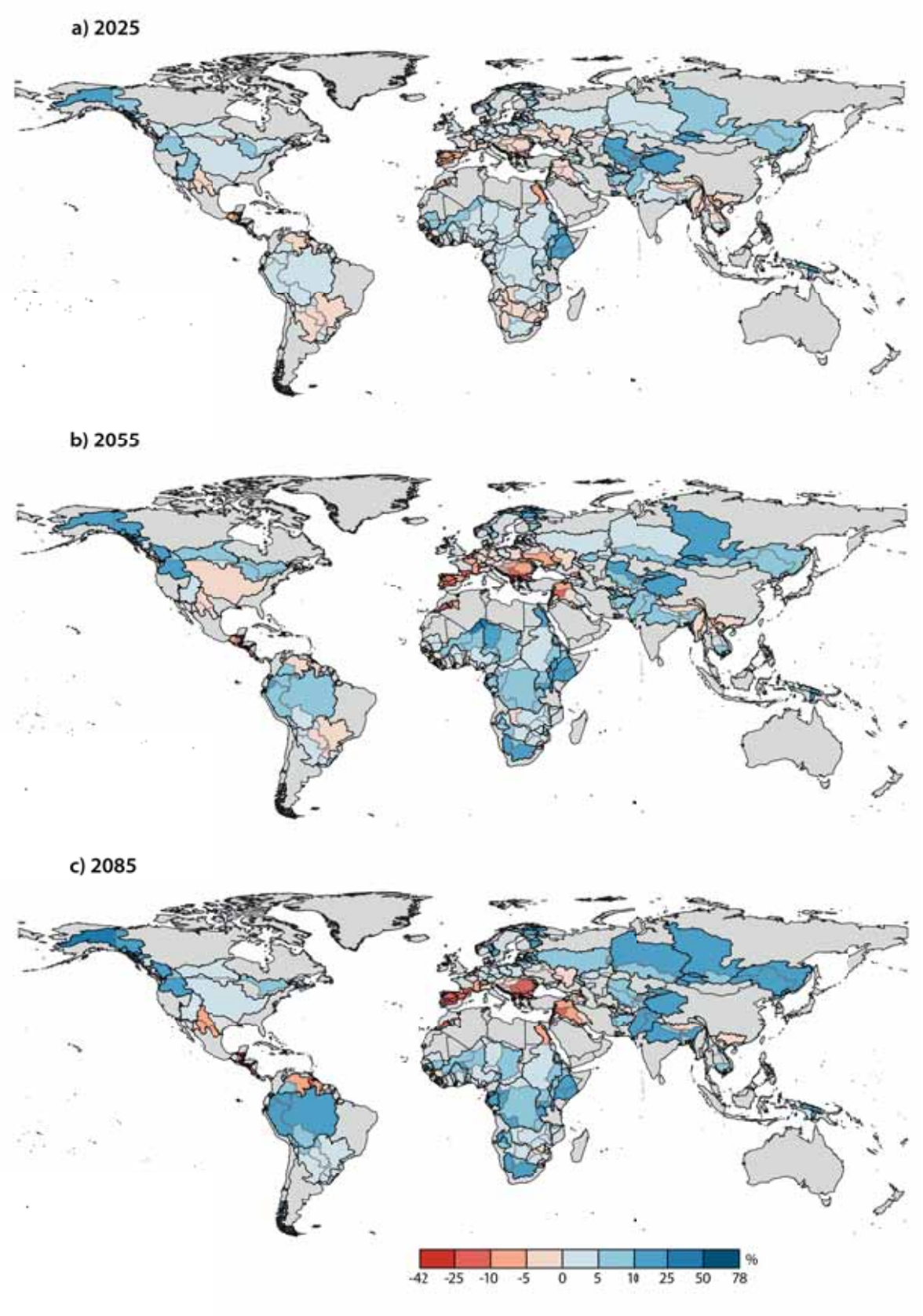


Figure 3.5.: Changes in precipitation in world's international river basin in three future time periods in the B1 emission scenario.

### 3.2.2. Changes in the aridity index

The Aridity Index was calculated to analyse future changes in the water balance of the BCPs. In the control period, 17.5% of the BCPs worldwide are hyper-arid to semi-arid with an AI $< 0.5$, around 6% are dry sub humid ($0.5 <$ AI $< 0.65$) and the rest is classified as humid. In the future time periods, the developments of the AI for the two emission scenarios differ (Tab. 3.1).

Table 3.1.: Number of BCPs of each classification in the Aridity Index in the three time periods and both scenarios

| AI | Control | A2 | | | B1 | | |
|---|---|---|---|---|---|---|---|
| | | 2011 - 2040 | 2041 - 2070 | 2071 - 2100 | 2011 - 2040 | 2041 - 2070 | 2071 - 2100 |
| $< 0.03$ | 3 | 3 | 4 | 4 | 3 | 3 | 3 |
| 0.03 - 0.2 | 27 | 27 | 34 | 40 | 26 | 29 | 33 |
| 0.2 - 0.5 | 96 | 108 | 112 | 154 | 104 | 99 | 103 |
| 0.5 - 0.65 | 42 | 55 | 80 | 70 | 46 | 70 | 82 |
| $> 0.65$ | 549 | 524 | 487 | 449 | 538 | 516 | 496 |

In scenario B1, the number of BCPs being classified as arid (AI $< 0.5$) is projected to stay quite the same (18.5%, 18.2% and 19.3% for the three future time periods). In scenario A2, their number is similar in the near and medium future time period (2025: 19.2% and 2055: 20.9%) but in time period 2085 the projections show 10% more BCPs with an AI smaller 0.5. Noteworthy is that, the number of BCPs classified as hyper arid is remaining the same for the B1 scenario. The three BCPs with an AI smaller than 0.03 are located in Northern Africa: the two riparian states of the Atui River Mauritania and Western Sahara as well as the part in Egypt of the Nile river basin. In the A2 scenario the AI of the BCP Libya in the Lake Chad basin will decline from 0.039 (control) to 0.033 (2025) and to 0.026 in the far future.

In Figure 3.6 the AI for the BCPs is mapped for the control period and the far future time period 2085 for both emission scenarios. Areas with high projected changes can be identified: Southern Europe, South- Eastern Europe, parts of the Middle East and parts of Central Asia. The projected changes differ between the two scenarios. In Spain and Portugal, most BCPs will change from a humid AI classification to a semiarid in the A2 emission scenario. In the B1 scenario only the BCPs in the southern part of the countries show the same development. The Northern BCPs will change to dry sub humid AIs in this scenario. For South Eastern Europe similar developments are projected. The BCPs bordering the Aegean Sea as well as Moldova will change from a

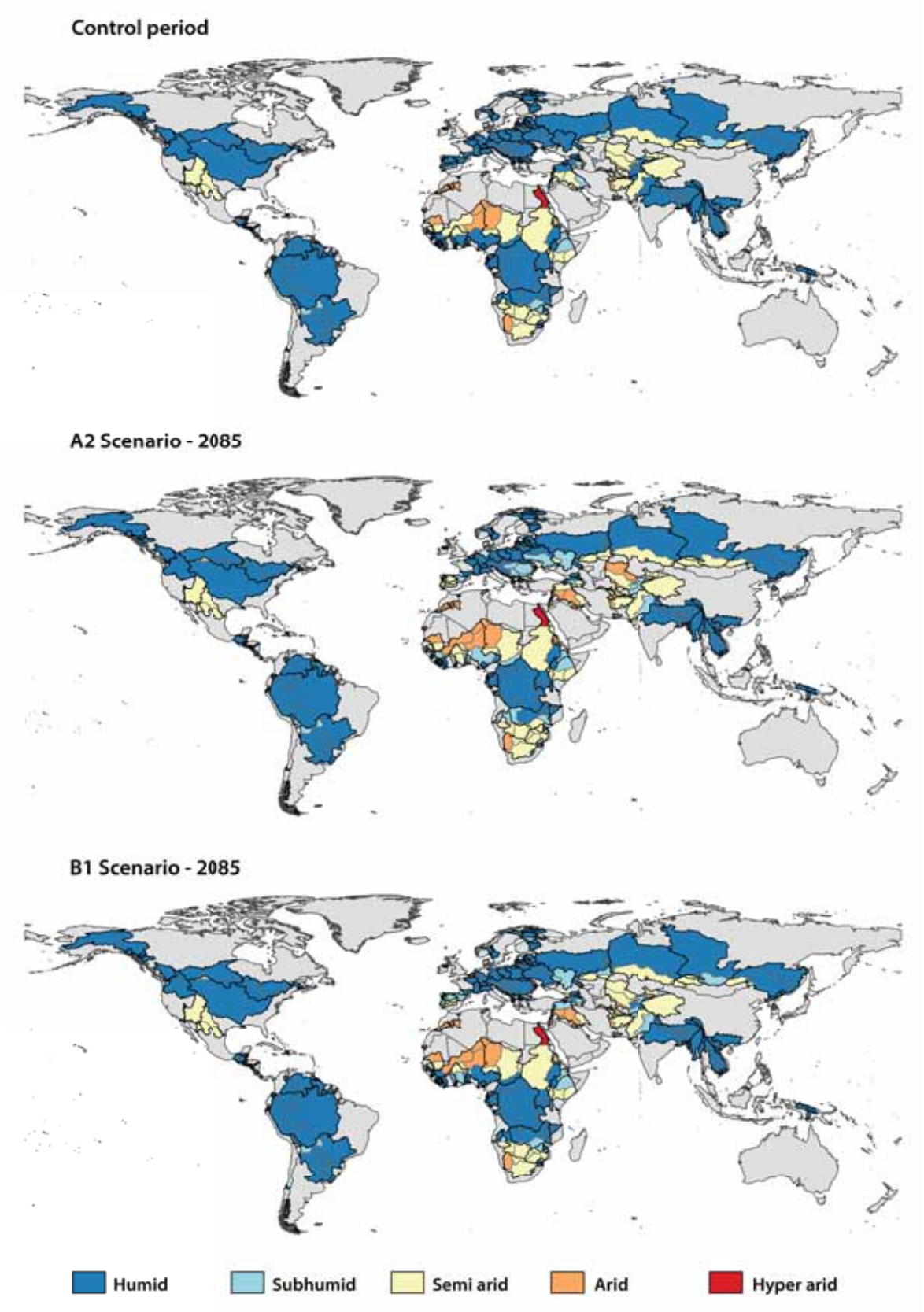


Figure 3.6.: Aridity index of the BCPs in the control period, the A2 scenario 2085 and the B1 sceanrio 2085.

humid water balance to an arid in the A2 scenario while they change to sub dry humid in the B2 scenario. The BCPs of Romania, Bulgaria, Hungary, Serbia, Ukraine will decrease to an AI in the sub humid classification (A2 scenario) while they will stay humid in the B1 scenario. This leads to a wide range in the AI of the riparian countries of the Danube basin because in the western part of it, the AI will be still in the range of a humid water balance.

In South Western Africa, projected changes compared among both scenarios are also quite high. In the control period BCPs in this region bordering the ocean are all classified as humid. In the A2 scenario only the BCPs of Liberia, Sierra Leone and Guinea and very small BCPs at the coast of Ghana and Nigeria are projected to stay humid. BCPs of Ivory Coast and Ghana will change to arid and BCPs of Burkina Faso, Togo and Nigeria will change to dry sub humid. In the B1 scenario only changes for the larger BCPs of Ivory Coast and Ghana are projected. They will have an AI classified as dry sub humid in 2085; all other BCPs will stay humid. For the Middle East and Central Asia, both scenarios project that semi arid BCPs will become arid and humid and dry sub-humid BCPs will change to semi-arid (especially in the Jordan basin, Tigris-Euphrates basin, the eastern BCPs or the Aral Sea basin and the BCPs of Afghanistan and India in the Indus basin). Changes in the range of a humid AI are not reflected by Figure 3.6. Because it only classifies the values of the AI for each time step the actual change is not listed. The highest decreases over time show basins in Chile and Argentina. In the Chico basin, for example, the AI decreases from 4.1 in the control period to 2.4 in the future (2085) in Argentina and from 3.3 to 1.8 in Chile. Also in Central and Eastern Europe these changes are projected. Most international river basins in this region have high AI values, so also when the changes are pretty high they still are classified as humid. These changes correspond with the decrease of runoff and AWR in Europe. There are also areas in which the AI will increase. This is projected for the Northern latitudes (Alaska, Canada and Northern Europe with Russia) and Western South America.

### 3.2.3. Changes in available water resources

To identify BCPs being vulnerable to climate change with respect to water availability, changes in available water resources (AWR) relative to the control period were calculated for both scenarios and the three future time periods from the multi model ensemble. BCP based maps which visualize the changes in AWR were created on basis of these calculations for scenario A2 (Fig. 3.7) and B1 (Fig. 3.8). Areas where AWR is expected to increase, can be identified for all future time periods. In both scenarios, the river basins in Sub-Saharan Africa expect more available water resources in the future. Highest changes are expected in the basins of the Sahel zone and the Juba-Shibeli basin in Eastern Africa.

In the Juba-Shibeli basin the AWR are expected to increase about 70% (A2 and B1) in 2025 and 150% (A2) and 55% (B1) in 2085. For the Volta basin a continuous increase of AWR is predicted from 25% (A2) and 16% (B1) in 2025 to 58% and 38% in 2085. It should be noted that the high percentage values result also from the low AWR in these basins. In the control period, the AWR in the Volta basin are 213 mm/y and in the Juba-Shibeli 103 mm/y.

For the Nile basin an increase of 28% (A2) and 7% (B1) is projected by the multi model ensemble but its BCPs, individually, differ in their development. Even though there will be a strong increase of AWR in the BCPs of Kenya (73%) and Eritrea (47%), the AWR in the BCP Egypt is decreasing. This applies for the future time period 2085 and the A2 emission scenario. But for the other future periods the differences between the riparian countries are similar with a lower rate of increase. For the different time periods there is a continuous increase predicted, while for the B1 scenario the greatest change in most BCPs is expected in the time period 2055.

The predictions for the international river basins situated in the belt between the Congo and South Africa differ from the increasing trend in Sub-Saharan Africa. The projections do not show a continuous trend and there are big differences of expected changes between both scenarios. In the Okavango basin, for example, AWR will increase in the first two future time periods (2025 and 2055) and are expected to decrease in the time period 2085 in the A2 scenario. The same applies to the Buzi basin and the Limpopo basin except for the BCP of Mozambique. For the B1 scenario this trend only applies to the BCPs of the Okavango excluding Angola where a decrease is expected for the first two future time periods and an increase for the last time period.

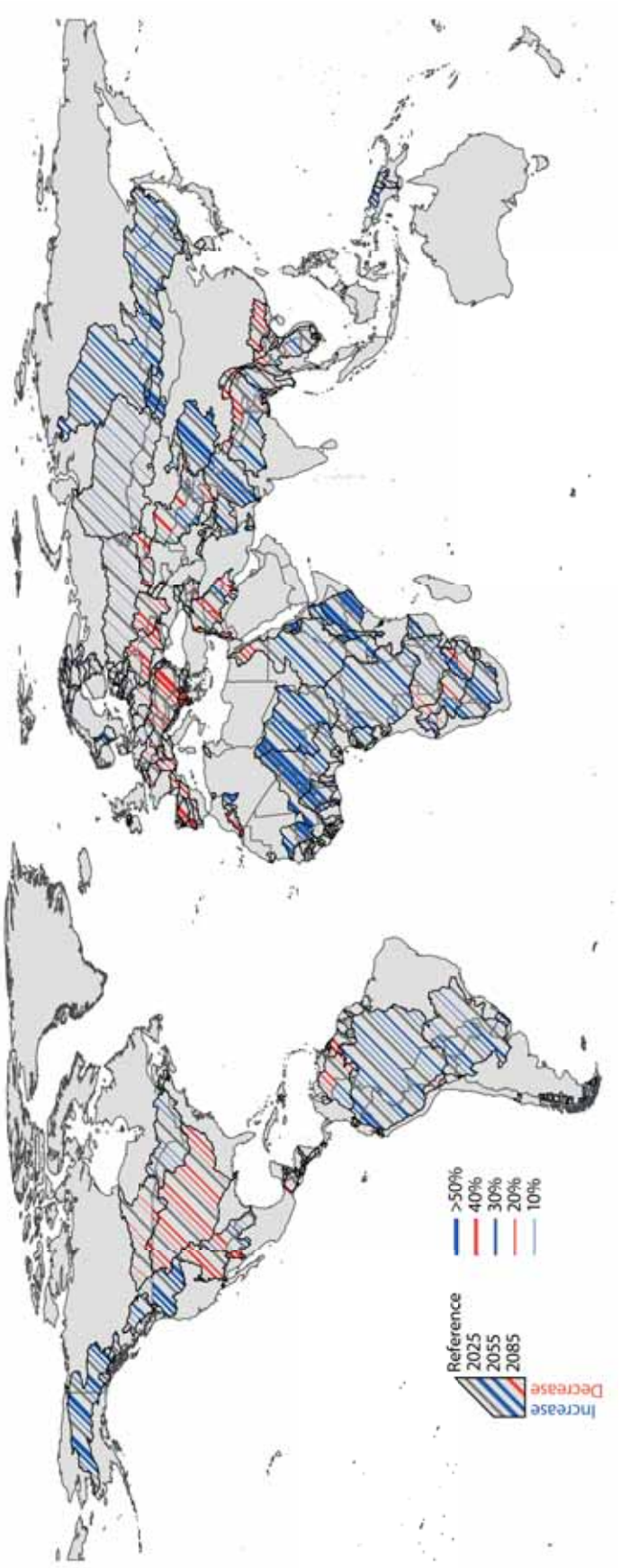


Figure 3.7.: Changes in available water resources in world's international river basin in three future time periods in emission scenario A2.

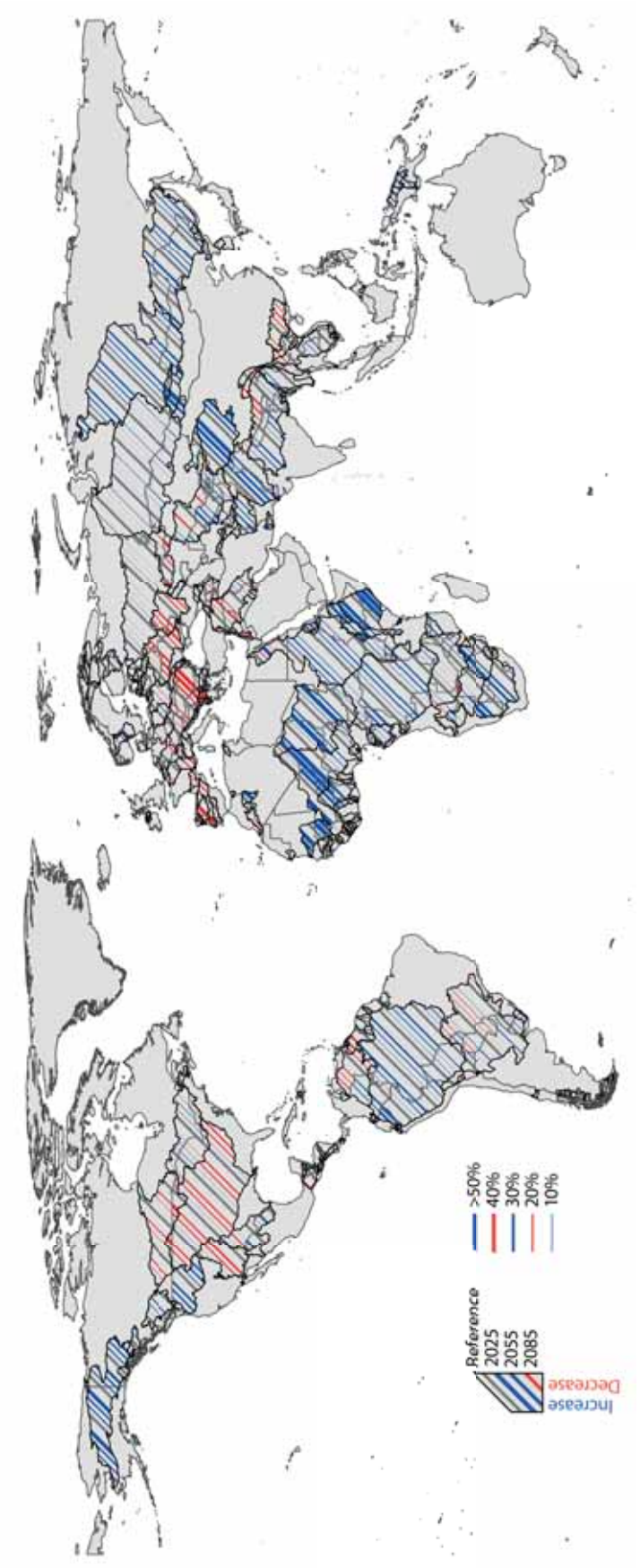


Figure 3.8.: Changes in available water resources in world's international river basin in three future time periods in emission scenario B1.

In the Buzi basin, there are nearly no changes projected for the time periods 2025 and 2085 (about 1% increase and decrease, respectively), but for the time period of 2055 an increase of 20% for both riparian countries is projected.

The absolute changes in AWR of the BCPs in the Limpopo basin are illustrated in figure 3.9.

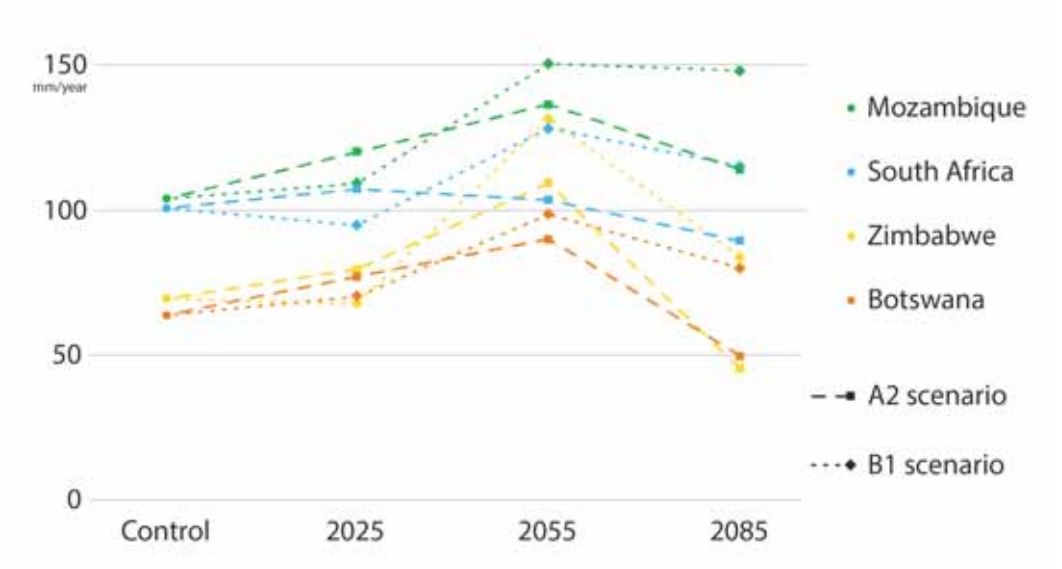


Figure 3.9.: Changes in available water resources in the riparian countries of the Limpopo river.

The BCPs can be subdivided into two groups: Mozambique and South Africa with annual mean AWR of about 100 mm/y and Zimbabwe and Botswana with AWR of about 65 mm/y. The projected changes differ among the BCPs and the emission scenarios.

In the near future time period 2025 and scenario A2, in all BCPs a decrease is expected. In the B1 scenario, the BCPs of South Africa and Zimbabwe will experience a slight decrease while AWR will increase in Botswana and Mozambique. For both scenarios and the future time period 2055, a strong rise in AWR is predicted in all BCPs excluding South Africa in scenario A2. Noteworthy is the expected high rise in Zimbabwe from 68 mm/y to 130 mm/y, which exceeds AWR in South Africa. In the future time period after it, AWR will decline again. The most decline is projected for Zimbabwe (both scenarios) followed by Botswana (A2) and Mozambique (A2). In South Africa (both scenarios) and Botswana (B1) only slight decreases a detected relative to the time period before. In the B1 scenario, AWR of Mozambique will be nearly the same as in 2055.

When taking only the changes of the far future relative to the control period into ac-

count, an increase of AWR is expected for all riparian countries in scenario B1 and the BCP of Mozambique in scenario A2 while South Africa and with more significance Botswana and Zimbabwe will experience a decrease in AWR.
In the Zambezi basin will be big differences in the future changes between the countries within the basin. In Zambia, the projections of scenario A2 show a slight increase of about 5% for all time periods, in comparison scenario B1 predicts a slight increase for the first time period but a slight decrease for the other time periods. In both scenarios, a decrease is projected in the BCPs of Angola, Botswana and with the highest strongest in the time period 2055 with about 10% to 15%. In the other riparian countries (Mozambique, Malawi, Tanzania, Zambia and Zimbabwe) AWR will increase with major changes in scenario A2.
International river basins with predicted increases in AWR are: Tarim basin, Indus basin except of the BCP of China and the river basins situated in Alaska, Scandinavia, Great Britain and Ireland, North Eastern Asia, Malaysia, Indonesia, Papua New Guinea and the basins in most parts of Southern America. Exceptions are La Plata BCP of Brazil and Paraguay, where a decrease about 5% to 8% is predicted in the time periods 2025 and 2055 (only B1 scenario), the Cancoso, Valdivia, Puelo, Comau and Palena basins shared between Chile and Argentina, and the river basins and BCPs located in Venezuela, Guyana and Suriname. In these basins, AWR will decrease about 5% to 10% in the first two time periods and about 20% in 2085.
In the international river basins in Southern, Central and Eastern Europe both scenarios predict a decrease in AWR. Overall, it can be said that the changes have the same trend for both scenarios but the decrease in AWR will be higher in the A2 scenario. The decrease in Central Europe is lower than in Southern and Eastern Europe. The international river basins Maritsa, Nestos, Lake Prespa, Struma and Vardar (all shared by bordering countries of the Aegean Sea) have the highest predicted decrease with an average of 20% in 2025, 40% in 2055 and 60% in 2085. The AWR in the river basins shared by Portugal, Spain and France indicate a decrease in AWR of about 40 – 50% in 2085. Predictions for the rivers in Central Europe, for example the river basins Rhine, Elbe, Rhone and Po show a decrease between 10% and 20% for the different time periods.
In the Middle East a decrease of AWR is expected for most transboundary river basins and BCPs. Especially for the river basins with parts in Lebanon, Syria, Jordan, Israel and Turkey the predictions show significant decreases. The river basins Asi, An Nahr Al Kabir, Nahr El Kebir, Wadi Al Izziyah and Jordan will experience an average de-

cline of AWR of about 10% (A2) and 5% (B1) in the near future (2025), 35% (both scenarios) in the time period 2055 and 70% (A2) and 45% (B1) in the far future. These values are similar to the ones in the Sahel zone. Due to very small amounts of AWR in these regions major relative changes arise. For example, in the Asi river basin the available water resources in the control period are 165 mm/y in Lebanon, 221 mm/y in Syria and 312 mm/y in Turkey. These values decrease to 100 mm/y, 42 mm/y and 64 mm/y, respectivly, in the future time period 2085 for the A2 scenario.
Future changes in AWR in the Tigris-Euphrates basins are displayed in figure 3.10.

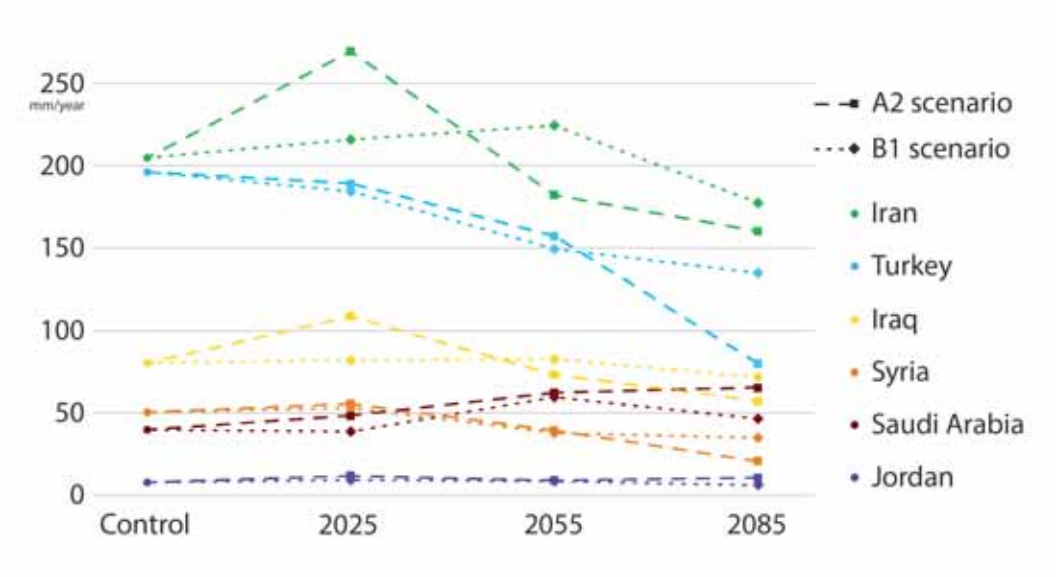


Figure 3.10.: Changes in available water resources in the riparian countries in the Tigris-Euphrates river basin.

Compared to the other BCPs, the riparian countries Iran and Turkey can be identified as AWR rich of about 200 mm/y. In these two BCPs, the most decreases in AWR are expected in the far future time period relative to the control period. Especially in the BCP of Turkey, where AWR will fall below 150 mm/y in emission scenario B1 and below 100 mm/y in scenario A2. Decreases in AWR are also projected inthe BCPs of Iraq and Syria in future. However, changes from one future time period to the next differ. In the near future and scenario A2, the BCP of Iran and Iraq will experience high increases and the BCP of Syria a slight increase while in Turkey the predictions show a slight decrease. In the B1 scenario, changes show the same direction but will be smaller. In the next future time step, in these BCPs a decrease of AWR is projected except for the Iran and Iraq in scenario B1. Projections show decreases for all BCPs in both scenarios in the far future time period.

The changes in the riparian countries Jordan and Saudi Arabia differ from the other four. The BCP with the lowest share of area in the basin and the lowest AWR (8 mm/y) is Jordan, where AWR will remain more or less the same in all time periods. In Saudi Arabia, AWR will slightly increase in future.
In the Northern American basins Mississippi, Nelson, Colorado and Rio Grande BCP of the USA, the emission scenarios predict a decreasing trend of AWR. In average, the changes will be about -10% in 2025 and -30% in 2085.
In Central American basins both emission scenarios show strong decreases in AWR in future. Especially the river basins shared by Haiti and the Dominican Republic show a continuous decrease from approximately 20% in 2025 to 60 - 70% in 2085. Also on the mainland a significant decrease is projected with approximately 15 to 30 % in the far future period 2085.
In South East Asian international river basins, a decrease in AWR is projected in the time period 2025. Exceptions are the Ganges BCPs of Nepal and India with a slight increase (2% and 4%). The B1 scenario predicts changes that are similar but additional BCPs will experience slight increases in AWR: Bangladesh and Bhutan in the Ganges basin, India in the Irrawaddy basin as well as Cambodia in the Mekong basin. During the time period 2055, AWR will decrease in the Northern BCPs of South East Asia while the more Southern BCPs will have an increase. A significant increase in AWR is expected about 10 to 25% depending on the emission scenario for whole Southern South East Asias in the far future time period 2085.

### 3.2.4. Changes in water reliability

As an index for the reliability of water resources the temporal (inter-annual) and spatial variability within a BCP was calculated for the hydrological variables runoff and precipitation. Figure 3.11 illustrates the inter-annual variability of precipitation (a) and runoff (b) for the control period. High inter-annual variability ($> 0.75$) is found in the international river basins of Northern and Southern Africa as well as the Juba-Shibeli basin in Eastern Africa, the Indus basin, the Helmand basin and the basins shared by Iran and Pakistan. The index shows the same spatial patterns for runoff and precipitation but the values differ. The values calculated for runoff are higher than those for precipitation. For example, the highest value for inter-annual variability for precipitation is 0.74 in the Nile BCP of Egypt while it is 1.04 for runoff. There's the

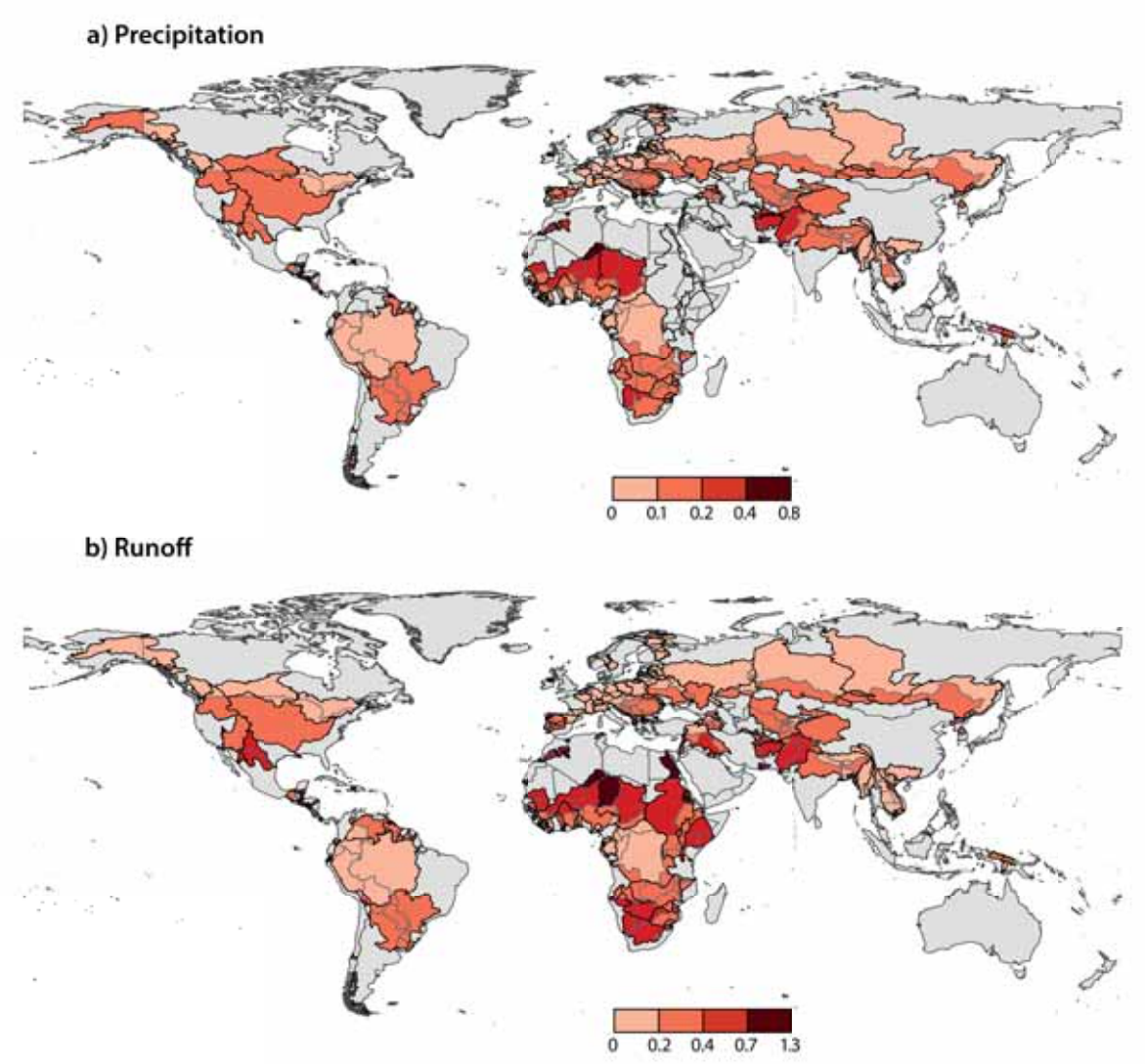


Figure 3.11.: Inter annual variability of precipitation (a) and runoff (b)for the contol period.

assumption that through intensification by the hydrological cycle the values for run-off are higher than for precipitation. On this basis, in the following, only changes in inter-annual variability of runoff will be analysed.

The predicted changes of inter-annual variability of runoff for the near future period 2025 based on BCP are mapped in figure 3.12 for both emission scenarios.
In the A2 scenarios no significant changes are expected in the international river basins on the American continent, both South and North, with the exception of the BCPs in Peru, the Colorado BCP of Mexico and the Pedernales basin shared by Haiti and the Dominican Republic. Also in the Northern latitudes of Europe and Asia the variability will stay quite the same as now. Increase of temporal variability is predicted for the

river basins in Southern Europe, South East Asia, Northern Africa and some BCPs in Southern Africa like the BCPs of Zimbabwe and Namibia in the Zambesi basin, the Kunene and Etosha basin as well as the Sabi basin. In the BCPs of Algeria the highest changes about 0.3 to 0.4 are expected. Also in the Baraka basin shared by Eritrea and Sudan increases in inter-annual variability of about 0.35 are predicted. In these areas the changes are rather severe because the inter-annual variability is already in the control period higher than 0.65. The most decreases ($> 0.2$) are projected in the Niger BCP of Algeria and the Jodan BCP of Saudi Arabia. Decreases are also expected in the Helmand basin in Central Asia and in some BCPs in Africa. Examples are the BCPs of Benin, the BCPs of Mali and Burkina Faso in the Niger basin, of the Lake Natron basin, the Nile BCPs of Tanzania and Kenya and the BCPs of Namibia and Botswana in the Orange basin.

In the B1 scenario the changes are similar. The river basins in Southern Europe and Northern Africa also expect an increase of the inter-annual variability of runoff. Nevertheless, the increase will be higher than in the A2 scenario. The predicted increase for the BCPs of Algeria is about 0.4 to 0.53.

Differences between the scenarios are in the BCPs of Iraq and Syria in the Euphrates-Tigris basin in some BCPs of Southern Africa like the Orange BCP of Namibia and the BCPs of Zimbabwe of the Limpopo and Sabi basin as well as in the BCPs of Northern Central America. In these BCPs an increase is predicted for the B1 scenario and a decrease for the A2 scenario. The BCPs of Niger and Chad in the Lake Chad basin, the BCP of Egypt in the Nile basin and the Rio Grande River basin in Northern America show the opposite.

In the far future period 2085 (Fig. 3.13) the regions with decreases of inter–annual variability of runoff are similar for the both scenarios. Decreases are projected for the Juba-Shibeli basin, the Southern BCPs of the Nile basin, the BCPs of Mali and Burkina Faso in the Niger basin as well as the BCP of Burkina Faso in the Volta basin, the Pu-Lun-T'o BCP of China and the Har Us Nur BCP of Mongolia. More areas in which the temporal variability will increase are projected for the A2 scenario. In Europe, the increase is not only limited to the river basins in Southern Europe as it is in the B1 scenario, it will also reach parts of Central Europe like the Po BCP of Italy or the Northern BCPs of the Danube basin like Austria, Czech Republic and Slovakia. Also in Southern East Europe the BCPs of countries bordering the Aegean Sea increases are projected. Other river basins are situated in the Middle East and Central Asia. For example, in the Euphrates-Tigris basin an increase in all BCPs is predicted for

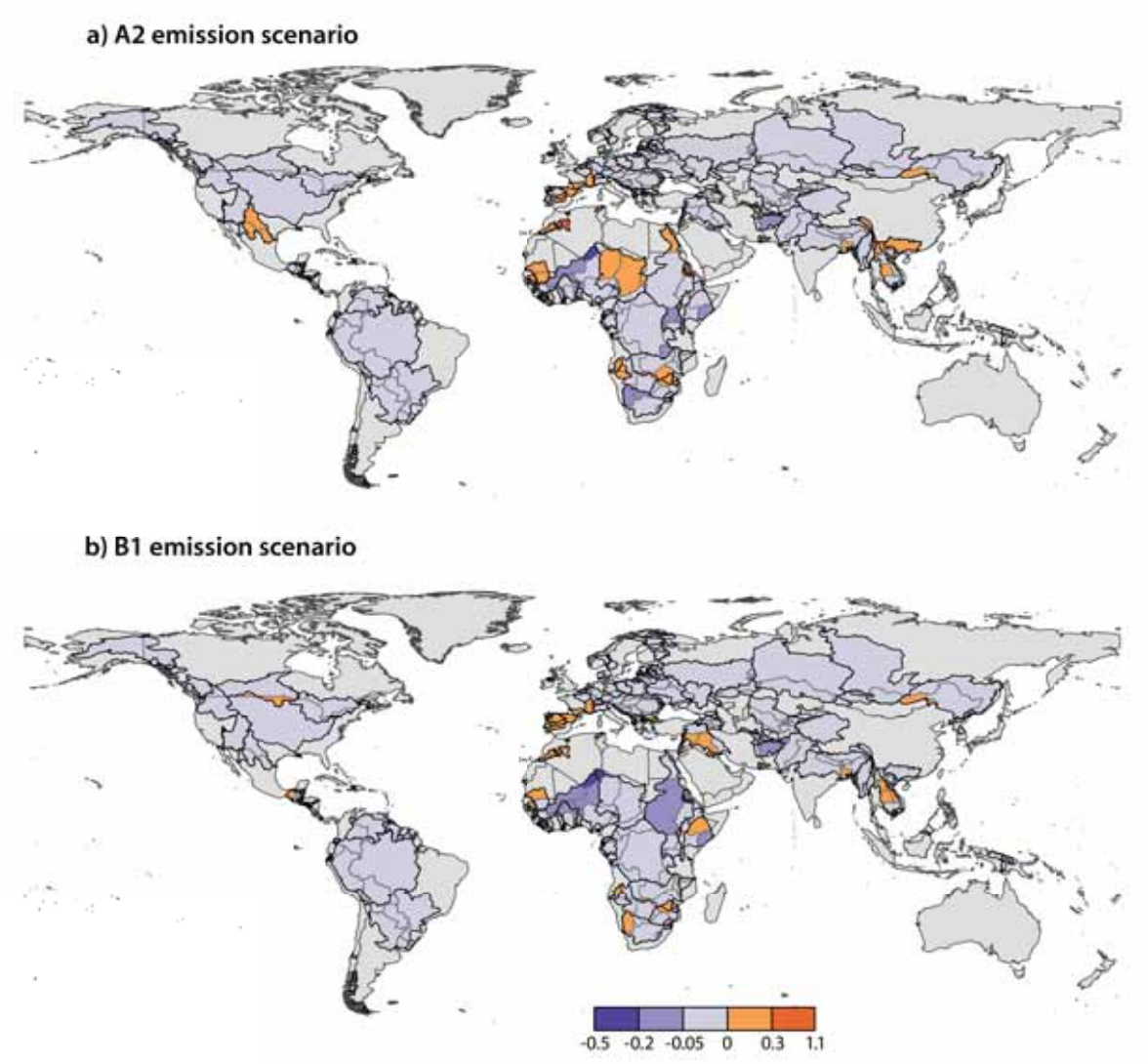


Figure 3.12.: Changes of inter-annual variability of runoff for the A2 (a) and B1 (b) emission scenario in the future time period 2025.

the A2 scenario but only the B1 scenario th BCP of Iran is affected. Furthermore, all international river basins in the Southern part of Africa are expected to experience an increase of inter-annual variability of runoff while this prediction only applies to some BCPs in the B1 scenario.

In some parts the projections of the both scenarios are more consistent. Both scenarios show increases in the Colorado and Rio Grande basin in Northern America, the Jordan and Asi basin in the Middle East, the BCPs of Egypt and Sudan of the Nile river, the BCPs of Chad and Niger in the Lake Chad basin and the basins situated in the Northern Sahara. For these basins also the most increases are projected with an average increase of about 0.5 to 1.

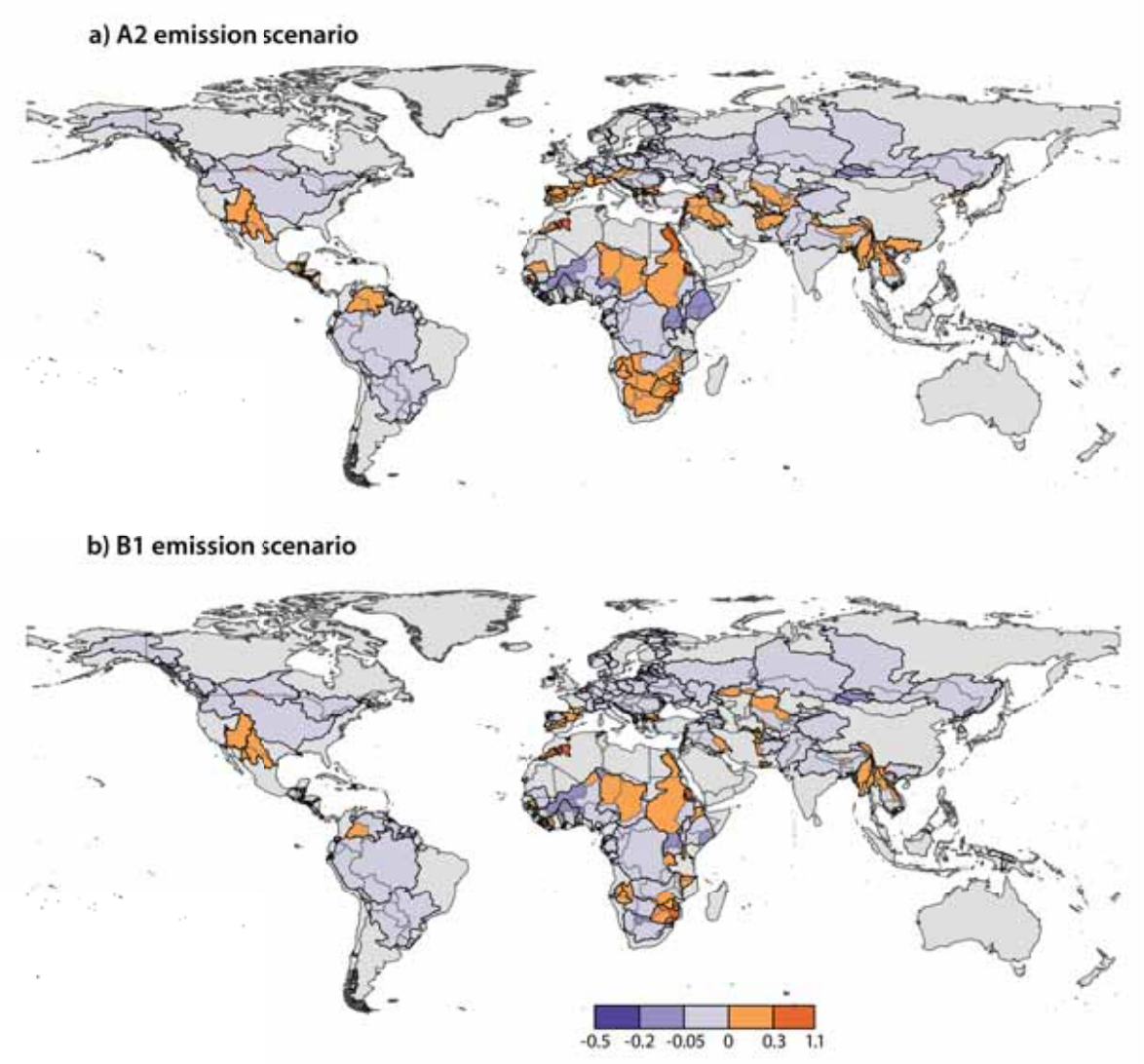


Figure 3.13.: Changes of inter-annual variability of runoff for the A2 (a) and B1 (b) emission scenario in the future time period 2085.

The spatial variability within one BCP is assumed to not have a significant influence for the interaction between two riparian countries of a river basin but it intensifies the vulnerability of BCPs with high temporal variability by hydro-climatic factors. To indicate the world regions where these effects are significant scatter plots with the temporal variability of runoff and the spatial variability of precipitation were created. The world was subdivided into eight regions for this analysis. The plots are depicted in figure 3.14 for the control period as well as for the future periods 2025 and 2071 for both emission scenarios.

Four different groups were subdivided by the combination of the temporal and spatial variability. The threshold for the temporal variability is set to 0.75 following De Stefano

et al. (2012). For the spatial variability the threshold of the vulnerability is set to 0.3. BCPs with small to medium vulnerability regarding the variability of runoff and precipitation are displayed in the left down corner. In this group the inter-annual variability of runoff is smaller than 0.75 and spatial variability of precipitation is smaller than 0.3. Most of the BCPs of the world's international river basins belong to this group. The group of BCPs with a high spatial variability (greater than 0.3) within the basin and low to medium temporal variability are mapped in the top left corner. In these two groups, all world regions are represented. For the future no big changes are projected for these groups.

BCPs with a combination of high inter-annual variability (greater than 0.75) and a spatial variability (smaller 0.3) are mapped in the bottom right corner. The group consists of five African BCPs and a BCP of the Middle East (the Euphrates-Tigris BCP of Saudi Arabia) in the control period. For the A2 scenario, the projections show an increase in the number of BCPs of Africa and the Middle East to eleven and two, respectively, for the near future period 2025. For the B1 scenario, the same number of BCPs of the Middle East is expected to be in this group but only five BCPs from Africa. For the far future time period (2085) an increase in the number of BCPs grouped into this class is projected for both scenarios. For the A2 scenario, 18 BCPs composed of one of North America, five of the Middle East and eleven of Africa will have the spatial – temporal variability combination, while it will be 20 BCPs for the B1 Scenario. These will be composed of two BCPs of North America, five of the Middle East and 13 of Africa. Not only the number of BCPs with high temporal variability of runoff will increase but also the value of variability. While the highest value in the control period is about 1.3, the value will increase to 1.9 (A2) and 1.85 (B1) in the future time period 2085.

In the top right corner BCPs most vulnerable to temporal and spatial variability are mapped. Five BCPs, all located in Africa, are grouped into the most vulnerable class with regard to both variability indices in the control period. For the first future time period 2025 and the A2 emission, one additional BCP from Africa will be grouped into this class as well as one from South America (Chico in Peru) and one from North America (Colorado BCP of Mexico). In the B1 scenario only the additional African BCP will be added to the group. For the far future (2085), this group will consist of mainly African BCPs (seven for A2, eight for B1 scenario). In the A2 scenario, it is predicted that also the Helmand BCP of Pakistani will have a combination of high variability values. These plots show that most of the BCPs with high inter-annual

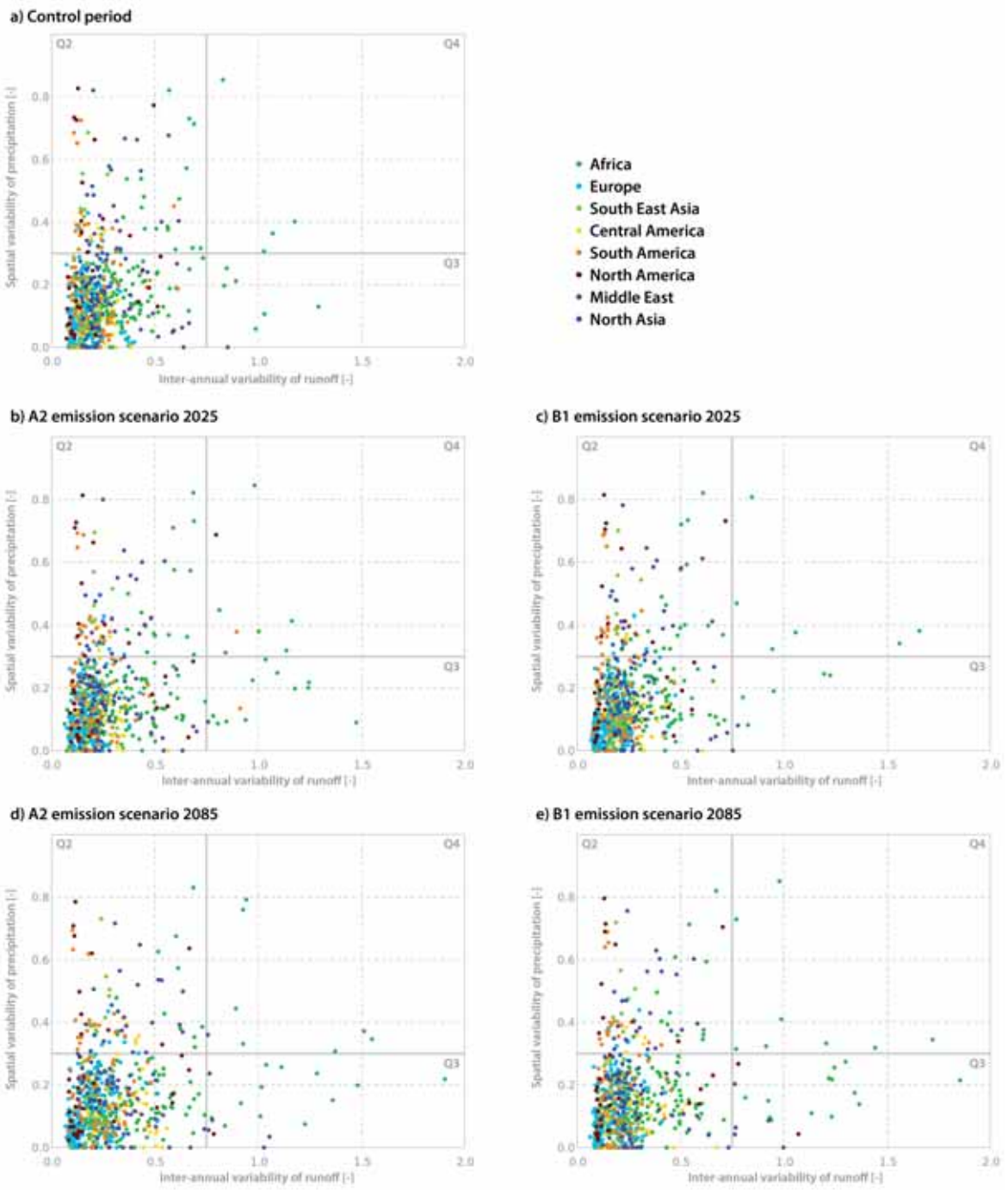


Figure 3.14.: Spatial and inter-annual variability of runoff in the BCPs of different world regions in the control period (a), the future time periods 2025 (b, c) and 2085 (d, e) and both emission scenarios.

variability of runoff and the BCPs with additional high values of spatial variability of precipitation are situated in Africa and some of them in the Middle East. Also the spatial variability within one BCP is most in the BCPs of these two regions.

### 3.2.5. Changes in available water per person

The water available for use per person was calculated and BCPs with water scarcity identified. Over the whole time period the number of countries experiencing water stress and water scarcity is increasing. Table 3.2 shows the number of BCPs of the different classes and the spatial distribution for the two emission scenarios in figure 3.16 and 3.17.

Table 3.2.: Number of BCPs classified by their available water per person in the three future time periods and both emission scenarios

| $Q_{cap}$ | | | A2 | | | B1 | |
|---|---|---|---|---|---|---|---|
| [$m^3$/y per cap] | Control | 2011 - 2040 | 2041 - 2070 | 2071 - 2100 | 2011 - 2040 | 2041 - 2070 | 2071 - 2100 |
| $< 500$ | 3 | 12 | 26 | 34 | 10 | 14 | 13 |
| 500 - 1000 | 11 | 34 | 38 | 41 | 34 | 42 | 41 |
| 1000- 1700 | 31 | 40 | 41 | 38 | 37 | 37 | 34 |
| $> 1700$ | 682 | 631 | 612 | 604 | 636 | 624 | 625 |

In the control period 46 BCPs (6.5%) have less than 1700 $m^3$ per person water available which is according to Falkenmark et al. (1989) the threshold to water stress (Fig. 3.15). Three BCPs have absolute water scarcity (Water per person and year $<$ 500 $m^3$/cap), namely the riparian states of the Oued Bon Naima basin (Algeria and Morocco) and the Nile BCP of Egypt. Other areas with water stress are situated in Europe (BCPs of Rhine and Scheldt in the Netherlands, the German BCPs of Rhine and Elbe and the BCPs of the basins in Moldova), in the Middle East (BCPs of Syria, Lebanon and Jordan) and in Southern Asia (Pakistani BCP of the Indus). There are no BCPs on the American and South American continent with water stress.

In the first future time period 2025 the changes for the two emission scenarios are quite similar. The BCPs with water scarcity increase to a number of 86 for the A2 scenario and 81 for the B1 scenario. BCPs with absolute water scarcity increase to 12 and 10, accordingly. Most of them are situated in the Middle East. The whole Jordan

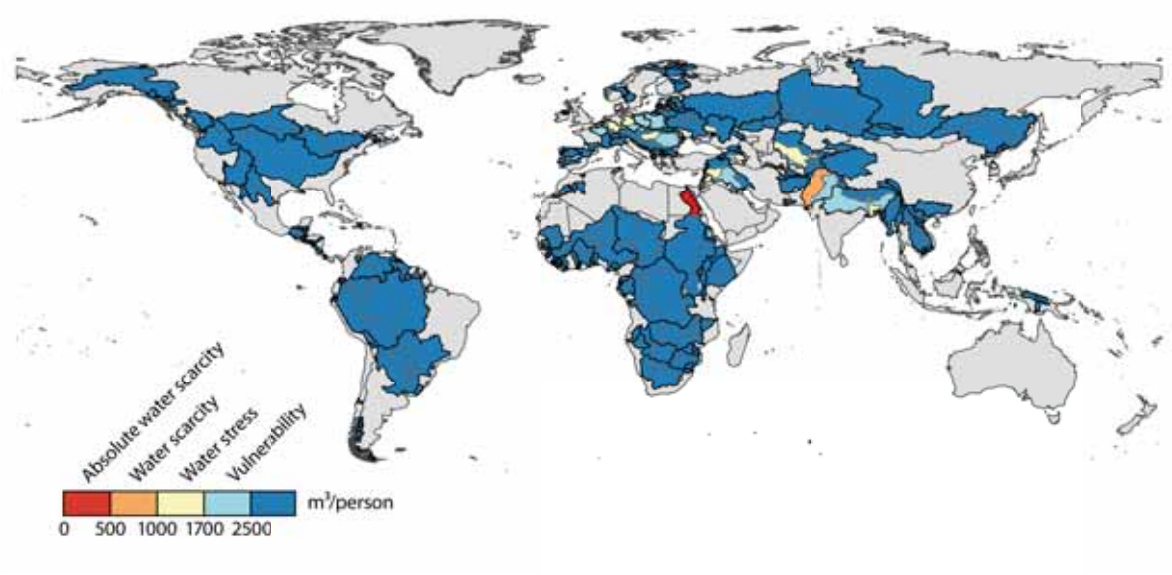


Figure 3.15.: Water availability per person year in the control period.

basin is under these conditions as well as the BCPs of the rivers in Syria.
In the time period 2055 there are big changes projected for Central America with both scenarios. Until this time period there are only two BCPs with water stress conditions but an increase to six BCPs experiencing water scarcity and six BCPs experiencing water stress is projected. The BCPs are situated especially in Guatemala, El Salvador, Haiti and the Dominican Republic. These projections will continue for the next time period when already the BCPs in Haiti and the Dominican Republic will experience absolute water scarcity.

Differences between the two scenarios are in the number of BCPs experiencing absolute water scarcity. For the B1 scenario it is projected that only 13 BCPs experience these conditions, while for the A2 scenario it will be 26. For example, the Nile BCPs of Rwanda and Burundi as well as the Euphrates-Tigris BCP of Iraq, the riparian countries of the Medjerda basin and the Maritsa BCP of Turkey are expected to experience water scarcity in the A2 scenario but water stress in the B1 scenario. In the time period 2085, the available water per person will develop different for the both emission scenarios. For the B1 scenario the number of BCPs under the threshold of 1700 $m^3$ /cap is again decreasing. While it will have been 13.2% of the BCPs in the time period before it will be 12.4% for this one. The number of BCPs below the threshold to water stress will still increase in the A2 scenario. 15.8% of the BCPs will experience water stress in 2085. Relative to the control period there will be an increase from 3 to 34 BCPs experiencing water scarcity, especially the Middle East, the river basins in

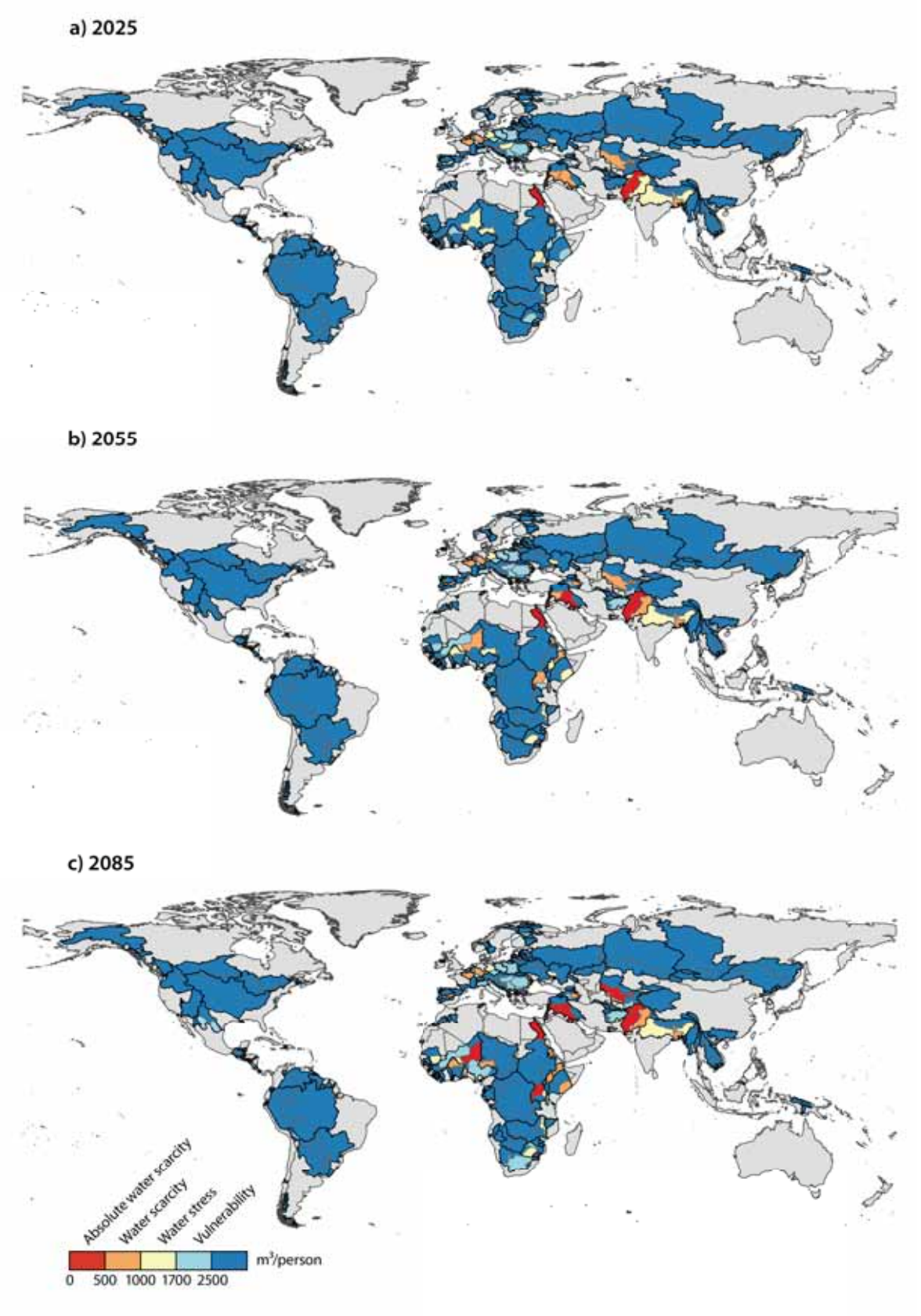


Figure 3.16.: Expected water availability per person and year in the three future time periods in emission scenario A2.

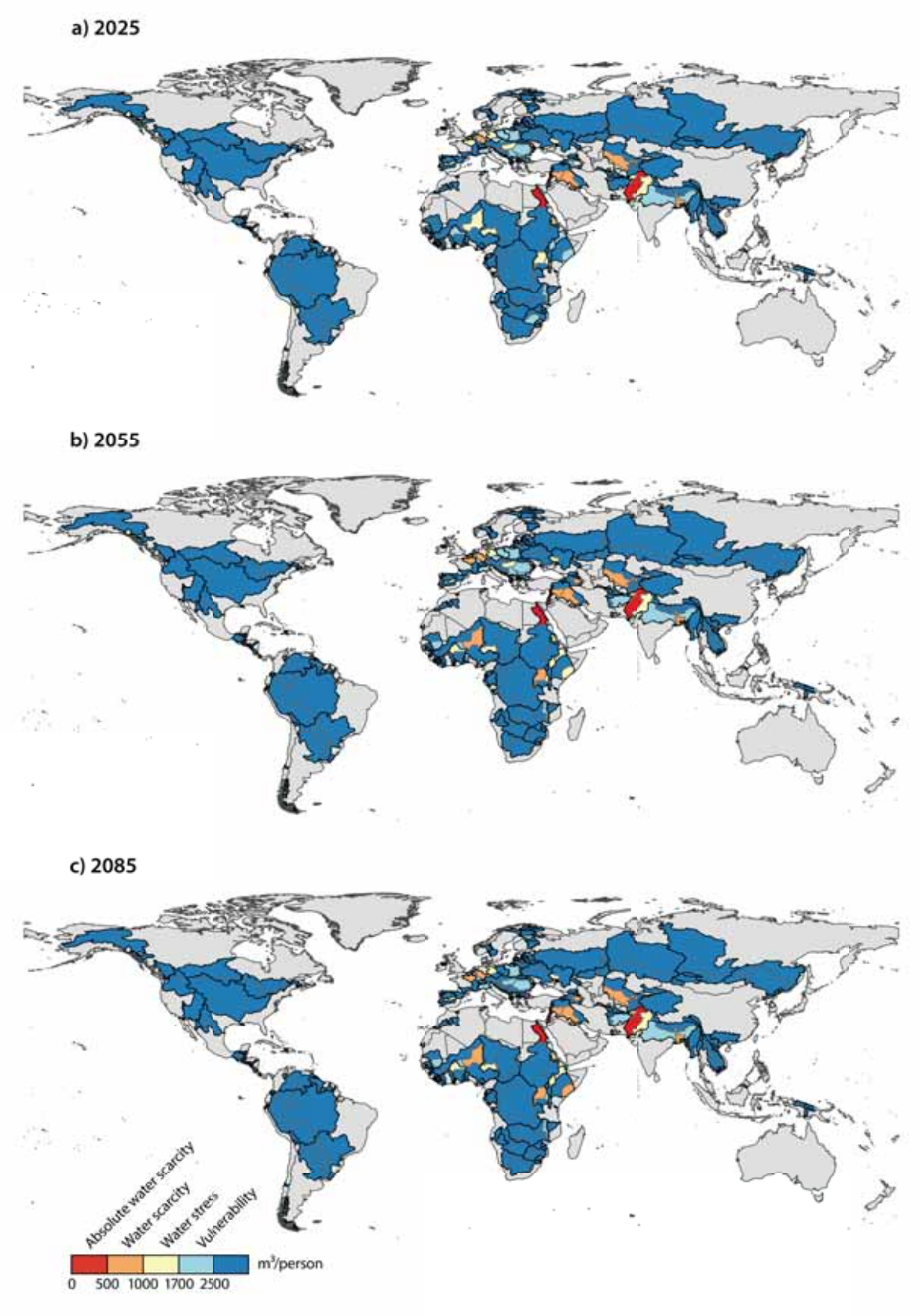


Figure 3.17.: Expected water availability per person and year in the three future time periods in emission scenario B1.

Ruanda, Uganda, Burkina Faso, Haiti, Dominican Republic and South Asia.
Overall there are no countries and basins under water stress in South America, North America, Northern Europe and Northern Asia. Significant future changes in water per capita can be seen in Central America, especially in Haiti and the Dominican Republic, in the basins of the Middle East, the Indus basin and the Aral Sea catchment. In Africa are decreases of available water per person in the Eastern and Western parts to highlight are Egypt, Uganda, Rwanda and Burundi within the Nile basin and the Niger basin (especially the BCP of Niger). Western Europe is another part of the world with a high rate of BCPs in water stress: the Seine basin, the Scheldt basin, the Rhine basin and the Dniester basin.
Also differences between BCPs within one international river basin are increasing in future. These following differences between the riparian states in one basin are all based on the projections of the far future period 2085 relative to the control period for the A2 emission scenario. In the B1 scenario these are lower.
Again, the river basins Nile, Niger and Euphrates- Tigris are to mention. In the Nile basin there is only Egypt under absolute water scarcity conditions in the control period. In 2085 also Uganda, Rwanda and Burundi will experience absolute water scarcity, Kenya will be under water scarcity conditions while there won't be any water stress in Sudan and Ethiopia.
Within the Niger basin there are Burkina Faso and Niger under water stress while the rest of the riparian states have available water per person above 1700 $m^3$.
In the A2 scenario, the Ganges-Brahmaputra-Meghna basin shows big differences. While Bangladesh experiences water scarcity and India water stress, in the headwater countries Nepal, China and Bhutan of the basin will be enough water per person available.

### 3.2.6. Hydro-climatic vulnerability index

With all indices stating the water availability situation of a BCP regarding to its hydro-climatic conditions a hydro-climatic vulnerability index (hcVI) was calculated for each BCP. The index ranges from 0 to 1 with one as most vulnerable situation. BCPs with a hcVI value greater than 0.7 have a severe vulnerability to hydro-climatic conditions. A hcVI between 0.5 and 0.7 shows high vulnerability while a hcVI between 0.3 and 0.5 shows moderate and a hcVI below 0.3 low vulnerability due to hydro-climatic conditions with respect to water availability. In figure 3.18 the results for the

index are presented for the control period.

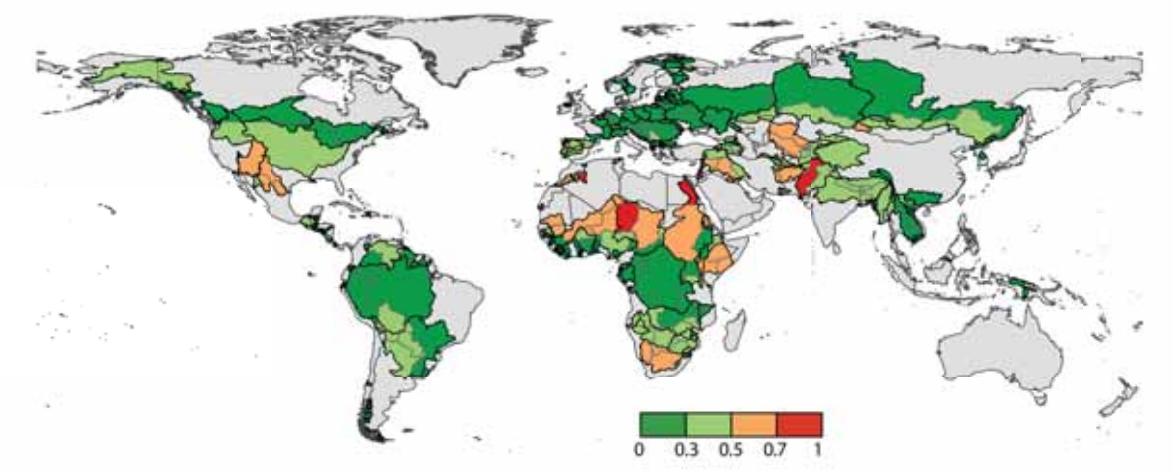


Figure 3.18.: Hydro-climatic vulnerability Index in the control period.

The map shows that no BCP of an international river basin with high vulnerability (hcVI $> 0.5$) is situated in Northern Asia, South East Asia, Europe, Central Africa and the American continent except the BCPs in the Colorado, Yaqui and Rio Grande basin, shared by the USA and Mexico. These basins have an hcVI of 0.55. BCPs with high vulnerability to hydro-climatic conditions are the whole Pu-Lun-T'o basin, the riparian countries Uzbekistan, Kazakhstan and Turkmenistan of the Aral Sea basin, the Murgab BCP of Turkmenistan, the whole Helmand basin, the Dasht BCP of Pakistan and the parts of Syria and Iraq in the Tigris-Euphrates basin. Other BCPs are situated in Southern Africa (the Orange basin except Lesotho and in the Kunene basin the part of Namibia) and in Northern Africa. River basins situated in the Sahara and countries in sub-Saharan Africa partly situated in the Sahel zone have at least a vulnerability index greater than 0.5. In this region most of the BCPs with severe vulnerability due to hydro climatic conditions are situated in this region: the Nile BCP of Egypt, the whole Atui basin, the Lake Chad BCP of Niger and the part of Algeria in the Guir basin. Two further BCPs with a hcVI above 0.7 are located outside that area: the Jordan BCP of Jordan and the part of the Indus basin in Pakistan.
The expected changes of the hcVI in both scenarios and all three future time periods are listed in table 3.3 due to their decreases and table 3.3 due to their increases for selected BCPs . The changes show no clear spatial patterns. In most of the BCPs, the changes are continuous and higher for the A2 emission scenario. Table 3.3includes the BCPs with the highest predicted decreases in the index for the far future period. For all BCPs, the changes for the different emission scenarios are comparable. The most

Table 3.3.: Selected Basin Country Polygons with their future decreases in the hydro-climatic vulnerability index for both emission scenarios

| Basin country polygon | | Index | A2 | | | B1 | | |
|---|---|---|---|---|---|---|---|---|
| River | Country | Control | 2025 | 2055 | 2085 | 2025 | 2055 | 2085 |
| Tumbes | Peru | 0.49 | 0 | -0.13 | -0.18 | -0.1 | -0.07 | -0.17 |
| Chira | Peru | 0.58 | 0.05 | -0.07 | -0.11 | -0.09 | -0.01 | -0.09 |
| Pu-Lun-T'o | China | 0.55 | -0.02 | -0.04 | -0.1 | -0.02 | -0.05 | -0.06 |
| Pu-Lun-T'o | Mogolia | 0.56 | -0.05 | -0.07 | -0.1 | -0.06 | -0.08 | -0.1 |
| Zarumilla | Ecuador | 0.43 | 0.05 | -0.08 | -0.1 | -0.04 | -0.05 | -0.1 |
| Juba Shibeli | Kenia | 0.58 | -0.02 | -0.02 | -0.09 | -0.02 | -0.03 | -0.01 |
| Tumbes | Ecuador | 0.29 | 0.03 | -0.08 | -0.08 | -0.02 | -0.05 | -0.09 |
| Lake NatronUmba | Tanzania | 0.36 | -0.05 | -0.04 | -0.07 | -0.01 | -0.07 | 0.04 |
| Har us Nur | China | 0.43 | -0.01 | -0.03 | -0.07 | -0.03 | -0.06 | -0.04 |
| Seno Union | Argentina | 0.29 | -0.02 | -0.02 | -0.07 | -0.02 | -0.04 | -0.04 |
| Yukon | USA | 0.31 | 0 | -0.03 | -0.07 | -0.03 | -0.05 | -0.04 |
| Atui | Mauretania | 0.82 | -0.06 | -0.07 | -0.07 | -0.07 | -0.07 | -0.07 |
| Zarumilla | Peru | 0.4 | 0.05 | -0.08 | -0.07 | -0.07 | -0.04 | -0.09 |
| Chira | Ecuador | 0.21 | 0.02 | -0.06 | -0.06 | -0.02 | -0.05 | -0.08 |

decreases are expected in the Tumbes-Poyango and the Chira BCP in Peru of about 0.18 and 0.11 (A2) for the far future (2085). So, both BCPs will change from a high to medium vulnerability categorization due to hydro climatic factors. The same applies to the Pu-Lun-T'o basin where a decrease of 0.1 for both BCPs (A2 scenario), 0.1 for Mongolia and 0.06 for China for the B1 is expected.

The BCPs with highest increases in vulnerability to hydro-climatic factors because of water availability are listed in table 3.4. The highest changes are predicted for riparian countries in the river basins (An)Nahr el Kebir and Nahr el Kabir with changes of about 0.35 for the A2 and 0.27 for the B1 scenario. Also in other BCPs in the Middle East the predictions show great changes. For example, the Asi BCP of Syria, Tigris BCP of Iraq and the Jordan BCP of Israel will experience in the far future a severe hydro climatic vulnerability while it is high in the control period. Other areas experiencing increase of hcVI are situated in the southern part of Eastern Europe. Changes range between 0.25 and 0.33 in the A2 scenario. For the B1 scenario they are slightly smaller compared to the A2 scenario.
In the A2 scenario, very high changes are expected for the BCPs of Mozambique in the river basins Incomati and Umbulezi. The changes will be 0.37 and 0.33, respectively, while the predictions with increases about 0.15 are much smaller for the B1 scenario.

Table 3.4.: Selected basin country polygons with future increases in the hydro-climatic vulnerability index for both emission scenarios

| Basin country polygon | | Index | A2 | | | B1 | | |
|---|---|---|---|---|---|---|---|---|
| River | Country | Control | 2025 | 2055 | 2085 | 2025 | 2055 | 2085 |
| Nahr el Kebir | Turkey | 0.11 | 0.23 | 0.28 | 0.37 | 0.21 | 0.25 | 0.29 |
| Incomati | Mozambique | 0.36 | 0.15 | 0.29 | 0.37 | 0.16 | 0.2 | 0.17 |
| Nahr el Kabir | Lebanon | 0.1 | 0.22 | 0.28 | 0.35 | 0.2 | 0.24 | 0.27 |
| Nahr el Kabir | Syria | 0.1 | 0.22 | 0.28 | 0.35 | 0.2 | 0.24 | 0.27 |
| Nahr el Kebir | Syria | 0.2 | 0.18 | 0.24 | 0.33 | 0.16 | 0.2 | 0.22 |
| Umbulezi | Mozambique | 0.28 | 0.15 | 0.26 | 0.33 | 0.14 | 0.16 | 0.15 |
| Artibonite | Haiti | 0.21 | 0.18 | 0.3 | 0.32 | 0.16 | 0.25 | 0.32 |
| Asi | Syria | 0.46 | 0.2 | 0.26 | 0.32 | 0.2 | 0.23 | 0.26 |
| Rezvaya | Bulgaria | 0.13 | 0.2 | 0.29 | 0.32 | 0.19 | 0.23 | 0.25 |
| Rezvaya | Turkey | 0.16 | 0.19 | 0.29 | 0.32 | 0.18 | 0.23 | 0.25 |
| Maritsa | Turkey | 0.17 | 0.13 | 0.26 | 0.3 | 0.11 | 0.19 | 0.21 |
| Lempa | El Salvador | 0.19 | 0.07 | 0.17 | 0.3 | 0.07 | 0.11 | 0.12 |
| Pedernales | Dom. Rep. | 0.26 | 0.17 | 0.26 | 0.29 | 0.15 | 0.17 | 0.29 |
| Pedernales | Haiti | 0.26 | 0.17 | 0.26 | 0.29 | 0.15 | 0.17 | 0.29 |
| Artibonite | Dom. Rep. | 0.23 | 0.07 | 0.24 | 0.29 | 0.04 | 0.13 | 0.24 |
| Medjerda | Tunisia | 0.42 | 0.14 | 0.27 | 0.29 | 0.14 | 0.21 | 0.2 |
| Tigris | Iraq | 0.59 | 0.1 | 0.21 | 0.29 | 0.16 | 0.23 | 0.2 |
| Medjerda | Algeria | 0.38 | 0.15 | 0.26 | 0.29 | 0.13 | 0.22 | 0.19 |
| Choluteca | Honduras | 0.27 | 0.06 | 0.16 | 0.29 | 0.04 | 0.14 | 0.17 |
| Asi | Lebanon | 0.28 | 0.03 | 0.17 | 0.28 | 0.02 | 0.08 | 0.09 |
| Struma | Bulgaria | 0.22 | 0.11 | 0.21 | 0.26 | 0.12 | 0.18 | 0.17 |
| Struma | Greece | 0.21 | 0.14 | 0.21 | 0.25 | 0.13 | 0.18 | 0.2 |
| Jordan | isreal | 0.62 | 0.16 | 0.18 | 0.25 | 0.15 | 0.2 | 0.19 |
| Wadi al Izziyah | Israel | 0.33 | 0.1 | 0.15 | 0.25 | 0.08 | 0.11 | 0.14 |
| Motaqua | Guatemala | 0.34 | 0.01 | 0.13 | 0.25 | 0.01 | 0.08 | 0.11 |
| Lempa | Guatemala | 0.24 | 0.03 | 0.12 | 0.25 | 0.04 | 0.07 | 0.09 |
| Tagus | Spain | 0.41 | 0.14 | 0.19 | 0.24 | 0.15 | 0.14 | 0.16 |
| Wadi al Izziyah | Lebanon | 0.25 | 0.1 | 0.15 | 0.24 | 0.08 | 0.11 | 0.14 |
| Indus | Afghanistan | 0.45 | 0.08 | 0.21 | 0.23 | 0.05 | 0.15 | 0.17 |
| Massacre | Dom. Rep. | 0.29 | 0.08 | 0.23 | 0.22 | 0.05 | 0.13 | 0.18 |
| Massacre | Haiti | 0.3 | 0.08 | 0.23 | 0.22 | 0.06 | 0.13 | 0.17 |
| Jordan | Lebanon | 0.38 | 0.09 | 0.14 | 0.21 | 0.08 | 0.11 | 0.13 |
| Goascoran | Honduras | 0.21 | 0.05 | 0.09 | 0.21 | 0.04 | 0.09 | 0.12 |

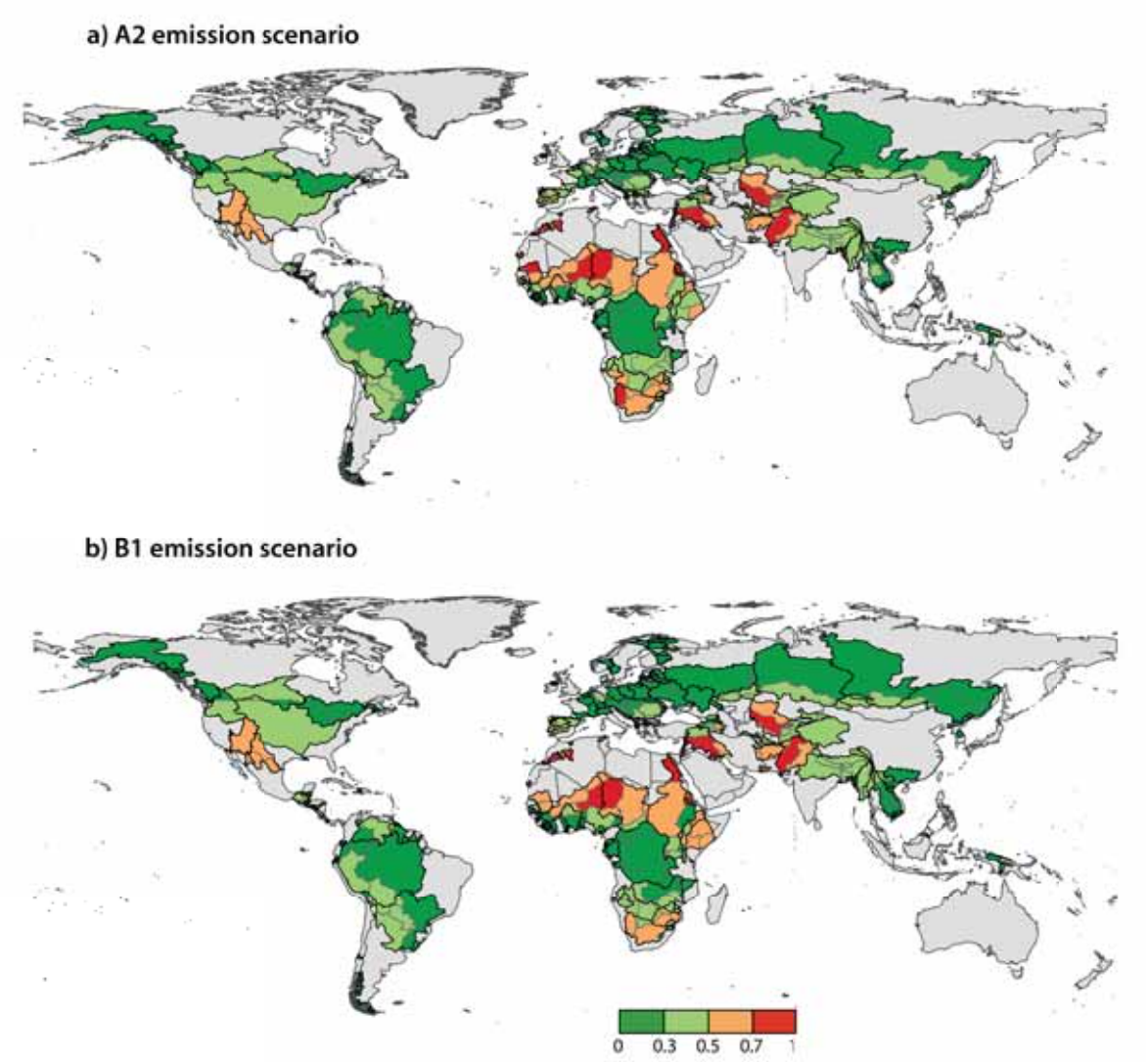


Figure 3.19.: Hydro-climatic vulnerability Index for the A2 scenario (a) and the B1 scenario (b) for the far future period 2085.

The same applies to the predicted changes in Central America. While they are quite similar for river basins shared by Haiti and the Dominican Republic for the both scenarios they differ for the BCPs on the mainland. Mostly, the changes expected for the A2 scenario are twice as severe as those expected for the B1 scenario. For example, the predicted change for the Motaqua BCP in Guatemala is 0.25 for the A2 scenario and 0.12 for the B1 scenario. These changes in the hcVI can also be seen in figure 3.19 picturing the hcVI for the far future time period (2085) for the both scenarios.

BCPs categorized with severe hydro climate vulnerability to water availability increase to a number of 24 for the A2 scenario and 17 for the B1 scenario. In contrast, only 7 BCPs have this categorization in the control period. Most BCPs in which

the hydro climatic vulnerability will degrade to a severe level are located in Northern Africa, the Middle East and Central Asia. For both scenarios, the part of Mexico in the Colorado basin, the Medjerda and Dra basins in the Sahara, the part of Niger in the Niger basin, the Tigris- Euphrates BCPs of Syria and Iraq, the part of Syria in the Asi basin, the whole Jordan basin and the Aral Sea BCP of Uzbekistan should be mentioned. In the A2 scenario the following BCPs are expected additionally to experience severe vulnerability: the Namibian part of the Orange basin, in the Senegal basin the part of Mauretania, the Gash BCP of Eritrea and the Baraka BCP of Sudan. Moreover, there are also some areas where degradation from a moderate to high categorization of vulnerability will happen: in the Tigris- Euphrates BCP of Iran, in the Indus basin except Pakistan (where it is severe), the riparian countries of Limpopo River except Botswana, all BCPs located in Namibia (only A2 scenario) and the Tagus BCP of Spain. In the other South European and South Eastern European river basins the values of the hcVI are expected to change to values greater 0.3 and the vulnerability category will change to moderate.

## 3.3. Comparison of water availability within one international river basin

In a next step, values of the indices aridity index, annual mean precipitation, available water resources and inter-annual variability of runoff, respectively of each riparian country to the concerning international river basin. The normalized range ($R_{norm}$) was calculated for each basin and time period as an index to express the disparity between riparian countries. Thus, it is possible to identify river basins with big variability in the different indices among their neighbouring countries. The higher the normalized range value, the higher the disparities within the basin. Additionally, the future changes in these inequalities between riparian countries are considered. The mean value of the basin will change through the different future time periods. Because of this and the mean value has an greater influence on the normalized range value for all time periods the basin mean value of the control period is used for normalization.
In the analysis only countries within the river basin, that has a territorial quota higher than 3%, are considered. Exceptions are made when the part, which is shared in the river basin is greater than one third of the total area of the country. Examples for

these exceptions are Luxemburg and Liechtenstein in the Rhine river basin as well as Ruanda and Burundi in the Nile basin.
For each index, tables with the $R_{norm}$ values are available in Appendix A. Therein, the international river basins are ranked according to their normalized range values in the control period. Only basins, which have a value greater than 0.3, are included. To evaluate the values if the disparity within the basin rises or declines, the mean value of all future time periods and both scenarios will be calculated. Additionally, the future time period-scenario combination with the highest change relative to conditions in the control period was highlighted.

Precipitation

The calculated normalized range of annual mean precipitation of world's international river basins is depicted in figure 3.20a for the control period. All river basins located on the border of the Sahara and sub-Saharan Africa show normalized range values greater than 1.0. This means there are high disparities in precipitation between the countries within one basin. In the control period, the river basin with highest inequalities is the Lake Chad basin with a normalized range of 2.07, followed by the Niger (1.71), Senegal (1.42) and Nile (1.41) basin. Also the Awash and the Lotagipi Swamp basins in North Eastern Africa, as well as the Orange basin in Southern Africa, the Ganges-Brahmaputra-Meghna basin in South East Asia and the Alsek basin shared by Canada and the USA have high differences ($R_{norm}$ >1) in precipitation among their riparian states.
In table A.1 (in the Appendix) the international river basins are ranked by their normalized range in annual precipitation in the control period. The table shows that there will be more river basins in which the range between its neighbouring countries will increase. The first nine basins have a $R_{norm}$ greater 1.0 in the control period. The Gash, Danube and Seno Union basins, $R_{norm}$ will exceed the value of 1.0 in future. In the Gash and Seno Union basin, this will happen in the near future. In the Danube basin the value of 1.0 will be transcended in the medium future (2055) in the B1 scenario. In the B1 scenario, the highest disparity of annual mean precipitation will be in 2055 with a $R_{norm}$ of 1.07 while a continuous increase with the highest value in the far future is predicted in the A2 scenario.
Selected river basins with high future decreases or increases in the normalized range of precipitation are listed in table 3.5.

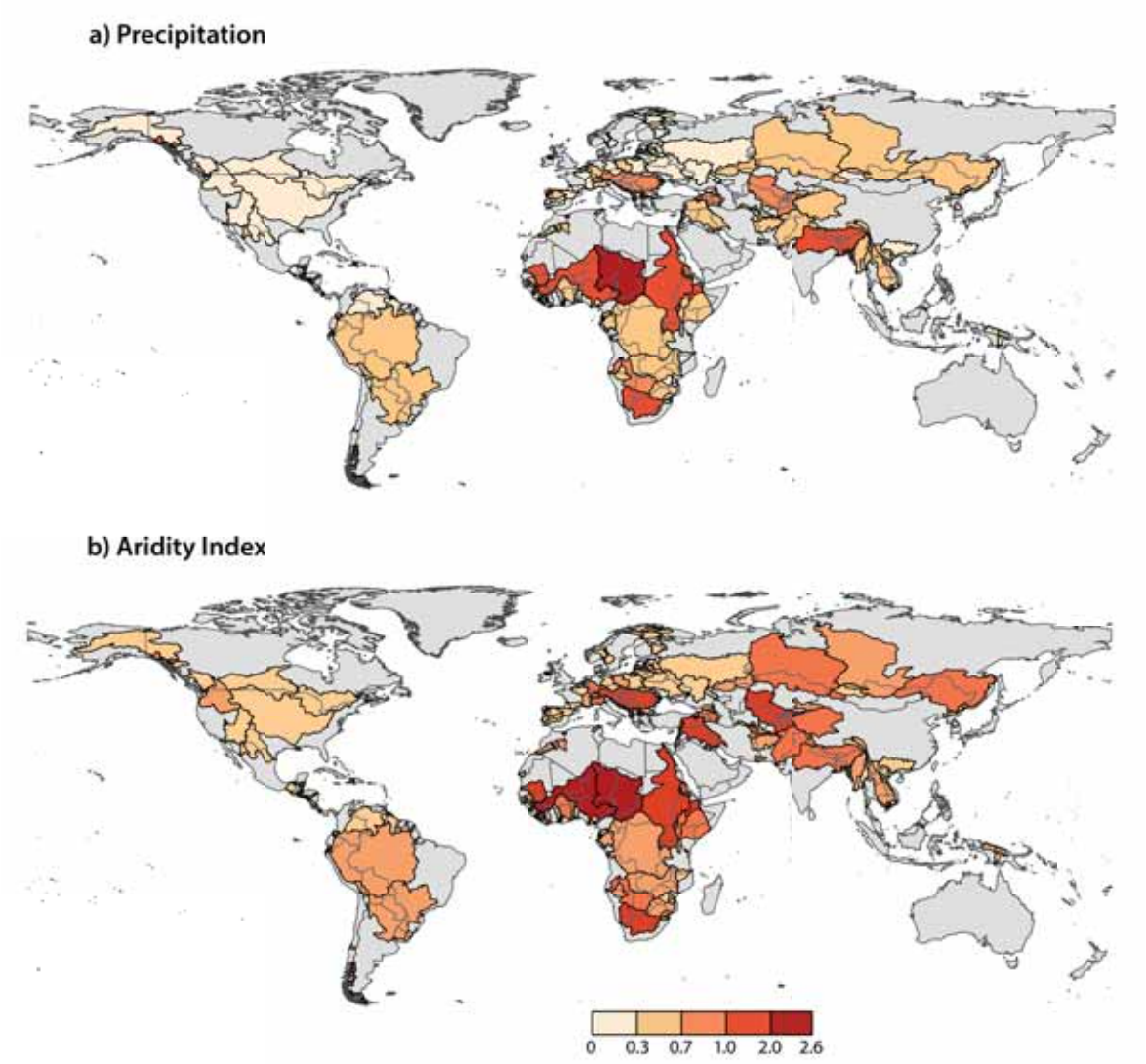


Figure 3.20.: Normalized range of international river basins for precipitation (a) and the aridity index (b) in the control period.

The river basins with the highest predicted increase in the range of annual mean precipitation are the Seno Union and Gallegos basin, both shared by Argentina and Chile, and the Orinoco basin shared by Columbia and Venezuela. Although $R_{norm}$ with 0.17 is low in the Orinoco basin the increase of 0.25 for the A2 scenario and 0.17 for the B1 scenario are notable. With an annual average about 2500 mm/y precipitation for the control and far future time period the basin has a quite high precipitation rate. But while Columbia gets about 8% more precipitation and Venezuela 8% less precipitation relative to the basin average value, it is expect to rise to a difference of about +/- 20%. However, the increase in the two other mentioned basins is more significant. With a $R_{norm}$ of 0.93 in the Seno Union and 0.83 in the Gallegos basin and an increase of

Table 3.5.: Selected river basins with high changes in the normalized range of precipitation

| Rank | River basin | Control period | A2 2025 | A2 2055 | A2 2085 | B1 2025 | B1 2055 | B1 2085 |
|---|---|---|---|---|---|---|---|---|
| 1 | Lake Chad | 2.07 | 2.08 | 2.17 | 2.29 | 2.13 | 2.11 | 2.16 |
| 2 | Niger | 1.71 | 1.76 | 1.85 | 1.94 | 1.76 | 1.79 | 1.81 |
| 5 | Orange | 1.27 | 1.33 | 1.28 | 1.3 | 1.27 | 1.28 | 1.29 |
| 7 | Awash | 1.18 | 1.19 | 1.14 | 1.19 | 1.23 | 1.18 | 1.21 |
| 10 | Gash | 0.98 | 1.04 | 1.02 | 1.15 | 1.08 | 1.08 | 1.08 |
| 11 | Danube | 0.94 | 0.9 | 0.96 | 0.96 | 0.94 | 1.01 | 0.98 |
| 13 | Seno Union | 0.93 | 1.06 | 1.11 | 1.26 | 1.01 | 1.08 | 1.14 |
| 16 | Gallegos | 0.86 | 0.98 | 1.03 | 1.16 | 0.94 | 1 | 1.06 |
| 36 | Dra | 0.52 | 0.44 | 0.4 | 0.33 | 0.45 | 0.46 | 0.41 |
| 37 | Tarim | 0.49 | 0.52 | 0.45 | 0.34 | 0.51 | 0.48 | 0.42 |

about 0.33 and 0.3, respectively, the normalized range will exceed 1.

The predicted increase of $R_{norm}$ about 0.22 in the Lake Chad basin for the far future and the A2 scenario will have a greater impact than in the before mentioned basins. The inequality in annual mean precipitation among the riparian countries is already very high in the control period($R_{norm} = 2.07$). Through changes in precipitation in the riparian states caused by climate change the normalized range will increase to 2.29 in the far future (2085). The range will rise from 1316 mm/y to 1456 mm/y.

In the Niger basin, $R_{norm}$ will rise of about 0.25 for the A2 scenario and about 0.1 for the B1 scenario. Accordingly, the range of annual mean precipitation among the riparian countries will get smaller relative to the basins mean value. The annual precipitation average in the basin is for the control and future about 1100 mm/y but has a range of 1650 mm/y in the control period and will rise to 1870 mm/y in the A2 scenario and 1915 mm/y in the B1 scenario in the future period 2085.

The neighbouring countries of the river basin Dra will experience the highest decreases in differences of precipitation. $R_{norm}$ will decline from 0.52 to 0.33 in the far future for the A2 scenario and to 0.46 for the B1 scenario. In the basins Tarim and Daoura (shared by Morocco and Algeria) the precipitation differences will also decrease. $R_{norm}$ will decline of 0.15 from value of 0.49 and 0.47. Overall, the increase and also decrease in disparities in precipitation between countries sharing the area of a river basin is expected to be stronger for the A2 scenario.

Aridity Index

To evaluate the general water balance of a BCP in comparison to the water balance of the whole river basin, the normalized range of the aridity index of each river basin was calculated. A comparison of figure 3.20b showing the normalized range of the aridity index for each international river basin and figure 3.20a (normalized range for precipitation) remarks that the normalized range is higher for the AI. Worldwide seen there are 35 international river basins with a $R_{norm}$ greater than 0.7 for AI while the number for precipitations is 23 in the control period. The higher values are probably caused by the small AI values (mostly between 0 and 1), but the number of basins with a normalized range higher than 1.0 is similar. The basins with the highest ranges are the same as for the normalized range of precipitation; Lake Chad (2.25), Niger (2.02), Orange (1.79), Senegal (1.78) and Nile (1.29). The Awash, the Gash and the Lotagipi Swamp basin have also high disparities between its countries as they do in precipitation. Further, the Danube, the Tigris and the Aral Sea basin have high normalized ranges in the AI. Additionally, the Seno Union located in South America has a high range between its riparian states. It's shared by Chile and Argentina and has a $R_{norm}$ of 1.03.

The future developments of the range in the AI within a basin differ slightly (A.2). Contrary to the other indicators, in more basins the differences in AI among its sharing countries will decrease. High decreases in the normalized range are expected for the Lake Chad and Senegal basin. (3.6). In the Lake Chad basin, the normalized range of 2.02 will decrease to 1.74 in the far future and A2 scenario. In the control period the AI of the BCP of Algeria is about 0.31 below the basins mean AI while the value of the Central Republic of Africa is 0.47 above the average. This will decrease to 0.22 and 0.37, respectively. In the Senegal basin, the range will decreases from 0.65 to 0.47.

Highest decreases in the variations of AI are projected for the Seno Union and Gallegos

Table 3.6.: Selected river basins with high changes in the normalized range of the aridity index

| Rank | River basin | Control period | A2 | | | B1 | | |
|---|---|---|---|---|---|---|---|---|
| | | | 2025 | 2055 | 2085 | 2025 | 2055 | 2085 |
| 1 | Lake Chad | 2.25 | 2.14 | 2.05 | 1.74 | 2.22 | 2.08 | 1.99 |
| 4 | Senegal | 1.78 | 1.76 | 1.64 | 1.31 | 1.77 | 1.7 | 1.63 |
| 12 | Seno Union | 1.03 | 1.15 | 1.19 | 1.31 | 1.17 | 1.24 | 1.31 |
| 15 | Gallegos | 0.94 | 1.05 | 1.09 | 1.19 | 1.07 | 1.12 | 1.19 |
| 90 | Orinoco | 0.26 | 0.3 | 0.37 | 0.4 | 0.28 | 0.32 | 0.36 |
| 92 | Catatumbo | 0.25 | 0.29 | 0.33 | 0.39 | 0.29 | 0.32 | 0.38 |

basin with a decline of $R_{norm}$ of about 0.33 and 0.25, respectively. In the Seno basin, for example, the range in AI will change from 1.59 in the control period to 1.26 in the far future and scenario A2. Basins with low normalized range values in AI but the greatest increases (0.14) are the Orinoco and Catatumba basin shared by Columbia and Venezuela.

Available water resources

For differences of available water resources among countries within a basin, more basins with high disparities can be counted than in the other indices (Tab. A.3). For a number of 26 international river basins, a normalized range of AWR greater than 1.0 was determined for the control period. The river basins with high normalized ranges are distributed more globally than in the other indices (Figure 3.21).

As for all other indices, in the river basins in the northern part of sub-Saharan Africa and in the Orange basin in Southern Africa the differences among the riparian countries are greatest with a normalized range greater than 2.0. River basins with a $R_{norm}$ between 1.0 and 2.0 are, for example, the basins Danube, Aral Sea, Lotagipi Swamp, Okavango, Pu Lun T'o, Kura-Araks, Awash and Rhine. Also river basins, which have not been noticed having great disparities in the other indices, can be identified to have a high normalized range for available water resources. To mention are the Hari basin shared by Afghanistan, Iran and Turkmenistan, the Gallegos and Seno Union basins shared by Argentina and Chile, the Amazon and La Plata basin in South America as well as the Yenisei basin shared by Mongolia and Russia and the Amur basin with the additional neighbouring country China.
Analysing the direction of change for the range of AWR between riparian countries in basins with high normalized ranges, an increasing trend is predominant. Increases are projected for the river basins located in the transition zone between the Saharan and sub-Saharan Africa as well as the Zambezi, the Kunene and Limpopo basin in the southern part of Africa. Furthermore, the disparity among the riparian states will rise in some basins in the Middle East (Tigris-Euphrates, Kura-Araks and Suluk), some in Central Asia (Aral Sea and Tarim), in the river basins in South East Asia as well as in South America. A decreasing trend is projected for the river basins in Europe, the Indus, the Hari and Amur basin in Central Asia as well as in Africa the Congo, the Orange and the Okavango basin.
For basins having a normalized range value greater than 2.0 in the control period

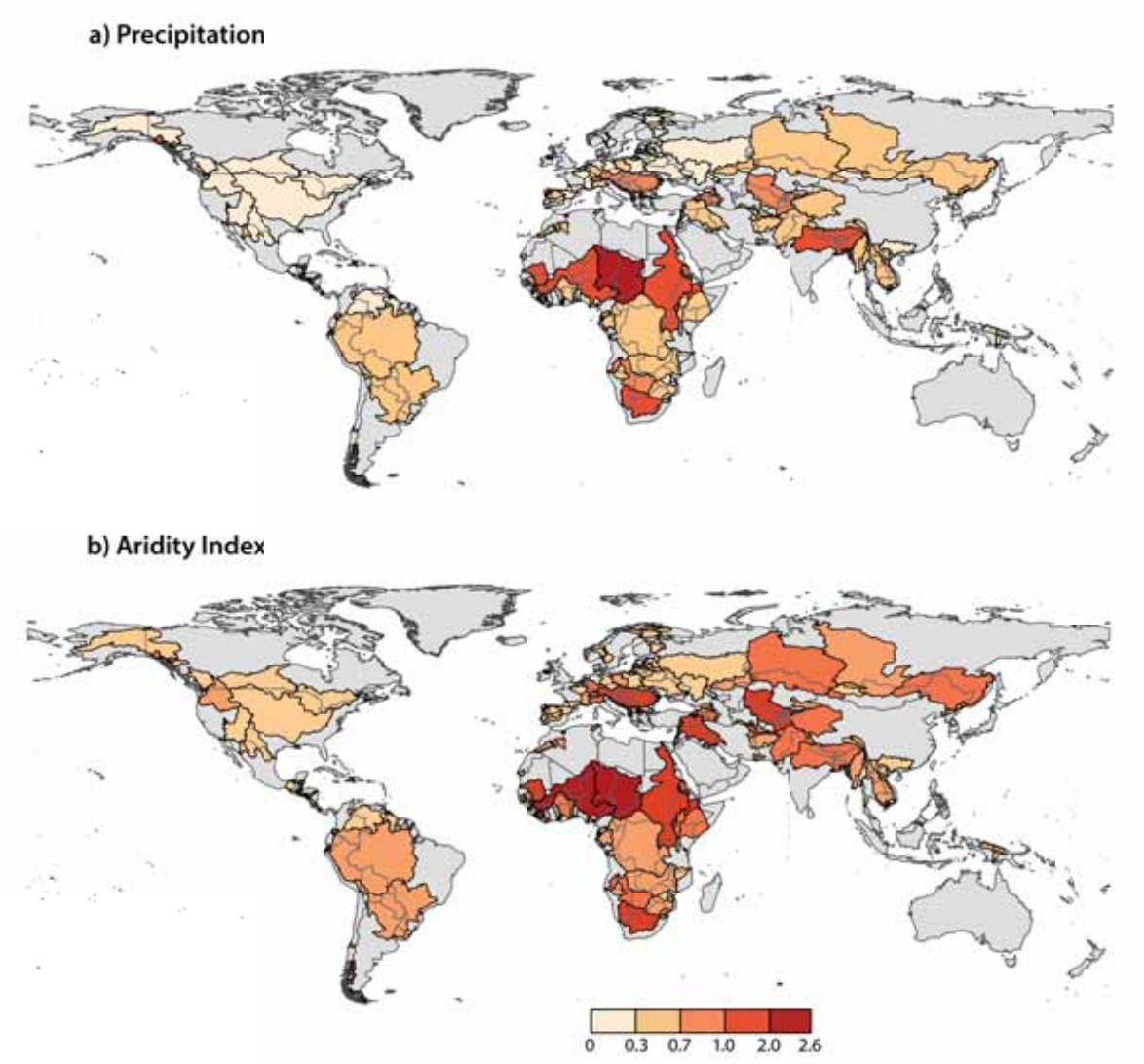


Figure 3.21.: Normalized range of international river basins for available water resources in the control period.

excluding the Orange river basin, an increase in the disparity of AWR between their countries are expected.

In the Orange basin a decline in the variability between its countries is predicted as a mean over all future time periods and scenarios with the smallest range in the far future and A2 scenario ($R_{norm}$=1.72). Nevertheless, in the A2 scenario and near future time period, the normalized range rises to 2.48 (from 2.03 in the control period).

In the Niger basin, the mean value over all time periods and both scenarios of 2.28 (2.1 in the control period) will increase with the highest value in 2085 and the A2 scenario ($R_{norm}$=2.57). The most disadvantaged riparian country in the Niger basin according to AWR is Algeria. In the control period, it has 221 mm/y less AWR than

the calculated mean value (304 mm/y) of the entirely basin. Consequently Algeria has 507 mm/y less available water resources than the most advantaged country in the basin: Cameroon with a positive deviation from the mean value of 283mm/y. The range between these two countries will rise to 623 mm/y in the far future and the A2 scenario with an additional increase in water availability.
In the Nile basin, the normalized range in AWR is expected to increase. In Egypt, the country with the lowest water availability in the basin, AWR will decline from 8mm/y to 6mm/y while in Ethiopia, the country with the highest AWR, it will rise from 509 mm/y to 576 mm/y. This leads to a higher range between riparian countries.
In the Seno Union basin shared by Chile and Argentina the highest increase in unequal distribution of AWR is projected (Tab. 3.7). The normalized range will rise from 1.38 in the control period, to a future mean of 1.79 with the highest value in the A2 scenario and time period 2085. $R_{norm}$ will be 2.23 which means an increase in the range of about 211 mm/y. Similar development is observed for another basin shared by these two countries, the Gallegos basin. The range will rise of about 214 mm/y.

Table 3.7.: Selected river basins with high changes in the normalized range of AWR

| Rank | River basin | Control period | A2 | | | B1 | | |
|---|---|---|---|---|---|---|---|---|
| | | | 2025 | 2055 | 2085 | 2025 | 2055 | 2085 |
| 3 | Niger | 2.1 | 2.19 | 2.43 | 2.57 | 2.15 | 2.26 | 2.27 |
| 4 | Orange | 2.03 | 2.48 | 2 | 1.72 | 1.96 | 2.09 | 1.89 |
| 7 | Aral Sea | 1.71 | 1.86 | 1.71 | 1.73 | 1.9 | 1.89 | 1.71 |
| 10 | Seno Union | 1.39 | 1.74 | 1.84 | 2.23 | 1.59 | 1.76 | 1.94 |
| 11 | Hari | 1.35 | 1.44 | 0.93 | 0.83 | 1.4 | 1.2 | 1.11 |
| 13 | Gallegos | 1.33 | 1.66 | 1.76 | 2.1 | 1.53 | 1.69 | 1.84 |
| 15 | Pu Lun T'o | 1.29 | 1.18 | 1.05 | 0.92 | 1.11 | 1.17 | 1.04 |
| 18 | Awash | 1.18 | 1.19 | 0.79 | 0.82 | 1.33 | 1.11 | 0.98 |
| 20 | Tigris-Euphrates | 1.16 | 1.61 | 1.07 | 1.05 | 1.23 | 1.41 | 1.07 |
| 24 | Amazon | 1.06 | 1.06 | 1.33 | 1.57 | 1.08 | 1.23 | 1.34 |
| 31 | Yaqui | 0.91 | 0.72 | 0.51 | 0.32 | 0.85 | 0.82 | 0.8 |

Other basins with high $R_{norm}$ values in the control period and a rise in the normalized range between its countries are the Aral Sea basin, the Tigris-Euphrates basin and the Amazon basin. In the Amazon basin the range will change from 863 mm/y to 1081 mm/y. The advantaged country is Columbia and the most disadvantaged one is Bolivia. The highest decrease in differences between riparian countries is expected for the Yaqui basin. $R_{norm}$ will decrease of about 0.57. Also in the international basins Hari and

Pu-Lun-T'o high declines are predicted. Both basins have low AWR. The mean value for the future period is 62 mm/y for the Hari basin and 77 mm/y for the Pu-Lun-T'o basin. Hence, the expected decline of the range in AWR from 79mm/y in the control period to 49 mm/y for the far future period and A2 scenario for the Hari basin and from 92 mm/y to 65 mm/y is significant. In the Awash basin, the range in AWR between Djibouti and Ethiopia will decline from 147 mm/y to 132 mm/y in the future, in average. The highest fall is expected for the far future and the A2 scenario. Then, the range will be 45 mm/y smaller relative to the control period. Regarding the low basin mean of AWR (175mm/y) this will be a great improvement.

Inter-annual variability of annual mean runoff

Great inequality in the reliability of annual water resources can lead to a great potential of conflicts between the riparian states of an international river basin. In table **??** selected river basins are sorted by descending order of their normalized range of inter annual runoff variability in the control period All basins with a normalized range greater than 0.3 can be found in appendix A (A.4).

As in the other indices, inequality among the riparian countries due to the reliability of the water resources is projected to increase in future. Only in some river basins the projections show decreases. Examples are the La Plata and Orinoco basin in South America, the Danube basin in Europe, the Juba-Shibeli and Niger basin in Africa as well as the Ganges-Brahmaputra-Meghna and Indus basin in South East Asia and the Ob and Yenisey basin in the northern part of Asia.

The river basins Nile, Niger and Lake Chad have the highest disparities among their sharing countries. The Nile basin has a normalized range of 2.3 in the control period. The inter-annual variability ranges between 0.2 in Burundi, Ruanda and Ethiopia and 1.0 in Egypt. These disparities will intensify in future. In the A2 emission scenario, the range will increase with a peak in the medium future period. In the B1 scenario, it is projected to rise continuously until the far future time period.. Through the expected decline of inter-annual variability of runoff in Burundi and Ruanda to a value of 0.16 and a rise in Egypt to 1.4, the differences will become greater and the normalized range will be 3.4in the medium future period.

In the Niger basin, the value of normalized range in the variability of runoff will steadily rise to a value greater 1.92 for the B1 scenario (1.77 for the A2 scenario) after a decline in the near future. In the Lake Chad basin, $R_{norm}$ will decrease from a value of 1.32 in the control period to 1.1 in the near future, will peak in the medium future time

period with 1.99 for the A2 and 2.32 for the B1 scenario and will then decline again in the far future.

Table 3.8.: Selected river basins with high changes in the normalized range of inter-annual variability

| Rank | River basin | Control period | A2 | | | B1 | | |
|---|---|---|---|---|---|---|---|---|
| | | | 2025 | 2055 | 2085 | 2025 | 2055 | 2085 |
| 1 | Nile | 2.3 | 2.64 | 3.4 | 3.32 | 2.35 | 2.68 | 2.84 |
| 2 | Niger | 1.74 | 1.29 | 1.46 | 1.77 | 1.12 | 1.69 | 1.92 |
| 3 | Lake Chad | 1.32 | 1.3 | 1.99 | 1.75 | 1.1 | 2.32 | 1.32 |
| 5 | Danube | 0.93 | 0.81 | 0.9 | 0.62 | 0.6 | 0.73 | 0.55 |
| 6 | Volta | 0.91 | 1.27 | 0.92 | 0.71 | 0.63 | 0.74 | 0.83 |
| 7 | Pu Lun T'o | 0.84 | 0.56 | 0.55 | 0.45 | 0.56 | 0.46 | 0.44 |
| 10 | Gash | 0.72 | 1.05 | 2.15 | 2.01 | 0.45 | 0.74 | 1.98 |
| 14 | Orange | 0.65 | 0.49 | 0.97 | 1.15 | 0.81 | 0.79 | 0.72 |
| 38 | Kura-Araks | 0.35 | 0.32 | 0.22 | 0.65 | 0.42 | 0.51 | 0.35 |
| 60 | Incomati | 0.22 | 0.19 | 0.9 | 1.1 | 0.6 | 0.78 | 0.66 |
| 82 | Zambezi | 0.17 | 0.57 | 0.82 | 0.52 | 0.27 | 0.65 | 0.36 |
| 96 | Lotagipi Swamp | 0.14 | 0.93 | 0.28 | 0.32 | 0.46 | 0.14 | 0.21 |

Another basin with a high range in inter-annual variability of runoff situated in the sub-Saharan Africa is the Volta basin. Here, a high increase is predicted for the near future period and the A2 emission scenario. In Togo, the variability will decrease from 0.23 in the control period to 0.19, while it will increase from 0.51 to 0.6 in Mali. Thus, the range will enlarge about 0.23. Also in the medium future period, an increase of the normalized relative to the control period is expected. For the far future and all future time periods for the B1 scenario a decrease is projected.

In the Danube basin the normalized range is also high with a value of 0.93. But if one takes a closer look on the values of inter-annual variability for the riparian countries, they will show a range between low to medium variability. In the control period, Austria has the lowest variability in runoff with a value of 0.15, while Moldova has the highest with 0.35. The same applies to the Ganges basin. With the lowest variability in Bangladesh (0.13) and the highest in India (0.27), it gets a normalized range of 0.8. For both of these basins, a decline in the differences between the countries in inter-annual variability of runoff is predicted.

A basin with a slightly lower normalized range (0.72) but higher inter-annual variability is the Gash river basin. For the B1 scenario, the predictions show a decrease in the range of runoff variability within the basin for the near and medium future time period and an increase to a value of 1.98 in the far future. In the A2 scenario, a different

development is expected. The normalized range will slightly rise in the near future and high increases are projected for the medium and far future. In the time period 2055, the normalized range will peak with a value of 2.15. In this river basin, the development is severe, because not only the differences between the countries increase but also the inter-annual variability itself. While the average value in the control period is 0.66, it will rise to 1.15 in 2055. While water resources will be still quite reliable in Ethiopia (CV = 0.51), they will be very uncertain in the Sudan where inter-annual variability will be about 1.9.
Other basins with high increasing disparities in the reliability of runoff among its riparian countries due to climate change are the Orange, the Incomati and the Zambezi basin in Southern Africa, the Lotagipi Swamp in Eastern Africa and the Kura-Araks basin in the Middle East.

### 3.3.1. Selected basins with high disparities among riparian countries

In the following, selected international river basins with big differences in all indices or great projected changes in future will be highlighted. Moreover, disadvantaged and advantaged riparian countries will be identified. To simplify comparison, average values over all three future time periods and both emission scenarios are calculated. On the basis of these future averages the range of the four indices and the deviation from the basin mean value for each riparian country was build. For inter-annual variability, the direction of deviation was changed. That is done, because a variability above the basin's mean value means that the situation for the BCP is worse than the basin average. Results can be found in the appendix table A.5.
The four international river basins with highest differences in the indices among its riparian countries are all located on the border between the Sahara and sub-Saharan Africa. As an example for these, the mean deviations from the basin mean value are visualized for the Lake Chad basin (Fig. 3.22). In the bar chart, deviations are given in per cent.

In the Lake Chad basin, BCPs of Libya and Cameroon are not included into the comparison because the territorial area in the Chad basin is only 0.19% and 1.96%, respectively.
Countries in the Southern part of the basin are privileged. They are located at the

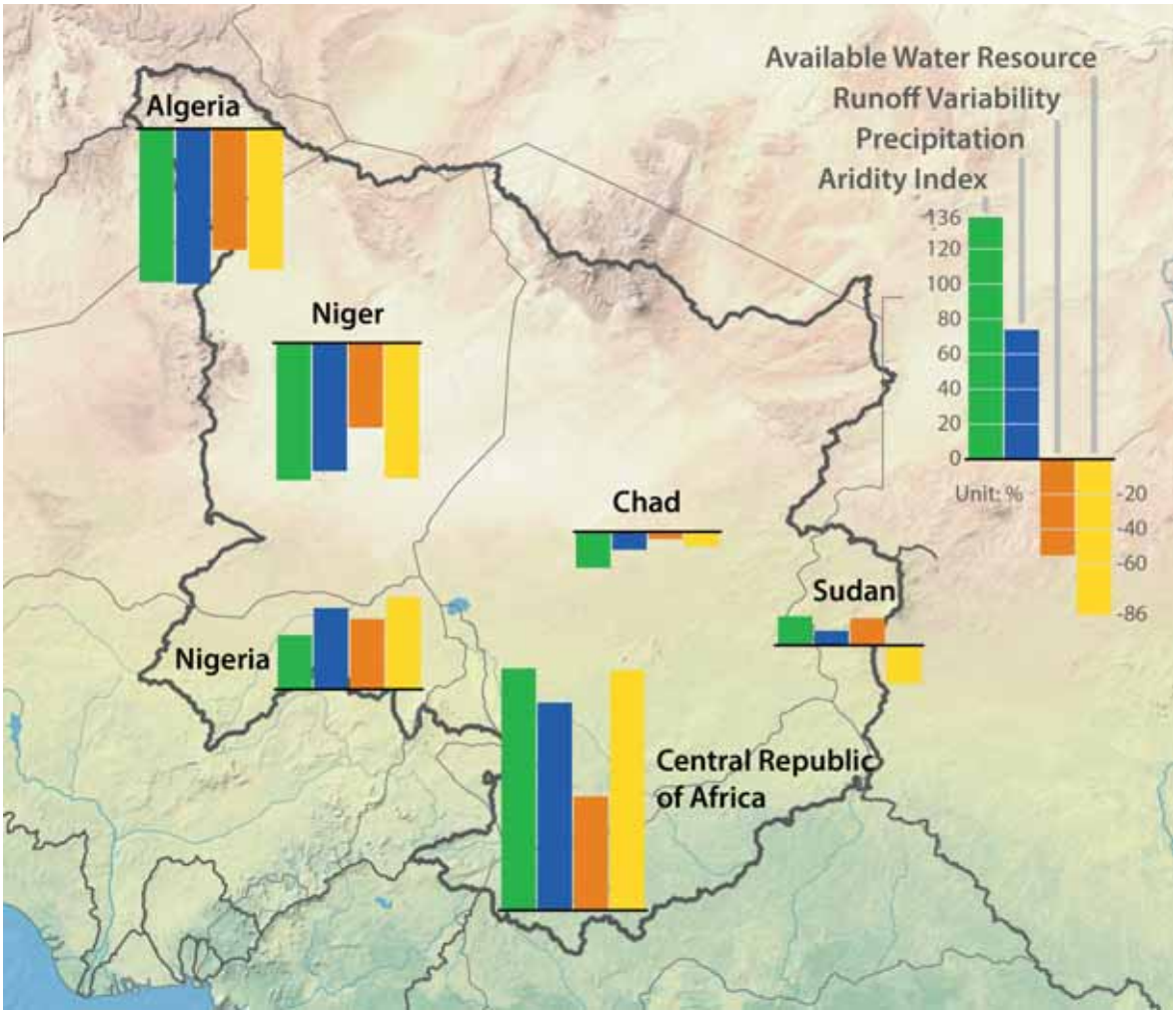


Figure 3.22.: Deviation from the basins average of the riparian countries in the Lake Chad basin.

beginning of the tropical climate zone, while the more northern BCPs are located in the arid Sahel zone. These climate differences are reflected by the differences of the indices. With an average AI of 0.38 the basin is characterized as semi-arid but the AI differs for the BCPs, respectively. The highest AI is detected for the Central Republic of Africa. Its AI is 134% higher than the basin average, while Algeria will have the lowest AI of 0.04. This is also reflected by precipitation and available water resources. The basin average of precipitation will be 666 mm/y and for AWR 156 mm/y. Chad and Sudan will have values near the mean. Sudan will have 53 mm/y more precipitation and 31 mm/y less AWR relative to the basins average. Chad will be have 73 mm/y less precipitation and 14 mm/y less AWR. For Nigeria and the Central Republic of Africa, values will be well above the basins mean. With a deviation of 117% in precipitation and 134% in AWR it will be the most advantaged BCP. Likewise, Ni-

geria will be privileged with 46% more precipitation and 51% more AWR. Located in the Northern part of the basin Algeria and Niger are the disadvantaged BCPs. With deviations of 79% and 77% less in precipitation and 88% and 73% less in AWR these basins have about 334 mm/y less water available than the southern BCPs. The same patterns are observed for the reliability of the water resources. Inter-annual variability is much higher in the northern BCPs of the basin compared to the South.

Similar patterns in distribution of precipitation and AWR as well as inter-annual variability of runoff are found in the neighbouring international river basins.
In the Niger basin, Algeria will be the most disadvantaged BCP as well. In all indices it will lie about 90% below the basin average. The BCP will have an inter-annual variability of 0.95. This is 0.77 higher than in Cameroon, which will have the lowest one. Also in the other indices, the BCP of Cameroon is most privileged followed by Guinea, Nigeria and Benin.
In the Nile basin, only the riparian countries Sudan and Egypt will have values below the basins average for all four indices. Particularly noticeable are high differences among the riparian countries in inter-annual variability of runoff. With a basin mean value of 0.38, the reliability of the runoff will be in a medium range but for the BCPs Sudan and Egypt very high values are projected. In Egypt, the variability will be more than two times higher compared to the basin average.
In the Senegal basin, in Mali the values for the different indices will be near its basin mean. Guinea is the privileged country regarding to water availability. Especially the aridity index and AWR in Guinea will deviate from the mean basin values (AI = 0.33, AWR= 214 mm/y). Its AWR are 135% higher than the basin average. The disadvantaged BCP in the Senegal basin is Mauretania. For all indices, excluding the inter-annual variability of runoff the value is more than 60% below the basins mean.
Furthermore, in the Orange basin in Southern Africa similar inequality patterns are observed among the countries located in different climate zones. For all indices, the BCP of Lesotho will have values above the basin's mean. It is the headwater of the basin and located in a very mountainous and water-rich area. The countries bordering the Orange river get more arid the further away from its spring. In future, in South Africa a mean value for precipitation near the basin's average (499 mm/y) is predicted while the mean values for precipitation of Botswana and Namibia are 16% and 52%, respectively, above the basins mean value. Also the AWR of these countries differ greatly from the future mean value of 80 mm/y. While Lesotho has 120 % more AWR,

Namibia has 71% less water available relative to the mean value.// In Eastern Africa, in all three river basins shared by Ethiopia and its neighbouring countries, Ethiopia is the privileged BCP. In the Awash basin, Djibouti will have 636 mm/y less precipitation and 132 mm/y less AWR than Ethiopia. With the small availability of water resources, differences between the countries are quite significant. The same applies to the Gash basin. It is shared by Ethiopia, Eritrea and Sudan. While Eritrea will have index values near the basin's mean, the values for Ethiopia will be above and the values for Sudan below average. Also in the Logatipi Swamp, Ethiopia will be advantaged. While it will have AWR 114% higher than the basins average of 176 mm/y, in Sudan AWR are 3% lower than the average and in Kenia and Uganda, AWR are about 40% lower.

The international river basins with high differences between its riparian countries are not only situated in Africa. In the Middle East, the Tigris-Euphrates basin is the most affected one due to disparities in water availability among its sharing countries. The little water, which will be available (basin mean = 121 mm/y), is quite reliable with an inter-annual variation of runoff about 0.38. The BCP with the highest variability is Iraq with 0.52, while the variation will be just 0.24 in the BCP of Turkey. These differences are also given in the other indices. While Turkey and Iran will be well above the basins average of the indices, Iraq and Syria will receive less precipitation and will have fewer AWR. The most disadvantaged country will be Syria.
In the Aral Sea basin, the availability of water resources will be low. In future, it will have mean annual precipitation of 368 mm/y. The range will be about 316 mm/y with the highest value in Afghanistan and Tajikistan (about 515 mm/y) and the lowest in Turkmenistan with 207 mm/y. The same BCPs show the same variation for AWR. The range between Turkmenistan and Tajikistan will be 256 mm/y at a mean value of 148 mm/y. Furthermore, the BCPs of Uzbekistan as well as Kazakhstan have AWR below the basin's average.

Disparities in water availability in the Danube basin, the international basin shared by the most countries (18), is visualized in figure 3.23. BCPs not included because of their small area within the basin are those of Albania, Italy, Poland and Switzerland. The basin stretches from its spring in Germany through South Eastern Europe to the Black Sea. Countries bordering the rivers basin have different water balances. Slovenia is the country with the highest AI of 1.91 in future, followed by Austria (1.82) and Germany (1.58). All these countries are classified as humid, while the AI in Moldavia will be

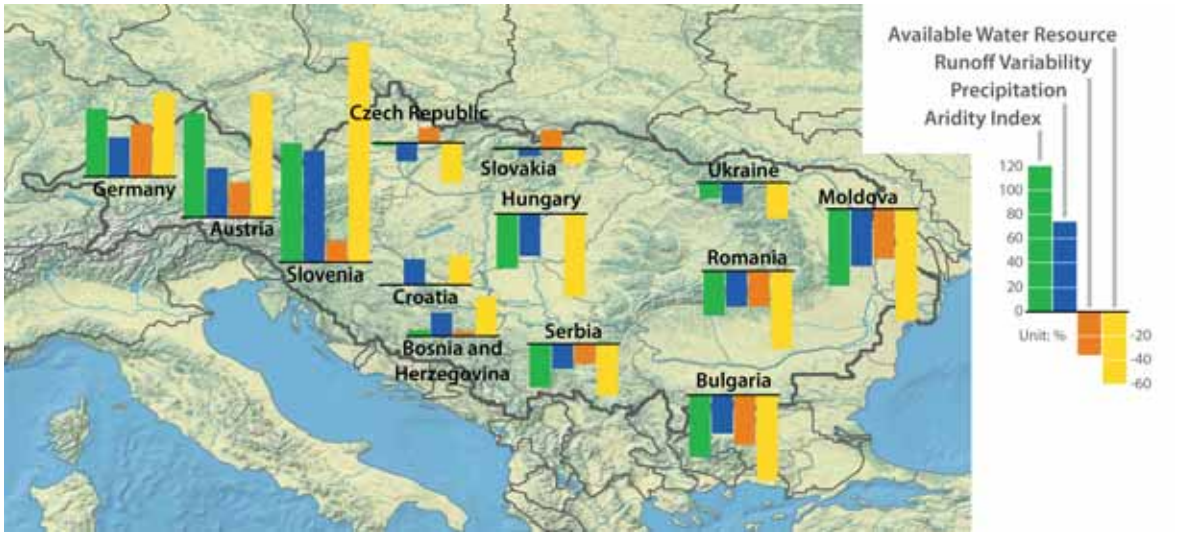


Figure 3.23.: Deviation from the basins average of the riparian countries in the Lake Chad basin.

0.62, which is already categorized as dry sub-humid. Also other BCPs in the South Eastern part of the basin will have AI below 1. These differences in the water balance are also found in the precipitation index and with higher ranges for AWR. The basin's mean value of precipitation will be 822 mm/y with a range of 825 mm/y among the riparian countries. Again, Slovenia will have the highest value with 66% below the mean. Other BCPs which will be advantaged in precipitation are Germany (41%), Austria (30%), Croatia (15%) and Bosnia and Herzegovina (15%). In the remaining BCPs, precipitation values in future will be below the basin average. Deviations above 20% are expected in the Czech Republic, Slovakia, Ukraine and Serbia, while in Hungary, Bulgaria and Romania the differences from the basin's mean annual precipitation will be about 20% to 25%. In Moldova, the BCP's mean value will be 34% above. AWR will show the same patterns of differences of the countries relative to the basin's mean but the range will be greater. Slovenia will have AWR of 131% higher than the basin average. Moldova will be 66% above this value. The yearly reliability of runoff is high with an inter-annual variability of 0.22. The range with a value of 0.16 in this index between the BCPs is small.

The analysis and the figure show, that the privileged countries in the Danube basin are located in the North East of the basin. The closer the BCPs are situated to the estuary (in the Black Sea), the more disadvantaged they will be. Additionally, as shown before these BCPs will be the ones with high decreases in precipitation and AWR in the future due to climate change.

## 3.4. Uncertainty analysis

Uncertainties due to the choice of the model are reflected by the spread of the model results. The normalized standard deviation of the model results due to the choice of the model is visualized in BCP based maps.
For evapotranspiration, the spread due to the choice of GHM is high (Fig. 3.24a,b). Especially in the international river basins Nile, Lake Chad, Niger and Senegal the standard deviation (CV) is above 1.4. In the Congo basin as well as in the northern BCPs of the Zambezi basin, the spread due to the choice of GHM is high with values above 1. Similarly high CV values are evaluated in the river basins of South East Asia and South America. Acceptable are the predicted changes in Northern America, Southern and South Eastern Europe as well as in North East Asia. The uncertainty in the changes is smaller with the choice of GCM compared to the choice of GHM. The CV does not exceed the value of 1.65. In sub-Saharan Africa the spread in the projected changes is mostly below 1, only in some BCPs the CV exceeds that value. Also in South East Asia and South America the uncertainties after choosing GCM are lower than due to the choice of GHM.
This comparison between the spread with respect to the choice of the model, that uncertainties in evapotranspiration are mainly originate by the choice of GHM.

On global basis, the uncertainties in the projected changes of AWR are higher due to the choice of GCM (Fig. 3.24c,d). Especially on the African continent, the Amazon BCP of Brazil, in the river basins of South East Asia and in the basins in Central and Eastern Europe high spreads are detected in the projected changes due to the choice of GCM. In the international river basins in these regions the spreads regarding to the choice of GHM are lower but in other regions the spreads are higher. This applies to the river basins in Southern Africa (located South of the Congo), in Eastern Europe and in Middle North Asia. These results show that uncertainties of the predicted change of AWR due to the choice of GCM are comparable to the choice of GHM. It depends on the region if the uncertainty in the change sis projected by the change of GHM or GCM.

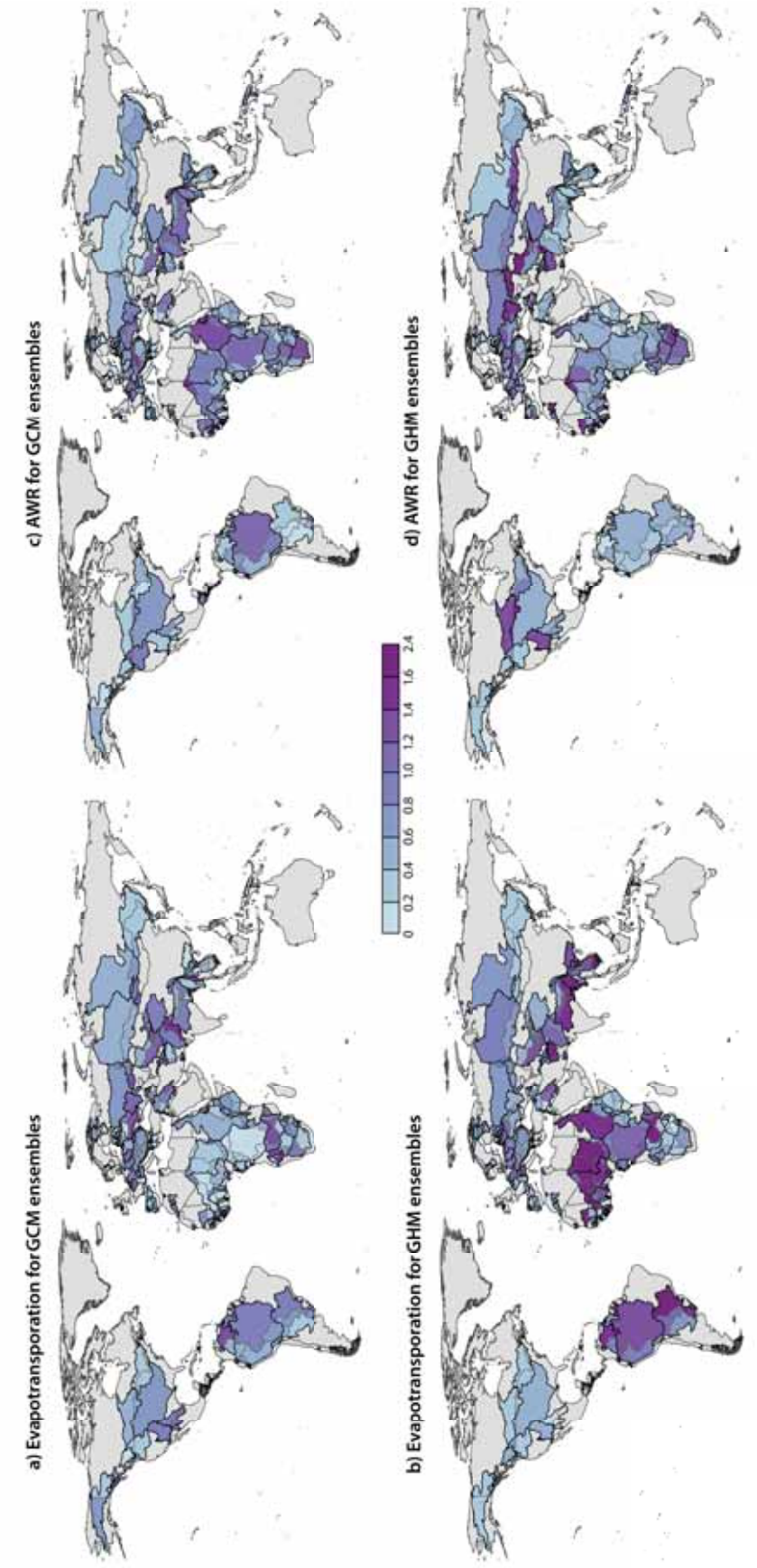


Figure 3.24.: Uncertainties of the changes due to the choice of the model. Mapped is the coefficiant of variation in evapotranspiration due to the choice of GCM (a) or GHM (b) and AWR due to the choice of GCM (c) and GHM (d).

# 4. Discussion

The results of this study show that inequality in the distribution of available water resources due to climate change are increasing, both on a global basis and within international river basins.
The available water resources in international river basins situated in already water scarce areas (Southern Europe, northern parts of Africa, Middle East and parts of Central Asia and northern parts of the USA) are expected to decrease, while at the same time the projections show increases in international basins in the high latitudes and the tropical regions, which are generally wetter and have more water resources available.
Furthermore, on the level of international river basins individually, the results show that in many basins the disparities among the riparian countries will increase. It is projected that the gap of water availability between the disadvantaged and privileged countries within one basin will get larger.

The two factors with major effects on future global water availability are the changes in precipitation and temperature due to climate change (Alcamo et al., 2007). Projected continuous increases in precipitation until the far future time period 2085 are projected for the river basins in the high latitudes, in Central Asia, the northern parts of sub-Saharan Africa and most BCPs in South America while the basins in the southern part of the USA, Mexico and Central America, Southern Europe, many basins in the Middle East, the river basins situated in the Sahara and in the southern part of Africa will experience a decrease in precipitation. These changes in precipitation and also in evapotranspiration and runoff are consistent with those of previous studies (Bates et al., 2008; IPCC, 2007; Chen et al., 2011; Milly et al., 2005). Future changes in evapotranspiration and runoff follow the changes in precipitation. For evapotranspiration, the main influencing factor is the increase in temperatures due to climate change. Thus in most of the river basins evapotranspiration will increase apart from the once where less water is available due to precipitation decreases. This is projected, for ex-

ample, in Southern Europe and the Middle East. The changes in precipitation and evapotranspiration interact and raise or lower the runoff volume. AWR changes are similar to those in runoff because they are depending on it. These follow the changes in precipitation as well.

For precipitation as well as AWR, the same river basins show a discontinuous change over the three future time periods. Moreover, high differences in change between the BCPs of one international river basin are expected in some of these basins. The basins in South East Asia show a projected decrease of AWR in the near future, but an increase in the far future. The river basins in Central Asia will experience a higher increase in precipitation and AWR in the near future than in the two later future time periods. In the Tigris-Euphrates basin, it is projected that the riparian countries will experience an increase in precipitation in the near future but a decrease in the future period afterwards. Additionally, between the BCPs of this basin there are high differences in changes. This becomes clear in the projections of AWR for the near future period where a decrease in AWR is projected for the BCP of Turkey, while the other countries will experience a slight increase in AWR. In the far future period, in the whole Tigris-Euphrates basin AWR are expected to decrease, but in the BCPs of Turkey and Syria they will be twice as high as in Iraq and Iran.

Other basins with high differences in changes between its riparian countries are the Nile basin, where only for the BCP of Egypt a decrease is projected, as well as the Zambezi and Limpopo basin in Southern Africa. Basins with high differences are not only restricted to the African continent. In the Orinoco basin, Venezuela will experience decreases and the available water resources in Bolivia will increase, in the La Plata basin the size of change increases from West to East.

These results of changes in precipitation, evapotranspiration and AWR show, that water resources will mostly decrease in international river basins situated in regions with low water availability while they are increasing in water-rich transboundary river basins.

Changes in these components of the water balance show for the A2 emission scenario and the B1 emission scenario in most of the international river basins and BCPs, individually, the same direction of change, but there are also regions where, due to the scenario differences also the predicted changes differ. Notably, the projected changes differ in the La Plata basin in South America, in basins in Central Europe and the river basins located in the belt between the Congo and South Africa.

Generally, projected changes have higher values for the A2 scenario compared to the

B1 scenario. This applies to all analysed indices. This is probably due to the higher projected increase of temperature for the A2 scenario. Thereby, the intensification of the hydrological cycle could lead to higher precipitation but also to higher variability.

This is reflected in the analysis of the inter-annual variability of runoff. The results of changes show that climate change does not only influence water availability, but also the reliability of precipitation and runoff. Analyses of the inter-annual variability as an index for the yearly reliability of the water resource showed that the changes will be much more significant and more river basins will be affected in the far future period 2085. Affected are predominantly river basins where AWR are also decreasing. Highest increases are projected in the arid and semi-arid regions of the Middle East and Northern Africa with high differences between the BCPs in the Lake Chad and Nile river basin. This increase could be associated with changes in the monsoon pattern of the African monsoon. And the inter-annual variation of precipitation directly feeds through to runoff (Haddeland et al., 2011). The same applies to the projected increasing inter-annual variability of runoff in the international river basins in South-East Asia. Schewe and Levermann (2012) show in their study based on simulation results that through future warming conditions it will come to more frequent failures in the summer monsoon. The reasons are seen in increasing temperatures and changes in the strength of the Pacific Walker circulation in spring. Changes in southern parts of Africa could be explained by changes in the El Niño-Southern oscillation which is a dominant driver in inter-annual and seasonal changes.
Statements of projected changes in the components of the hydrological water balance and the inter-annual variability are all based on thirty-year mean values averaged of the annual mean values of the time period. This means, the results do not state anything about seasonality and if these intra-annual variation will change with climate change. Already today, large parts of monsoon Asia suffer from severe water scarcity in dry periods while the annual availability seems to be sufficient (Gain et al., 2012). In future an intensification of extreme events is predicted (Bates et al., 2008; IPCC, 2007; Alcamo et al., 2007). Through climate change an intensification of the hydrological cycle with an increase of hydrological extremes is predicted (IPCC, 2007). The intensity of the events is expected to increase especially in tropical regions and high latitudes. Also in areas where the projections show decrease in annual mean precipitation, the precipitation intensity will increase with larger gaps between rainfall events. Alcamo et al. (2007) show that through higher annual water availability the risk of extremely

high runoff and precipitation events in global river basins especially in humid regions will increase. For the 2050s and the A2 scenario, about 10% of the global river basins show higher risks of high runoff events which could result in a higher frequency of floods. In contrary, about 16% of the global river basins will experience more low flow events.
These studies show that it would be important to analyse also the changes in seasonality as well as extreme events in international river basins in further investigations. Extreme events can lead to great tension between riparian countries. A good knowledge about changes and developments of floods and drought is required to manage those.

The analysis about water stress using the index of water per capita and year shows that water stress will increase. Water stress is strongly depending on the population density within the BCP. After 2050, water stress will be more depended on the population density than on water availability. This becomes especially visible in the comparison of the BCPs in water stress of the far future time period (2085) between both emission scenarios. While the projections of the A2 scenario show the number of BCPs experiencing water stress is still increasing, the B1 emission scenario describes the number of BCPs with water stress is comparable to the one in the medium future time period (2055). This is explained by the differences in population growth. The high population scenario A2 is based on a population growth of 15 billion by 2100. Projections for the low population scenario B1 show a population growth to 9 billion by the middle of the century and a decline afterwards to 7 million people by 2100 (Nakicenovic et al., 2000). This shows that the population growth has a higher influence on water stress than the changes in the hydro-climatology. This is consistent with the studies of Voeroesmarty et al. (2000) and Alcamo et al. (2007) who state that population growth and increasing water demand outweighs climate change as factor of increasing water stress.
Comparing the water stress results of the BCPs with other studies on country or river basin level, they show that the water stress levels are significantly lower in this study. In studies including a whole country (FAO 2008), there are high differences in water stress between the country and the BCP of an international river basin. For example, Morocco and Algeria are classified experiencing water stress as countries, but the international river basins Guir, Daoura and Don have available water resources above the threshold for water stress. These differences can be explained by the availability of water is only ensured in these areas covered by the BCPs. In the atlas of freshwater

agreements (UNEP, 2002) a map is shown with water stress per international river basins. The water stress levels are higher as in this study. This results from different input variables as available water resource. They used the river discharge as available water while in this study total runoff is used which has higher values because it's not only restricted on the river itself.
Beside water availability, other factors influence a region that is under water stress. As already mentioned in the methods the here used Falkenmark index (Falkenmark et al., 1989) does not include these factors. One important issue if people will experience water stress is the availability of water infrastructure get access to the available water resources. As it was already observed, more and more people are living in urban areas. Water has to come from the surrounding areas to meet the needs of the people. But that is not always possible. Thus, from a local perspective, many cities, which are situated in the river basins, have or will become a water scarcity conditions in future.

The introduced hydro-climatic vulnerability index, that combines indicators stating water availability conditions, appears to summarize the general hydro-climatic situation of a BCP quite well. It is a good way to get an overall impression of the vulnerability of a BCP or region due to prevailing conditions. It brings together the single factors of the hydro-climatology and is a combination of the different factors influencing the vulnerability. The BCPs of the international river basins situated in the south western parts of the USA and South Mexico, in northern Africa and the transition zone to sub-Saharan Africa, in the southern parts of Africa and in the Middle East as well as some in Central Asia have a high to severe vulnerability to the hydro-climatic conditions. Furthermore, the index reveals once again, differences within a transboundary basin. To highlight are the Niger, Lake Chad and Nile basin in the transitional zone between Sahara and sub-Saharan Africa as well as the Tigris-Euphrates and the Aral Sea basin. In the Tigris-Euphrates basin, the BCP of Turkey is not vulnerable to the hydro-climatic conditions, but Syria and Iran have a high hydro-climatic vulnerability which gets worse to a severe vulnerability in future due to climate change.

The results of the comparison about the water availability in the countries within one international river basin indicate that the disparity among them is increasing. This applies to all indices except for the AI, meaning that the water balance of the riparian countries in a international basin will become more equal while the range in the thirty-year annual mean of precipitation, AWR and the inter-annual variability will increase.

This is especially expected in the river basins in transition zones like the river basin Nile, Niger, Lake Chad and Senegal with riparian countries in the Sahara and in sub-Saharan Africa and the Orange basin in Southern Africa. These five basins are with all indices ranked as the five basins with highest disparities among its riparian countries, except for inter-annual variability where the Senegal and Orange rivers are on rank as number 11 and 14, respectively. Besides their differences among the riparian countries, inter-annual water variability will increase in some BCP of these basins because of climate change. Furthermore, water stress is projected to increase in the Nile BCPs of Egypt, Uganda, Burundi and Ruanda, in the Niger basin the BCPs of Niger and Burkina Faso, the part of Nigeria in the Lake Chad basin and the BCP of South Africa in the Orange basin. These combinations could lead to tension between the riparian countries over the rare water resources in future.

Already in the past, there were conflicts among the countries of these basins (TFDD) . The most disadvantaged BCP of the basin, Egypt, was involved in 69 events of which 11 were conflictive. In the other four basins a lower number of events has happened (Orange 18, Senegal 14, Niger and Lake Chad 5) with one to three (Orange) conflictive ones. Changes due to climate change and high disparities among the countries make these transboundary basins highly vulnerable and there will be a risk of conflicts also favoured by the low institutional coverage (river basin organizations or water treaties) in future. De Stefano et al. (2012) developed a treaty-river basin score (treaty-RBO) ranging from zero (high vulnerability) to five (low vulnerability), which describes the institutional resilience of a basin and BCP. Out of the five before mentioned river basins, only the Orange and Nile basin have a treaty-RBO score of low vulnerability. The others have treaty-RBO scores of three in average. Moreover, there are BCPs with a treaty-BCP score of zero and one: the BCPs in the Lake Chad and Niger basin of Algeria as well as the Lake Chad BCP of Sudan.

All mentioned factors together intensify the risk of conflict. Wolf et al. (2003) characterized the Lake Chad, the Senegal and Orange basin as basins at risk for conflict in the near future. Also De Stefano et al. (2012) identified the Lake Chad basin and especially its BCPs Algeria, Libya and Sudan as well as the Niger basin with the BCPs of Algeria and Niger as basins with high hazard and vulnerability level because of its hydro-climatic changes in inter-annual variability in future.

Future hazard due to changes in water availability and reliability also applies to other basins in arid and semi-arid basins. Other basins which could be under risk are the Gash, Awash and Lotagipi Swamp basin in Eastern Africa due to their increasing high

differences in water availability among riparian countries and projected changes. These basins are also listed in De Stefano et al. (2012) as basins with high future hazard level. All of them have a treaty-RBO score of zero.
Furthermore, in one of the hydro-political hot spot basins, the Tigris-Euphrates basin, the projected developments will show risks in future. Additional to great differences of water availability between the riparian countries, the projected changes show increasing water availability for Turkey while it will decrease in Syria and Iran. These greater disparities could lead to more tensions between neighbouring countries.
However, not for all international river basins with high differences in the water availability between its riparian countries and projected decreases due to climate change, a risk of conflict is given. In the transboundary basins in North America, Europe and some basins in Africa, a high institutional coverage is given (De Stefano et al., 2012). Therefore, cooperation in the adaption to the future conditions is more likely. This proofs that a good knowledge of the conditions about water availability and reliability, to which this study contributes, is crucial. Furthermore, a greater knowledge of factors influencing the water availability in a basin and the political stability of countries within a basin should be needed.

However, the results of this study were obtained by analysing the multi-model ensemble comprising three GCMs and six GHMs. As mentioned before, these model runs do not include the direct impact on hydrology by humans. But it should be included because water is the primary medium through which climate change will influence the Earth's ecosystems and therefore people's wellbeing (Gain et al., 2012). Adaption to climate change, future demographic trends, improvements in technology, economic development and related land use changes are the indirect drivers in the increasing demand of water resources. Through these factors induced changes in human water requirements and withdrawals may affect the environment and will intensify the vulnerability of the different regions to projected climate change. Voeroesmarty et al. (2000) states that growing population density, which importance is underlined in the different emission scenario simulations, could outweigh climate change as a factor of increasing water stress. The principle cause of increasing water stress is the higher water consumption which is caused through the higher population density but also through a higher income in many regions of the world. Through growing living standard especially the water withdrawals in the domestic sector are expected to increase Alcamo et al. (2007).

Model uncertainties

The comparison of the simulations of the GHM and GCM model ensemble showed that uncertainties due to the choice of the model (GHM or GCM) cannot be ignored. As already shown in the global studies of Haddeland et al. (2011) and Hagemann et al. (2013), and now in this study with regard to international river basins the uncertainties resulting of the choice of GHM are higher than those resulting of the choice of GCM. This becomes clear in the projected changes of evapotranspiration which show that the uncertainties are largely dominated by the choice of the GHM. These uncertainties can be explained by differences in the model formulation of the GHMs which represent the hydrological processes (Haddeland et al., 2011; Hagemann et al., 2013). As listed in 2.1 the used GHMs differ in their evapotranspiration as well as in their runoff scheme for soil moisture. Differences are especially given in the treatment of evapotranspiration through different model formulations like, for example, Penman-Monteith (in Gwava, MacPDM, Vic) or Priestley-Taylor (in LPJml and WaterGAP). That explains the higher uncertainty due to the choice of GHM in evapotranspiration. For the predicted changes in runoff in most areas the uncertainties due to the GCM exceed the GHM ones. This shows that differences in the runoff scheme of the GHMs have smaller influence on the uncertainties of the model results.
Deeper analysis of the reason for uncertainties is beyond the scope of this study. For the interactions between the processes in the model simulations a wider understanding of each GCM and GHM would be needed.
The approach of the multi model ensemble of different climate impact models (GHMs) forced by different GCMs is a good one because of these uncertainties in the projected changes depending on the choice of GCM or GHM. Multi model ensembles of climate impact models should be used in future studies as it is already proposed by Haddeland et al. (2011) and Hagemann et al. (2013). With the knowledge of the uncertainties it is important that conclusions about the impacts of climate changes should not be based on the results of one GHM (Haddeland et al., 2011), because the differences among them are high, so that only one model is not representative.

# 5. Conclusion

Changes in water availability due to climate change in the 279 international river basins and the bordering BCPs are highly geographically dependent. There are regions, in which precipitation is expected to increase and likewise the water availability. This will occur mainly in the transboundary basins in the Northern latitudes, in the tropical parts of Africa and South America, in Central and North Asia as well as in South East Asia. In the contrary, the available water resources will decrease in the basins of the North West of the USA and Central America, Southern and South Eastern Europe, the northern and southern parts of Africa and the Middle East. Additionally, in many basins with decreasing water availability the inter-annual variability of precipitation and runoff will rise.

Furthermore, the gap in water availability within one international river basin will become greater between the riparian countries. This is projected for nearly all basins but especially for those in climate transition zones.

All these factors could lead to greater tension between the riparian countries in future. Therefore, a good knowledge of the changes due to climate change and the hydro-climatic variability is crucial for the management and better cooperation in international river basins. The analysis of the spread in the results due to the model choice shows that the uncertainties of the projected changes are quite high in some regions. Nevertheless, the use of the model ensemble is the best approach but more model inter-comparison are needed to validate and improve the single climate and climate impact models.

Further investigations should be done to analyze the indirect and direct human impact on available water resources because the availability of the water resources also depend strongly on these factors.

# Bibliography

Alcamo, J., Flörke, M., and Märker, M. (2007). Future long-term changes in global water resources driven by socio-economic and climatic changes. *Hydrological Sciences Journal*, 52(2):247–275.

Bates, B., Kundzewicz, Z., Wu, S., and Palutikof, J. (2008). Climate change and water. Technical paper of the intergovernmental panel on climate change, IPCC Secretariat, Geneva.

Center for International Earth Science Information Network (CIESIN)/Columbia University and United Nations Food and Agriculture Programme (FAO) and Centro Internacional de Agricultura Tropical (CIAT) (2005). Gridded population of the world, version 3 (gpwv3): Population count grid.

Chen, C.and Hagemann, S., Clark, D.and Folwell, S., Gosling, S., Haddeland, I., Hanasaki, N., Heinke, J., Ludwig, F., Voss, F., and Wiltshire, A. (2011). Projected hydrological changes in the 21st century and related uncertainties obtained from a multi-model ensemble. Technical report, Watch Technical Report No.45.

Christensen, N., Wood, A., Voisin, N., Lettenmaier, D., and Palmer, R. (2004). The effects of climate change on the hydrology and water resources of the colorado river basin. *Climatic Change*, 62(1-3):337–363.

CSC (2013). Climate change scenarios for the congo basin. [haensler a., jacob d., kabat p.,ludwig f. (eds.)]. Climate service centre report no. 11, Hamburg, Germany. ISSN: 2192-4058.

De Stefano, L., Duncan, J., Dinar, S., Stahl, K., Strzepek, K. M., and Wolf, A. T. (2010). Mapping the resilience of international river basins to future climate change-induced water variability. In *Water Sector Board discussion paper series paper*, volume 2. The Worldbank, Washington D.C.

De Stefano, L., Duncan, J., Dinar, S., Stahl, K., Strzepek, K. M., and Wolf, A. T. (2012). Climate change and the institutional resilience of international river basins. *Journal of Peace Research*, 49(1):193–209.

Doell, P., Kaspar, F., and Lehner, B. (2003). A global hydrological model for deriving water availability indicators: model tuning and validation. *Journal of Hydrology*, 270(1–2):105 – 134.

El-Fadel, M., El-Sayegh, Y., El-Fadl, K., and Khorbotly, D. (2003). The nile river basin: a case study in surface water conflict resolution. *Journal of Natural Resources & Life Sciences Education*, 32:107–117.

Falkenmark, M., Lundqvist, J., and Widstrand, C. (1989). Macro-scale water scarcity requires micro-scale approaches. *Natural Resources Forum*, 13(4):258–267.

Gain, A. K., Giupponi, C., and Renaud, F. G. (2012). Climate change adaptation and vulnerability assessment of water resources systems in developing countries: A generalized framework and a feasibility study in bangladesh. *Water*, 4(2):345–366.

Gosling, S. N. and Arnell, N. W. (2011). Simulating current global river runoff with a global hydrological model: model revisions, validation, and sensitivity analysis. *Hydrological Processes*, 25(7):1129–1145.

Greenhouse Gas Initiative (GGI) Program of the International Institute for Applied Systems Analysis (IIASA) (2007). Ggi downscaled spatially explicit socio-economic scenario data.

Gruebler, A., O'Neill, B., Riahi, K., Chirkov, V., Goujon, A., Kolp, P., Prommer, I., Scherbov, S., and Slentoe, E. (2007). Regional, national, and spatially explicit scenarios of demographic and economic change based on {SRES}. *Technological Forecasting and Social Change*, 74(7):980 – 1029. <ce:title>Greenhouse Gases - Integrated Assessment</ce:title>.

Haddadin, M. J. and Shamir, U. (2003). Jordan case study. UNESCO-IHP.

Haddeland, I., Clark, D. B., Franssen, W., Ludwig, F., Voß, F., Arnell, N. W., Bertrand, N., Best, M., Folwell, S., Gerten, D., Gomes, S., Gosling, S. N., Hagemann, S., Hanasaki, N., Harding, R., Heinke, J., Kabat, P., Koirala, S., Oki, T., Polcher,

J., Stacke, T., Viterbo, P., Weedon, G. P., and Yeh, P. (2011). Multimodel estimate of the global terrestrial water balance: Setup and first results. *Journal of Hydrometeorology*, 12:869–884.

Hagemann, S., Chen, C., Clark, D. B., Folwell, S., Gosling, S. N., Haddeland, I., Hanasaki, N., Heinke, J., Ludwig, F., Voss, F., and Wiltshire, A. J. (2013). Climate change impact on available water resources obtained using multiple global climate and hydrology models. *Earth System Dynamics*, 4(1):129–144.

Harding, R., Warnaars, T., Weedon, G., Wiberg, D., Hagemann, S., Tallaksen, L., van Lanen, H., Blyth, E., Ludwig, F., and P., K. (2011). Executive summary of the completed watch project. Technical report, Watch Technical Report No.56.

IPCC (2007). *Climate Change 2007 - The Physical Science Basis: Working Group I Contribution to the Fourth Assessment Report of the IPCC*. Cambridge University Press, Cambridge, UK and New York, NY, USA.

Middleton, N., Thomas, D., and Programme, U. N. E. (1992). *World Atlas of Desertification*. Arnold.

Milly, P., Dunne, K., and A., V. (2005). Global pattern of trends in streamflow and water availability in a changing climate. *Nature*, 438(9066):347–350.

Nakicenovic, N., Alcamo, J., Davis, G., de Vries, B., Fenhann, J.and Gaffin, S., Gregory, K., Grübler, A., Jung, T., Kram, T., La Rovere, E., Michealis, L., Mori, S., Morita, T., Pepper, W., Pitcher, H., Price, L., Riahi, K., Roehrl, A., Rogner, H.-H. andSankovski, A., Schlesinger, M., Shukla, O.and Smith, S., Swart, R., van Rooijen, S., Victor, N., and Dadi, Z. (2000). *IPCC Special report on Emission Scenarios*. Cambridge University Press, Cambridge,UK and New York, NY, USA.

Piani, C., Weedon, G., Best, M., Gomes, S., Viterbo, P., Hagemann, S., and Haerter, J. (2010). Statistical bias correction of global simulated daily precipitation and temperature for the application of hydrological models. *Journal of Hydrology*, 395(3–4):199 – 215.

Rijsberman, F. R. (2006). Water scarcity: Fact or fiction? *Agricultural Water Management*, 80(1–3):5 – 22. <ce:title>Special Issue on Water Scarcity: Challenges and Opportunities for Crop Science</ce:title> <xocs:full-name>Selected plenary and

symposia papers from the theme, presented at the Fourth International Crop Science Congress, Brisbane, Australia, 26 September to 1 October 2004</xocs:full-name>.

Schewe, J. and Levermann, A. (2012). A statistically predictive model for future monsoon failure in india. *Environmental Research Letters*, 7(4):044023.

Schulzweida, U., Kornblueh, L., and Quast, R. (2012). *CDO User's Guide*, version 1.5.9 edition.

Smakhtin, V., Revenga, C., and Döll, P. (2004). A pilot global assessment of environmental water requirements and scarcity. *Water International*, 29(3):307–317.

Smith, S. E. and AI-Rawahy, H. M. (1990). The blue nile: Potential for conflict and alternatives for meeting future demands. *Water International*, 15(4):217–222.

Stahl, K. (2007). Hydrology of world's international river basins: Hydrological parameters for use in global studies of international water - relations. GRDC Report Series, Report 37, 52pp.

(TFDD), T. F. D. D. International freshwater treaty database. Oregon State University.

UN Water (2013). Un water - international year of cooperation 2013.

UNEP (2002). *Atlas of international freshwater agreements*. UNEP and Oregon State University, UNEP press, Nairobi, Kenya.

Unesco (1979). *Map of the world distribution of arid regions: explanatory note*. MAB technical notes. Unesco.

Voeroesmarty, C. J., Green, P., Salisbury, J., and Lammers, R. B. (2000). Global water resources: Vulnerability from climate change and population growth. *Science*, 289(5477):284–288.

Wolf, A. T., Natharius, J. A., Danielson, J. J., Ward, B. S., and Pender, J. K. (1999). International river basins of the world. *International Journal of Water Resources Development*, 15(4):387–427.

Wolf, A. T., Yoffe, S. B., and Giordano, M. (2003). International waters: Identifying basins at risk. In *In Water Policy 5:29-60 Wonink, S.J., Kok, M.T.J. and Hilderink, H.B.M. (2005). Vulnerability and Human Well-being. Report 500019003/2005. Netherlands Environmental Assessment Agency, Bilthoven World Bank*.

Yoffe, S., Fiske, G., Giordano, M., Giordano, M., Larson, K., Stahl, K., and Wolf, A. T. (2004). Geography of international water conflict and cooperation: Data sets and applications. *Water Resources Research*, 40(5).

## Declaration

I herewith declare that I have completed the present thesis independently and only making use only of the specified literature and aids.

Freiburg im Breisgau, 20. December 2013

Barbara Sailer

## Acknoledgements

I would like to thank the following people who have contributed to the outcome of this work:

- First of all, I like to thank Dr. Kerstin Stahl for making this work possible and all given support . item Thanks to Dr. Jens Lange for co-supervising this study.
- Thanks to Friedjoff Trautwein for his constructive and inspiring feedback in all cartographic questions and a special thanks for the ongoing moral support.
- Thanks to my friends Hedda Straehler-Pohl , Marleen Stuhr, Svenja Voss and Riona Patak for proofreading this work.
- Worries and laughs were also shared with other friends, family and flat mates I would like to thank greatly.
- Special thanks go to my parents for giving me the opportunity to study, their encouragement and indispensable support.

# List of Abbreviations

**AI** Aridity Index

**AWR** Awailable Water Resource

**BCP** Basin Country Polygon

**CDO** Climate Data Operators

**CV** Coefficant of Variation

**EWR** Environmental Requirements

**GCM** General Circulation Model

**GHM** Global Hydrological Model

**hcVI** Hydro-climatic Vulnerability Index

**IPCC** Intergovernmental Panel on Climate Change

**P** Precipitation

**RBO** River Basin Organisation

**SRES** IPCC Special Report on Emission Scenarios

**TFDD** Transboundary Freshwater Dispute Database

**WATCH** Water and global Change

# A. Appendix I: Tables of differences between the riparian states in a basin and their changes

In the following tables , the international river basins are ranked according to their normalized range in the control period of the different indices. The international river basin with the highest normalized range ,and therefore with the highest disparities between its riparian countries, is assigned to 1. Only basins are listed which have a normalized range value higher than 0.3 in the control period.

Table A.1.: Differences of precipitation between the riparian countries (expressed through the normalized range) of international river basins and its future changes

| Rank | River basin | Precipitation | | | | |
|---|---|---|---|---|---|---|
| | | Control Period | Future Mean | Trend | Highest change | |
| | | | | | When | Value |
| 1 | Lake Chad | 2.07 | 2.16 | increase | A2 2085 | 2.29 |
| 2 | Niger | 1.71 | 1.82 | increase | A2 2025 | 1.76 |
| 3 | Senegal | 1.42 | 1.43 | increase | A2 2055 | 1.48 |
| 4 | Nile | 1.41 | 1.51 | increase | A2 2085 | 1.57 |
| 5 | Orange | 1.27 | 1.29 | increase | A2 2025 | 1.33 |
| 6 | Ganges | 1.2 | 1.2 | decrease | A2 2025 | 1.13 |
| 7 | Awash | 1.18 | 1.19 | increase | B1 2025 | 1.23 |
| 8 | Alsek | 1.01 | 1.11 | increase | A2 2085 | 1.23 |
| 9 | Lotagipi Swamp | 1.01 | 1.11 | increase | A2 2085 | 1.2 |
| 10 | Gash | 0.98 | 1.08 | increase | A2 2085 | 1.15 |
| 11 | Danube | 0.94 | 0.96 | increase | B1 2055 | 1.01 |
| 12 | Kunene | 0.93 | 1.01 | increase | B1 2085 | 1.1 |
| 13 | Seno Union | 0.93 | 1.11 | increase | A2 2085 | 1.26 |
| 14 | Taku | 0.91 | 1 | increase | A2 2085 | 1.1 |
| 15 | Aral Sea | 0.89 | 0.93 | increase | B1 2025 | 0.97 |
| 16 | Gallegos | 0.86 | 1.03 | increase | A2 2085 | 1.16 |
| 17 | Coruh | 0.79 | 0.78 | decrease | A2 2085 | 0.76 |
| 18 | Okavango | 0.77 | 0.78 | increase | B1 2085 | 0.86 |
| 19 | Kura-Araks | 0.76 | 0.71 | decrease | A2 2085 | 0.68 |
| 20 | Aysen | 0.75 | 0.75 | decrease | A2 2085 | 0.69 |
| 21 | Lake Turkana | 0.7 | 0.73 | increase | B1 2085 | 0.75 |
| 22 | Mekong | 0.68 | 0.74 | increase | A2 2025 | 0.83 |
| 23 | Tigris-Euphrates | 0.68 | 0.73 | increase | A2 2085 | 0.77 |
| 24 | Rhine | 0.67 | 0.65 | decrease | A2 2085 | 0.75 |
| 25 | Salween | 0.67 | 0.68 | increase | A2 2085 | 0.63 |
| 26 | Pu-Lun-T'o | 0.66 | 0.62 | decrease | A2 2085 | 0.57 |
| 27 | Amazon | 0.61 | 0.7 | increase | A2 2085 | 0.81 |
| 28 | Volta | 0.6 | 0.57 | decrease | A2 2055 | 0.53 |
| 29 | La Plata | 0.59 | 0.56 | decrease | B1 2055 | 0.54 |
| 30 | Po | 0.59 | 0.58 | decrease | A2 2025 | 0.55 |
| 31 | Amur | 0.56 | 0.63 | increase | A2 2085 | 0.68 |
| 32 | Chira | 0.55 | 0.56 | increase | B1 2055 | 0.59 |
| 33 | San Juan | 0.55 | 0.57 | increase | A2 2025 | 0.51 |
| 34 | Hari | 0.53 | 0.51 | decrease | A2 2085 | 0.62 |
| 35 | Indus | 0.53 | 0.56 | increase | A2 2085 | 0.42 |
| 36 | Dra | 0.52 | 0.42 | decrease | A2 2085 | 0.33 |
| 37 | Tarim | 0.49 | 0.45 | decrease | A2 2085 | 0.34 |
| 38 | Baker | 0.47 | 0.51 | increase | A2 2055 | 0.52 |
| 39 | Daoura | 0.47 | 0.39 | decrease | A2 2085 | 0.32 |
| 40 | Irrawaddy | 0.46 | 0.54 | increase | A2 2085 | 0.63 |
| 41 | Congo | 0.44 | 0.5 | increase | A2 2025 | 0.51 |
| 42 | Helmand | 0.44 | 0.46 | increase | A2 2085 | 0.38 |

| Rank | River basin | Precipitation | | | | |
|---|---|---|---|---|---|---|
| | | Control Period | Future Mean | Trend | Highest change | |
| | | | | | When | Value |
| 43 | Oder (Odra) | 0.44 | 0.41 | decrease | A2 2085 | 0.53 |
| 44 | Red | 0.44 | 0.45 | increase | A2 2085 | 0.47 |
| 45 | Ob | 0.43 | 0.49 | increase | A2 2085 | 0.55 |
| 46 | Guir | 0.42 | 0.34 | decrease | A2 2085 | 0.35 |
| 47 | Yelcho | 0.42 | 0.4 | decrease | A2 2055 | 0.29 |
| 48 | Yenisey | 0.42 | 0.54 | increase | A2 2085 | 0.63 |
| 49 | Drin | 0.41 | 0.38 | decrease | B1 2025 | 0.39 |
| 50 | Gambia | 0.41 | 0.41 | increase | A2 2085 | 0.36 |
| 51 | Lake Titicaca | 0.41 | 0.46 | increase | A2 2085 | 0.39 |
| 52 | Tumbes | 0.41 | 0.4 | decrease | A2 2085 | 0.51 |
| 53 | Pascua | 0.4 | 0.44 | increase | A2 2085 | 0.36 |
| 54 | Terek | 0.4 | 0.39 | decrease | A2 2085 | 0.47 |
| 55 | Douro | 0.39 | 0.34 | decrease | A2 2085 | 0.31 |
| 56 | Etosha/Cuvelai | 0.38 | 0.41 | increase | B1 2085 | 0.47 |
| 57 | Puelo | 0.38 | 0.34 | decrease | A2 2085 | 0.26 |
| 58 | Yaqui | 0.38 | 0.34 | decrease | A2 2085 | 0.27 |
| 59 | Jordan | 0.37 | 0.3 | decrease | A2 2085 | 0.43 |
| 60 | Ogooue | 0.37 | 0.4 | increase | A2 2085 | 0.22 |
| 61 | Skagit | 0.37 | 0.41 | increase | A2 2085 | 0.42 |
| 62 | Juba-Shibeli | 0.36 | 0.41 | increase | A2 2085 | 0.47 |
| 63 | Lake Prespa | 0.36 | 0.33 | decrease | A2 2085 | 0.3 |
| 64 | Mino | 0.36 | 0.31 | decrease | A2 2085 | 0.28 |
| 65 | Sepik | 0.34 | 0.39 | increase | A2 2085 | 0.52 |
| 66 | Zambezi | 0.34 | 0.39 | increase | A2 2085 | 0.44 |
| 67 | Little Scarcies | 0.32 | 0.32 | decrease | A2 2085 | 0.31 |
| 68 | Palena | 0.32 | 0.3 | decrease | A2 2085 | 0.26 |
| 69 | Limpopo | 0.31 | 0.31 | decrease | A2 2085 | 0.34 |
| 70 | Oral | 0.31 | 0.32 | increase | B1 2085 | 0.34 |
| 71 | Incomati | 0.3 | 0.3 | increase | A2 2055 | 0.29 |

Table A.2.: Differences of the aridity index between the riparian countries (expressed through the normalized range) of international river basins and its future changes

| Rank | River basin | Aridity Index | | | | |
|---|---|---|---|---|---|---|
| | | Control Period | Future Mean | Trend | Highest change | |
| | | | | | When | Value |
| 1 | Lake Chad | 2.25 | 2.04 | decrease | A2 2085 | 1.74 |
| 2 | Niger | 2.02 | 1.85 | decrease | A2 2085 | 1.57 |
| 3 | Orange | 1.79 | 1.77 | decrease | A2 2085 | 1.61 |
| 4 | Senegal | 1.78 | 1.64 | decrease | A2 2085 | 1.31 |
| 5 | Nile | 1.39 | 1.39 | decrease | B1 2025 | 1.46 |
| 6 | Awash | 1.37 | 1.35 | decrease | A2 2085 | 1.25 |
| 7 | Aral Sea | 1.28 | 1.31 | increase | A2 2085 | 1.15 |
| 8 | Gash | 1.27 | 1.32 | increase | A2 2055 | 1.24 |
| 9 | Lotagipi Swamp | 1.16 | 1.11 | decrease | A2 2085 | 1 |
| 10 | Danube | 1.11 | 0.96 | decrease | A2 2085 | 0.84 |
| 11 | Tigris-Euphrates | 1.09 | 0.99 | decrease | A2 2085 | 0.77 |
| 12 | Seno Union | 1.03 | 1.23 | increase | A2 2085 | 1.31 |
| 13 | Kura-Araks | 0.98 | 0.83 | decrease | A2 2085 | 0.68 |
| 14 | Rhine | 0.97 | 0.78 | decrease | A2 2085 | 0.64 |
| 15 | Gallegos | 0.94 | 1.12 | increase | A2 2085 | 1 |
| 16 | Taku | 0.94 | 0.95 | increase | A2 2085 | 1.19 |
| 17 | Baraka | 0.93 | 0.87 | decrease | A2 2085 | 0.8 |
| 18 | Kunene | 0.92 | 0.95 | increase | B1 2085 | 1.05 |
| 19 | Alsek | 0.91 | 0.93 | increase | A2 2085 | 1.04 |
| 20 | Pu-Lun-T'o | 0.9 | 0.82 | decrease | A2 2085 | 0.67 |
| 21 | Okavango | 0.87 | 0.85 | decrease | A2 2085 | 0.76 |
| 22 | Lake Turkana | 0.84 | 0.83 | decrease | A2 2085 | 0.76 |
| 23 | Indus | 0.82 | 0.69 | decrease | A2 2085 | 0.52 |
| 24 | Tarim | 0.82 | 0.73 | decrease | A2 2085 | 0.64 |
| 25 | Aysen | 0.79 | 0.75 | decrease | A2 2085 | 0.63 |
| 26 | Po | 0.79 | 0.65 | decrease | A2 2085 | 0.5 |
| 27 | Ganges | 0.78 | 0.73 | decrease | B1 2085 | 0.81 |
| 28 | Ob | 0.78 | 0.78 | decrease | A2 2025 | 0.68 |
| 29 | Hari | 0.77 | 0.74 | decrease | A2 2085 | 0.57 |
| 30 | Volta | 0.77 | 0.71 | decrease | A2 2055 | 0.66 |
| 31 | Amur | 0.75 | 0.77 | increase | A2 2055 | 0.79 |
| 32 | Coruh | 0.71 | 0.63 | decrease | A2 2085 | 0.53 |
| 33 | Juba-Shibeli | 0.71 | 0.8 | increase | A2 2085 | 0.85 |
| 34 | Dra | 0.69 | 0.55 | decrease | A2 2085 | 0.4 |
| 35 | Yenisey | 0.67 | 0.76 | increase | A2 2085 | 0.82 |
| 36 | Chira | 0.66 | 0.65 | decrease | A2 2025 | 0.61 |
| 37 | Terek | 0.66 | 0.55 | decrease | A2 2085 | 0.68 |
| 38 | Tumbes | 0.66 | 0.64 | decrease | A2 2085 | 0.4 |
| 39 | Amazon | 0.64 | 0.68 | increase | A2 2085 | 0.77 |
| 40 | Guir | 0.63 | 0.52 | decrease | B1 2025 | 0.63 |
| 41 | Baker | 0.62 | 0.65 | increase | A2 2085 | 0.59 |
| 42 | Daoura | 0.62 | 0.51 | decrease | A2 2085 | 0.4 |

| Rank | River basin | Aridity Index | | | | |
|---|---|---|---|---|---|---|
| | | Control Period | Future Mean | Trend | Highest change When | Value |
| 43 | Gambia | 0.6 | 0.56 | decrease | A2 2085 | 0.48 |
| 44 | Helmand | 0.59 | 0.58 | decrease | A2 2025 | 0.66 |
| 45 | Oder | 0.59 | 0.47 | decrease | B1 2085 | 0.69 |
| 46 | Pascua | 0.59 | 0.65 | increase | A2 2085 | 0.38 |
| 47 | Lake Titicaca | 0.58 | 0.56 | decrease | B1 2025 | 0.54 |
| 48 | San Juan | 0.58 | 0.55 | decrease | A2 2085 | 0.48 |
| 49 | Columbia | 0.57 | 0.5 | decrease | A2 2025 | 0.51 |
| 50 | La Plata | 0.57 | 0.59 | increase | A2 2085 | 0.45 |
| 51 | Ili | 0.53 | 0.54 | increase | A2 2085 | 0.43 |
| 52 | Yelcho | 0.52 | 0.46 | decrease | A2 2085 | 0.34 |
| 53 | Incomati | 0.5 | 0.47 | decrease | A2 2085 | 0.45 |
| 54 | Irrawaddy | 0.48 | 0.49 | increase | B1 2025 | 0.52 |
| 55 | Jordan | 0.47 | 0.38 | decrease | A2 2085 | 0.31 |
| 56 | Palena | 0.47 | 0.41 | decrease | A2 2085 | 0.25 |
| 57 | Struma | 0.47 | 0.34 | decrease | A2 2085 | 0.24 |
| 58 | Asi | 0.45 | 0.36 | decrease | A2 2055 | 0.46 |
| 59 | Congo | 0.45 | 0.43 | decrease | A2 2085 | 0.37 |
| 60 | Oral | 0.45 | 0.43 | decrease | A2 2085 | 0.37 |
| 61 | Sepik | 0.45 | 0.44 | decrease | A2 2085 | 0.25 |
| 62 | Rhone | 0.44 | 0.38 | decrease | A2 2085 | 0.29 |
| 63 | Drin | 0.43 | 0.35 | decrease | A2 2085 | 0.27 |
| 64 | Limpopo | 0.42 | 0.39 | decrease | A2 2055 | 0.36 |
| 65 | Puelo | 0.42 | 0.34 | decrease | A2 2085 | 0.23 |
| 66 | Etosha | 0.4 | 0.4 | decrease | B1 2085 | 0.46 |
| 67 | Murgab | 0.4 | 0.39 | decrease | A2 2085 | 0.3 |
| 68 | Dniester | 0.39 | 0.37 | decrease | A2 2085 | 0.32 |
| 69 | Skagit | 0.37 | 0.4 | increase | A2 2085 | 0.35 |
| 70 | Torne | 0.37 | 0.37 | decrease | B1 2085 | 0.45 |
| 71 | Mekong | 0.35 | 0.36 | increase | A2 2085 | 0.32 |
| 72 | Ogooue | 0.35 | 0.31 | decrease | A2 2085 | 0.27 |
| 73 | Neretva | 0.32 | 0.23 | decrease | B1 2025 | 0.29 |
| 74 | Roia | 0.32 | 0.24 | decrease | A2 2085 | 0.35 |
| 75 | Tami | 0.32 | 0.32 | decrease | A2 2085 | 0.17 |
| 76 | Zarumilla | 0.32 | 0.33 | increase | A2 2085 | 0.19 |
| 77 | Sulak | 0.31 | 0.28 | decrease | A2 2085 | 0.21 |
| 78 | Zambezi | 0.31 | 0.35 | increase | A2 2085 | 0.44 |
| 79 | Lake Prespa | 0.3 | 0.24 | decrease | A2 2085 | 0.2 |
| 80 | Little Scarcies | 0.3 | 0.25 | decrease | A2 2085 | 0.2 |
| 81 | Nestos | 0.3 | 0.2 | decrease | A2 2085 | 0.15 |
| 82 | Yaqui | 0.3 | 0.24 | decrease | A2 2085 | 0.13 |

Table A.3.: Differences of available water resources between the riparian countries (expressed through the normalized range) of international river basins and its future changes

| Rank | River basin | Available water resources | | | | |
|---|---|---|---|---|---|---|
| | | Control Period | Future Mean | Trend | Highest change | |
| | | | | | When | Value |
| 1 | Senegal | 2.35 | 2.5 | Increase | A2 2055 | 2.81 |
| 2 | Lake Chad | 2.29 | 2.46 | Increase | A2 2085 | 2.84 |
| 3 | Niger | 2.1 | 2.28 | Increase | A2 2085 | 2.57 |
| 4 | Orange | 2.03 | 2.02 | decrease | A2 2025 | 2.48 |
| 5 | Nile | 2.02 | 2.2 | Increase | A2 2085 | 2.3 |
| 6 | Danube | 1.76 | 1.64 | decrease | A2 2085 | 1.5 |
| 7 | Aral Sea | 1.71 | 1.79 | Increase | B1 2025 | 1.9 |
| 8 | Lotagipi Swamp | 1.65 | 1.9 | Increase | A2 2085 | 2.33 |
| 9 | Gash | 1.55 | 1.72 | Increase | A2 2085 | 1.93 |
| 10 | Seno Union | 1.39 | 1.78 | Increase | A2 2085 | 2.23 |
| 11 | Hari | 1.35 | 1.18 | decrease | A2 2085 | 0.83 |
| 12 | Okavango | 1.34 | 1.21 | decrease | B1 2085 | 1.47 |
| 13 | Gallegos | 1.33 | 1.7 | Increase | A2 2085 | 2.1 |
| 14 | Ganges | 1.3 | 1.33 | Increase | A2 2025 | 1.14 |
| 15 | Pu-Lun-T'o | 1.29 | 1.11 | decrease | A2 2085 | 0.92 |
| 16 | Amur | 1.22 | 1.35 | Increase | A2 2085 | 1.44 |
| 17 | Kura-Araks | 1.22 | 1.04 | decrease | A2 2085 | 0.82 |
| 18 | Awash | 1.18 | 1.06 | decrease | B1 2025 | 1.33 |
| 19 | Rhine | 1.16 | 1.02 | decrease | A2 2085 | 0.83 |
| 20 | Tigris-Euphrates | 1.16 | 1.23 | Increase | A2 2025 | 1.61 |
| 21 | Volta | 1.14 | 1.2 | Increase | A2 2085 | 1.43 |
| 22 | Yenisey | 1.14 | 1.31 | Increase | A2 2085 | 1.44 |
| 23 | La Plata | 1.13 | 1.19 | Increase | A2 2025 | 1.1 |
| 24 | Amazon | 1.06 | 1.24 | Increase | A2 2085 | 1.57 |
| 25 | Kunene | 1.03 | 1.18 | Increase | B1 2085 | 1.51 |
| 26 | Lake Turkana | 1.01 | 1.07 | Increase | B1 2055 | 1.13 |
| 27 | Indus | 0.99 | 0.8 | decrease | A2 2055 | 0.66 |
| 28 | Alsek | 0.95 | 1.03 | Increase | A2 2085 | 1.19 |
| 29 | Taku | 0.95 | 1.06 | Increase | A2 2085 | 1.23 |
| 30 | Aysen | 0.92 | 0.91 | decrease | A2 2085 | 0.79 |
| 31 | Yaqui | 0.91 | 0.7 | decrease | A2 2085 | 0.32 |
| 32 | Tarim | 0.9 | 0.91 | Increase | A2 2085 | 0.69 |
| 33 | Gambia | 0.89 | 0.87 | decrease | A2 2085 | 0.8 |
| 34 | Ili | 0.89 | 0.85 | decrease | A2 2055 | 0.92 |
| 35 | Coruh | 0.87 | 0.83 | decrease | B1 2025 | 0.89 |
| 36 | Po | 0.87 | 0.91 | Increase | A2 2055 | 0.94 |
| 37 | Oder (Odra) | 0.86 | 0.71 | decrease | A2 2085 | 0.54 |
| 38 | Terek | 0.86 | 0.79 | decrease | A2 2085 | 0.66 |
| 39 | Dra | 0.82 | 0.56 | decrease | A2 2085 | 0.32 |
| 40 | Mekong | 0.82 | 0.97 | Increase | A2 2085 | 1.11 |
| 41 | San Juan | 0.81 | 0.77 | decrease | A2 2085 | 0.65 |
| 42 | Tumbes | 0.81 | 0.84 | Increase | A2 2025 | 0.75 |
| 43 | Chira | 0.79 | 0.91 | Increase | A2 2085 | 1.1 |
| 44 | Baraka | 0.78 | 0.98 | Increase | A2 2085 | 1.53 |
| 45 | Juba-Shibeli | 0.78 | 0.97 | Increase | A2 2085 | 1.26 |
| 46 | Bia | 0.73 | 0.67 | decrease | A2 2085 | 0.61 |
| 47 | Lake Titicaca | 0.71 | 0.81 | Increase | A2 2085 | 0.93 |

| Rank | River basin | Available water resources | | | | |
|---|---|---|---|---|---|---|
| | | Control Period | Future Mean | Trend | Highest change | |
| | | | | | When | Value |
| 48 | Pascua | 0.71 | 0.83 | Increase | A2 2085 | 0.97 |
| 49 | Congo | 0.69 | 0.85 | Increase | A2 2085 | 0.97 |
| 50 | Douro | 0.69 | 0.55 | decrease | A2 2085 | 0.42 |
| 51 | Etosha/Cuvelai | 0.68 | 0.8 | Increase | B1 2085 | 1.19 |
| 52 | Incomati | 0.68 | 0.56 | decrease | A2 2085 | 0.42 |
| 53 | Murgab | 0.66 | 0.52 | decrease | A2 2085 | 0.35 |
| 54 | Columbia | 0.63 | 0.51 | decrease | A2 2085 | 0.43 |
| 55 | Asi | 0.62 | 0.47 | decrease | A2 2085 | 0.25 |
| 56 | Salween | 0.62 | 0.77 | increase | A2 2085 | 1.03 |
| 57 | Red | 0.61 | 0.64 | increase | A2 2085 | 0.7 |
| 58 | Baker | 0.58 | 0.62 | increase | A2 2025 | 0.66 |
| 59 | Drin | 0.57 | 0.5 | decrease | A2 2025 | 0.55 |
| 60 | Lake Prespa | 0.56 | 0.46 | decrease | A2 2085 | 0.37 |
| 61 | Tano | 0.56 | 0.48 | decrease | A2 2085 | 0.41 |
| 62 | Helmand | 0.55 | 0.59 | increase | B1 2085 | 0.63 |
| 63 | Ogooue | 0.55 | 0.51 | decrease | A2 2085 | 0.71 |
| 64 | Sepik | 0.55 | 0.65 | increase | A2 2085 | 0.76 |
| 65 | Dniester | 0.52 | 0.5 | decrease | A2 2085 | 0.38 |
| 66 | Struma | 0.52 | 0.32 | decrease | A2 2085 | 0.16 |
| 67 | Yelcho | 0.52 | 0.49 | decrease | A2 2085 | 0.38 |
| 68 | Irrawaddy | 0.5 | 0.63 | increase | A2 2085 | 0.83 |
| 69 | Daoura | 0.49 | 0.34 | decrease | A2 2085 | 0.14 |
| 70 | Medjerda | 0.49 | 0.44 | decrease | A2 2085 | 0.38 |
| 71 | Mino | 0.49 | 0.36 | decrease | A2 2055 | 0.23 |
| 72 | Zarumilla | 0.49 | 0.53 | increase | A2 2025 | 0.46 |
| 73 | Puelo | 0.48 | 0.42 | decrease | A2 2085 | 0.32 |
| 74 | Limpopo | 0.47 | 0.4 | decrease | B1 2085 | 0.37 |
| 75 | Little Scarcies | 0.47 | 0.61 | increase | A2 2085 | 0.81 |
| 76 | Guadiana | 0.46 | 0.38 | decrease | A2 2085 | 0.22 |
| 77 | Nyanga | 0.45 | 0.51 | increase | B1 2085 | 0.56 |
| 78 | Skagit | 0.45 | 0.54 | increase | A2 2085 | 0.6 |
| 79 | Tumen | 0.45 | 0.4 | decrease | A2 2085 | 0.33 |
| 80 | Geba | 0.44 | 0.45 | increase | B1 2085 | 0.51 |
| 81 | Rhone | 0.43 | 0.42 | decrease | A2 2055 | 0.45 |
| 82 | Zambezi | 0.42 | 0.52 | increase | A2 2085 | 0.89 |
| 83 | Ob | 0.41 | 0.42 | increase | A2 2085 | 0.52 |
| 84 | Palena | 0.41 | 0.38 | decrease | A2 2085 | 0.3 |
| 85 | Torne | 0.4 | 0.46 | increase | B1 2025 | 0.43 |
| 86 | Komoe | 0.39 | 0.76 | increase | A2 2055 | 0.93 |
| 87 | Buzi | 0.38 | 0.4 | increase | 0 | 0.44 |
| 88 | Oral | 0.38 | 0.47 | increase | A2 2055 | 0.52 |
| 89 | Sassandra | 0.37 | 0.3 | decrease | B1 2085 | 0.25 |
| 90 | Tagus | 0.36 | 0.29 | decrease | A2 2085 | 0.15 |
| 91 | St. Paul | 0.35 | 0.37 | increase | A2 2085 | 0.47 |
| 92 | Tami | 0.35 | 0.33 | decrease | A2 2055 | 0.35 |
| 93 | Cross | 0.33 | 0.3 | decrease | B1 2025 | 0.66 |
| 94 | Guir | 0.33 | 0.27 | decrease | B1 2025 | 0.23 |
| 95 | Kemi | 0.33 | 0.34 | increase | A2 2085 | 0.32 |
| 96 | St. John | 0.33 | 0.34 | increase | A2 2025 | 0.33 |
| 97 | Mira | 0.31 | 0.34 | increase | A2 2085 | 0.38 |

Table A.4.: Differences of reliability of the water resources between the riparian countries (expressed through the normalized range) of international river basins and its future changes

| Rank | River basin | Inter-annual variability of runoff | | | | |
|---|---|---|---|---|---|---|
| | | Control Period | Future Mean | Trend | Highest change | |
| | | | | | When | Value |
| 1 | Nile | 2.3 | 2.87 | increase | A2 2055 | 3.4 |
| 2 | Niger | 1.74 | 1.54 | decrease | B1 2025 | 1.12 |
| 3 | Lake Chad | 1.32 | 1.63 | increase | B1 2055 | 2.32 |
| 4 | Indus | 0.98 | 0.93 | decrease | A2 2085 | 0.6 |
| 5 | Danube | 0.93 | 0.7 | decrease | B1 2085 | 0.55 |
| 6 | Volta | 0.91 | 0.87 | decrease | A2 2025 | 1.27 |
| 7 | Pu-Lun-T'o | 0.84 | 0.5 | decrease | B1 2085 | 0.44 |
| 8 | Ganges | 0.8 | 0.71 | decrease | A2 2085 | 0.56 |
| 9 | Tigris-Euphrates | 0.77 | 0.77 | increase | B1 2055 | 1.2 |
| 10 | Gash | 0.72 | 1.4 | increase | A2 2055 | 2.15 |
| 11 | Senegal | 0.67 | 0.73 | increase | A2 2085 | 0.99 |
| 12 | Chira | 0.66 | 0.57 | decrease | B1 2025 | 0.2 |
| 13 | Aral Sea | 0.65 | 0.85 | increase | A2 2085 | 1.06 |
| 14 | Orange | 0.65 | 0.82 | increase | A2 2085 | 1.15 |
| 15 | Awash | 0.63 | 0.98 | increase | B1 2085 | 1.63 |
| 16 | Tumbes | 0.61 | 0.56 | decrease | B1 2025 | 0.25 |
| 17 | Amazon | 0.53 | 0.65 | increase | B1 2055 | 0.76 |
| 18 | Orinoco | 0.53 | 0.48 | decrease | B1 2085 | 0.3 |
| 19 | Komoe | 0.52 | 0.24 | decrease | B1 2085 | 0.12 |
| 20 | Terek | 0.46 | 0.46 | increase | A2 2085 | 0.26 |
| 21 | Lake Titicaca | 0.45 | 0.44 | decrease | A2 2085 | 0.31 |
| 22 | Yenisey | 0.45 | 0.23 | decrease | B1 2055 | 0.09 |
| 23 | Dniester | 0.44 | 0.12 | decrease | B1 2055 | 0.03 |
| 24 | Irrawaddy | 0.44 | 0.53 | increase | A2 2025 | 0.6 |
| 25 | Lake Turkana | 0.44 | 0.46 | increase | A2 2085 | 0.67 |
| 26 | Sepik | 0.42 | 0.25 | decrease | A2 2085 | 0.18 |
| 27 | Ob | 0.41 | 0.27 | decrease | B1 2055 | 0.14 |
| 28 | Alsek | 0.4 | 0.41 | increase | B1 2055 | 0.29 |
| 29 | La Plata | 0.4 | 0.36 | decrease | A2 2085 | 0.29 |
| 30 | Cross | 0.39 | 0.39 | increase | B1 2055 | 0.44 |
| 31 | Limpopo | 0.39 | 0.8 | increase | B1 2055 | 1.62 |
| 32 | Okavango | 0.39 | 0.46 | increase | B1 2055 | 0.91 |
| 33 | Gambia | 0.38 | 0.7 | increase | B1 2085 | 0.84 |
| 34 | Kunene | 0.37 | 0.27 | decrease | A2 2055 | 0.17 |
| 35 | Columbia | 0.36 | 0.3 | decrease | B1 2025 | 0.59 |
| 36 | Taku | 0.36 | 0.35 | decrease | A2 2055 | 0.22 |
| 37 | Coruh | 0.35 | 0.1 | decrease | A2 2055 | 0.04 |
| 38 | Kura-Araks | 0.35 | 0.37 | increase | A2 2085 | 0.51 |
| 39 | Torne | 0.35 | 0.41 | increase | A2 2085 | 0.65 |
| 40 | Chiloango | 0.33 | 0.13 | decrease | B1 2055 | 0.08 |
| 41 | Kemi | 0.33 | 0.14 | decrease | A2 2025 | 0.09 |
| 42 | Congo | 0.32 | 0.4 | increase | B1 2085 | 0.77 |
| 43 | Dra | 0.31 | 0.45 | increase | B1 2025 | 0.62 |
| 44 | Seno Union | 0.31 | 0.25 | decrease | B1 2025 | 0.18 |
| 45 | Amur | 0.3 | 0.41 | increase | A2 2025 | 0.52 |
| 46 | Zarumilla | 0.3 | 0.29 | decrease | A2 2025 | 0.47 |

Table A.5.: Selected basins and their deviation basins average (all indices) in %

| River basin | Trend | Mean Range Country | Deviation from basins average [%] | | | |
|---|---|---|---|---|---|---|
| | | | Aridity Index | P | Qcvt | AWR |
| Lake Chad | increase but AI decrease | Mean [mm/y] | 0.32 | 666 | 0.64 | 156 |
| | | Range[mm/y] | 0.72 | 1365 | 0.92 | 334 |
| | | Algeria | -86.3 | -87.7 | -70.1 | -79.1 |
| | | Cen. Rep. Africa | 136.1 | 117.3 | 64.1 | 134.6 |
| | | Chad | -20.6 | -11.3 | -4 | -9 |
| | | Niger | -77.3 | -72.6 | -45.9 | -76.9 |
| | | Nigeria | 31 | 46 | 40.1 | 51.9 |
| | | Sudan | 17 | 8.3 | 15.7 | -20.9 |
| Niger | P and AI decrease, AWR and Qcvt increase | Mean | 0.47 | 1006 | 0.45 | 284 |
| | | Range | 0.95 | 1740 | 0.77 | 552 |
| | | Algeria | -90.9 | -91 | -109.3 | -89.4 |
| | | Benin | 20.4 | 31 | 35 | 32.5 |
| | | Burkino Faso | -38.2 | -22.5 | 5.1 | -45.8 |
| | | Cameroon | 112.7 | 81.9 | 60.3 | 106 |
| | | Guinea | 73.8 | 65.5 | 36.8 | 91 |
| | | Mali | -58.6 | -46.9 | -33.1 | -59.9 |
| | | Niger | -70 | -60.4 | -39.3 | -77.2 |
| | | Nigeria | 50.9 | 42.4 | 44.6 | 42.8 |
| Nile | increase but AI decrease | Mean | 0.81 | 1180 | 0.38 | 271 |
| | | Range | 1.13 | 1660 | 1.04 | 545 |
| | | Burundi | 33 | 19.1 | 50.1 | 25 |
| | | Egypt | -97.3 | -96.4 | -216.9 | -97.4 |
| | | Ethiopia | 40.9 | 44.1 | 42.4 | 104.1 |
| | | Kenia | 29 | 27.6 | 36.7 | 31.6 |
| | | Ruanda | 20.6 | 6.4 | 48.4 | -6.7 |
| | | Sudan | -64.1 | -46.6 | -92.6 | -60.9 |
| | | Tanzania | -0.1 | 9 | 28.7 | -9 |
| | | Uganda | 9.3 | 17.4 | 44.7 | 4.4 |
| Senegal | increase but AI decrease | Mean | 0.33 | 841 | 0.49 | 214 |
| | | Range | 0.61 | 1169 | 0.35 | 452 |
| | | Guinea | 109.9 | 76.3 | 38.3 | 135.9 |
| | | Mali | 0.1 | 13.3 | -4 | -13 |
| | | Mauretania | -72.3 | -62.6 | -33.7 | -76 |
| | | Senegal | -37.4 | -26.9 | -0.3 | -46.4 |
| Orange | P and Qcvt increase, AI and AWR decrease | Mean | 0.39 | 499 | 0.46 | 80 |
| | | Range | 0.69 | 609 | 0.36 | 145 |
| | | Bostwana | -38.7 | -16.3 | -4.1 | -15.3 |
| | | Lesotho | 112.4 | 70 | 42 | 110.3 |
| | | Namibia | -64.3 | -52.3 | -34.4 | -71.1 |
| | | South Africa | -9.7 | -1.6 | -3 | -23.7 |
| Awash | P and Qcvt increase, AI and AWR decrease | Mean [mm/y] | 0.36 | 611 | 0.59 | 175 |
| | | Range[mm/y] | 0.47 | 636 | 0.47 | 132 |
| | | Djibouti | -65.4 | -52.3 | -38.4 | -39.1 |
| | | Ethiopia | 65.4 | 52.3 | 38.4 | 39.1 |

| River basin | Trend | Mean Range Country | Deviation from the mean value [%] | | | |
|---|---|---|---|---|---|---|
| | | | Aridity Index | P | Qcvt | AWR |
| Logatipi Swamp | increase but AI decrease | Mean [mm/y] | 0.5 | 923 | 0.31 | 176 |
| | | Range[mm/y] | 0.57 | 921 | 0.11 | 276 |
| | | Ethiopia | 73.7 | 65.3 | 18.3 | 114.6 |
| | | Kenia | -40.3 | -34.9 | -6 | -41.9 |
| | | Sudan | -24 | -14.6 | -12.7 | -32.3 |
| | | Uganda | -9.7 | -15.4 | 0.6 | -40.4 |
| Gash | increase | Mean [mm/y] | 0.42 | 720 | 0.88 | 161 |
| | | Range[mm/y] | 0.57 | 723 | 0.86 | 216 |
| | | Eritrea | 3.6 | 8.1 | 8.6 | 8.3 |
| | | Ethiopia | 66.3 | 46.3 | 41.3 | 63.3 |
| | | Sudan | -69.6 | -54.4 | -50.1 | -71.9 |
| Danube | decrease but P increase | Mean [mm/y] | 1.12 | 822 | 0.22 | 214 |
| | | Range[mm/y] | 1.3 | 825 | 0.16 | 418 |
| | | Austria | 62 | 29.7 | 21.1 | 73.7 |
| | | Bulgaria | -37.1 | -23.1 | -30 | -50.9 |
| | | Belarus | 3.9 | 14.6 | 3.3 | 24 |
| | | Czech Republic | -2.4 | -11.7 | 8.9 | -23.6 |
| | | Germany | 41 | 23.7 | 32.3 | 50.6 |
| | | Croatia | 0.1 | 15.1 | 1 | 17.6 |
| | | Hungary | -33 | -25.4 | 0.6 | -49.1 |
| | | Moldova | -44.9 | -34.3 | -29.7 | -65.9 |
| | | Romania | -26.1 | -21 | -20.9 | -45.6 |
| | | Slovakia | 2.1 | -4.9 | 11.7 | -9.1 |
| | | Slovenia | 70.9 | 66.1 | 13 | 130.6 |
| | | Ukraine | -10 | -13.1 | 0 | -21.4 |
| | | Serbia | -26 | -15 | -11.9 | -30.3 |
| Ganges | decrease but AWR increase | Mean [mm/y] | 1.75 | 2161 | 0.21 | 890 |
| | | Range[mm/y] | 1.33 | 2536 | 0.13 | 1173 |
| | | Bangladesh | -10 | 26.4 | 13 | 13.9 |
| | | Bhutan | 9.9 | -3.4 | 2.4 | -2.4 |
| | | China | -27.7 | -61.3 | 3.1 | -60.1 |
| | | India | -28.4 | -10.3 | -37.9 | -18.3 |
| | | Myanmar | 47.1 | 56 | 22.7 | 71.6 |
| | | Nepal | 9.3 | -7.6 | -3.6 | -4.4 |
| Tigris | increase but AI decrease | Mean [mm/y] | 0.37 | 446 | 0.36 | 121 |
| | | Range[mm/y] | 0.4 | 337 | 0.28 | 163 |
| | | Iran | 32.1 | 36.1 | 5.7 | 71.6 |
| | | Iraq | -44.9 | -26.6 | -39.7 | -33.7 |
| | | Syria | -48.3 | -39.4 | -2.6 | -65.9 |
| | | Turkey | 61 | 29.7 | 36.7 | 28.1 |

| River basin | Trend | Mean Range Country | Deviation from the mean value [%] | | | |
|---|---|---|---|---|---|---|
| | | | Aridity Index | P | Qcvt | AWR |
| Aral Sea | increase | Mean [mm/y] | 0.43 | 368 | 0.29 | 148 |
| | | Range[mm/y] | 0.54 | 316 | 0.22 | 256 |
| | | Afghanistan | 44.9 | 40.4 | 10.1 | 52.4 |
| | | Kazakhstan | -46.7 | -30.7 | -7.7 | -52 |
| | | Kyrgyzstan | 47.9 | 23 | 37.1 | 41.4 |
| | | Tajikistan | 62.6 | 40.3 | 23.9 | 97.1 |
| | | Turkmenistan | -63.9 | -44.3 | -38.6 | -76.1 |
| | | Uzbekistan | -45.1 | -29 | -25 | -62.9 |
| Kura- Araks | decrease but Qcvt increase | Mean [mm/y] | 0.66 | 529 | 0.22 | 142 |
| | | Range[mm/y] | 0.6 | 377 | 0.09 | 165 |
| | | Azerbaijan | -18 | -6.6 | -4.4 | -25.3 |
| | | Georgia | 54.1 | 43.9 | 18.6 | 67.1 |
| | | Iran | -36.6 | -27.6 | -21.1 | -50.3 |
| | | Turkey | -1.7 | -8.3 | -1 | -0.3 |
| Pu Lun T'o | decrease | Mean [mm/y] | 0.37 | 207 | 0.25 | 77 |
| | | Range[mm/y] | 0.29 | 114 | 0.18 | 80 |
| | | Mongolia | -39.3 | -27.9 | -35.7 | -53.3 |
| | | Russia | 39.3 | 27.9 | 35.7 | 53.3 |
| Rhine | decrease | Mean [mm/y] | 1.73 | 1085 | 0.13 | 402 |
| | | Range[mm/y] | 1.58 | 719 | 0.03 | 438 |
| | | Belgium | -22.3 | -15.1 | 1.9 | -27.9 |
| | | Switzerland | 53.3 | 36.3 | 5.9 | 64.7 |
| | | Germany | -22.3 | -16.7 | -8.4 | -33 |
| | | France | -13.7 | -5 | -2 | -15.9 |
| | | Liechtenstein | 59 | 41.6 | -2.4 | 74 |
| | | Luxemburg | -22 | -16.7 | -0.9 | -27.4 |
| | | Holland | -32.4 | -24.6 | 5.7 | -34.6 |
| Okavango | AI and AWR decrease, P and Qcvt increase | Mean [mm/y] | 0.43 | 702 | 0.44 | 130 |
| | | Range[mm/y] | 0.38 | 540 | 0.17 | 158 |
| | | Angola | 58.3 | 51.3 | 20.7 | 83.1 |
| | | Botswana | -31.1 | -25.9 | -13 | -36.4 |
| | | Namibia | -25.1 | -23.4 | -2.4 | -38 |
| | | Zimbabwe | -2.1 | -1.7 | -5 | -8.7 |
| Seno Union | AI and AWR increase P and Qcvt decrease | | 1.43 | 693 | 0.15 | 302 |
| | | Range[mm/y] | 1.47 | 642 | 0.04 | 405 |
| | | Argentina | -51.3 | -46.3 | -12.9 | -67.4 |
| | | Chile | 51.3 | 46.3 | 12.9 | 67.4 |

# B. Appendix II: Map of the international river basins of the world

The map of the international river basins of the world is found in the back inside cover of the thesis.

*The map is found in the back inside cover of the thesis.*

Figure B.1.: Map of the international river basins of the world.

# International river basins

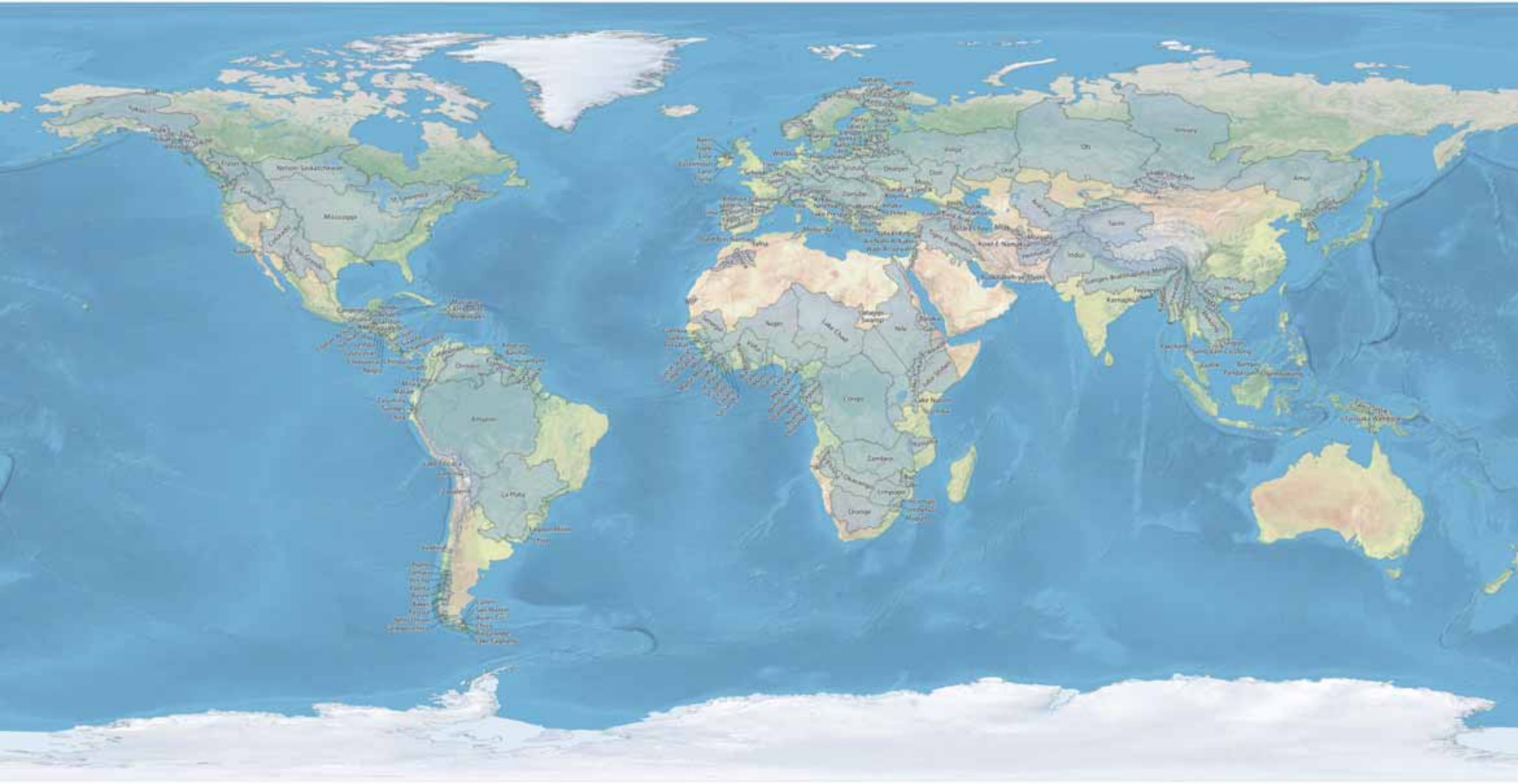

1000 0 1000 2000 3000 4000 5000 km

**Scale 1 : 67 020 000**

**Data**
River basins from Basins at Risk study (Yoffe et al. 2004).
Baselayer and countries from naturalearthdata.com.